NATIONAL ADVISORY COMMITTEE FOR AERONAUTICS

TECHNICAL NOTE 1945

AERODYNAMIC CHARACTERISTICS OF 15 NACA AIRFOIL SECTIONS AT SEVEN REYNOLDS NUMBERS FROM 0.7×10^6 TO 9.0×10^6

By Laurence K. Loftin, Jr. and Hamilton A. Smith

Langley Aeronautical Laboratory
Langley Air Force Base, Va.

Washington
October 1949

NATIONAL ADVISORY COMMITTEE FOR AERONAUTICS

TECHNICAL NOTE 1945

AERODYNAMIC CHARACTERISTICS OF 15 NACA AIRFOIL SECTIONS AT SEVEN REYNOLDS NUMBERS FROM 0.7×10^6 TO 9.0×10^6

By Laurence K. Loftin, Jr. and Hamilton A. Smith

SUMMARY

An investigation has been made of the two-dimensional aerodynamic characteristics of 15 NACA airfoils at four Reynolds numbers from 2.0×10^6 to 0.7×10^6. These data, together with those from previous NACA papers for the same airfoils at three Reynolds numbers from 3.0×10^6 to 9.0×10^6, are presented and analyzed in the present paper. The airfoils investigated consisted of 10 systematically varied NACA 6-series airfoils and 5 airfoils of the NACA 4- and 5-digit series. The NACA 6-series airfoils had thickness ratios varying from 9 to 18 percent of the chord, design lift coefficients varying from 0 to 0.6, and positions of minimum pressure on the basic thickness form at zero lift varying from 30 to 60 percent of the chord. The NACA 4- and 5-digit-series sections investigated consisted of the NACA 0012, and the NACA 44- and 230-series sections of 12-percent and 15-percent thickness. The tests were made for both smooth and rough surface conditions and also included the determination of the effectiveness of the different airfoils at various Reynolds numbers when equipped with split flaps.

The results of the investigation indicate that the drag coefficient at the design lift coefficient and the maximum lift coefficient are the important aerodynamic characteristics which are most affected by variations in the Reynolds number between 9.0×10^6 and 0.7×10^6. For each of the 15 airfoils in both the smooth and rough surface conditions, the drag coefficient at design lift increased as the Reynolds number was lowered from 9.0×10^6 to 0.7×10^6. For the smooth NACA 6-series airfoils the magnitude of this increase became larger with increasing airfoil thickness and with rearward movement of the position of minimum pressure on the basic thickness form at zero lift. In the rough surface condition and at the lower Reynolds numbers in the smooth surface

condition, the saving in minimum drag to be derived from the use of NACA 6-series as compared with NACA 5-digit series airfoil sections disappears.

Decreasing the Reynolds number from 9.0×10^6 to 0.7×10^6 caused reductions in the maximum lift of all the airfoils in both the smooth and rough surface conditions. The magnitude and character of this reduction varied rather inconsistently with airfoil design and surface condition, however, so that the comparative merits of a group of airfoils changed markedly and in a rather unpredictable manner with Reynolds number and surface condition.

INTRODUCTION

Two-dimensional aerodynamic data corresponding to Reynolds numbers of 3.0×10^6, 6.0×10^6, and 9.0×10^6 are now generally available (reference 1) for a rather large number of systematically derived NACA 6-series and 4-digit- and 5-digit-series airfoil sections. Although the range of Reynolds number covered by the investigations reported in reference 1 is reasonably wide, engineering design problems such as may be encountered in the selection of wing sections for small, personal-type airplanes may require data for a range of Reynolds number extending below 3.0×10^6.

With a view toward providing a basis upon which to choose airfoils for such applications, the two-dimensional aerodynamic characteristics of 15 NACA airfoil sections have been determined at Reynolds numbers of 0.7×10^6, 1.0×10^6, 1.5×10^6, and 2.0×10^6. The results of this investigation are given in the present paper. In order to give a more comprehensive picture of the manner in which the aerodynamic characteristics of the 15 airfoils vary with Reynolds number, data obtained for these airfoils at Reynolds numbers of 3.0×10^6, 6.0×10^6, and 9.0×10^6 (references 1 to 3 and previously unpublished data) are also presented.

The airfoils investigated consisted of 10 NACA 6-series sections and 5 airfoils of the NACA 4- and 5-digit-series groups. The airfoils were chosen to show the effect upon the resultant aerodynamic characteristics at different Reynolds numbers of systematic variations in airfoil thickness, camber, and thickness distribution. Lift, drag, and pitching-moment data are presented for each of the plain, smooth airfoils at the seven Reynolds numbers from 0.7×10^6 to 9.0×10^6. A

sufficient amount of data is also included to show the effects of leading-edge roughness and split flaps upon the characteristics of the airfoils.

SYMBOLS

c_d	section drag coefficient
c_l	section lift coefficient
$c_{l_{max}}$	maximum section lift coefficient
c_{l_i}	section design lift coefficient
$c_{m_{ac}}$	section pitching-moment coefficient about aerodynamic center
$c_{m_{c/4}}$	section pitching-moment coefficient about quarter-chord point
α_o	section angle of attack
α_{l_o}	section angle of zero lift
$dc_l/d\alpha_o$	section lift-curve slope
R	Reynolds number
c	airfoil chord
x	distance along chord
y	distance perpendicular to chord

AIRFOILS

The airfoils investigated consisted of 10 NACA 6-series sections and 5 NACA 4- and 5-digit-series sections. The airfoils were selected to show the effect upon the resultant aerodynamic characteristics of systematic variations in thickness, camber, and thickness distribution.

The 10 NACA 6-series airfoils can be grouped as follows to show the systematic variation in design parameters:

Thickness variation	Camber variation	Thickness-distribution variation
NACA airfoil		
64-409	64_1-012	63_2-415
64_1-412	64_1A212	64_2-415
64_2-415	64_1-412	65_2-415
64_3-418	64_1-612	66_2-415

The NACA 64-series thickness form was chosen for the basic investigation of the effects of thickness ratio and camber because, on the basis of the higher Reynolds number results presented in reference 1, this thickness form was believed to represent the best compromise between airfoil lift and drag characteristics in both the smooth and rough surface conditions. The use of an NACA 6A-series thickness form for the investigation of the 12-percent-thick airfoil with 0.2 design lift coefficient was prompted only by the availability of the test model. On the basis of the data presented in reference 3, the use of the slightly modified thickness form in this case would not be expected to alter the validity of the comparison of the more important effects of camber upon the aerodynamic characteristics of the airfoils. Except for the investigation of the effect of variation in amount of camber, the NACA a = 1.0 mean line cambered for a design lift coefficient of 0.4 was used in all cases, since the use of this mean line with 0.4 design lift coefficient generally results in good maximum lift characteristics without causing appreciable increases in the minimum drag or excessive values of the pitching moment (reference 1). Amounts of camber corresponding to design lift coefficients greater than 0.6 were not investigated because previous experience (reference 1) has indicated that such large amounts of camber have an adverse effect upon the drag without causing any marked improvement in maximum lift. Airfoils having thickness ratios not included in the range from 9 to 18 percent of the chord were not investigated because they were not thought to be of very great interest in the design of personal-type airplanes.

The NACA 4- and 5-digit-series airfoils for which experimental data were obtained are as follows:

NACA 0012 NACA 4412 NACA 23012

NACA 4415 NACA 23015

These particular airfoils were chosen for investigation because they have been employed quite extensively in the past; hence, a comparison of their merits relative to those of the NACA 6-series sections throughout the range of Reynolds number from 0.7×10^6 to 9.0×10^6 seemed desirable.

Complete descriptions, including the methods of derivation and theoretical pressure-distribution data, can be found in reference 1 for all the airfoils investigated except the NACA 64_1A212 section, for which corresponding information is included in reference 3. Ordinates for the 15 airfoils tested are presented in tables I to XV.

APPARATUS AND TESTS

Models.- The 24-inch-chord models of the airfoil sections tested were constructed of laminated mahogany. The surfaces of the models were lacquered and then sanded with No. 400 carborundum paper.

Wind tunnel and test methods.- The experimental investigation was conducted in the Langley two-dimensional low-turbulence tunnel. The test section of this tunnel measures 3 feet by 7.5 feet and, when mounted, the model completely spans the 3-foot dimension. Since this tunnel operates at atmospheric pressure only, the Reynolds number is varied by means of the tunnel airspeed. Lift measurements are usually made in this tunnel by taking the difference of the integrated pressure reaction upon the floor and ceiling of the tunnel (reference 4). Because of the small dynamic pressures involved in the present investigation, however, more accurate measurements of the lift were obtainable with the three-component balance which is part of the equipment of the low-turbulence tunnel. The pitching-moment measurements were also made with the balance.

For the tests using the balance, the models were supported in the tunnel on trunnions extending through the tunnel walls from the balance frame. A small gap was allowed between the ends of the model and the tunnel walls to insure freedom of movement of the balance. Since air leakage through these gaps was considered as a possible source of error, lift tests were made at Reynolds numbers of 2.0×10^6 and 1.5×10^6 with the gaps open and then sealed. The measurements for the gaps-sealed condition were made by means of the tunnel floor and ceiling pressure orifices; for the gaps-open tests the balance was used. Results obtained by the two methods agreed to within the experimental error for these Reynolds numbers and would be expected to agree equally well at the lower Reynolds numbers.

Similar comparative tests have shown, however, that more accurate measurements of the drag are possible with the wake-survey apparatus

than with the balance. Hence, all drag measurements were taken by the wake-survey method (reference 4) with the gaps between the model and tunnel walls sealed with felt packing.

Tests.- The tests of each smooth, plain airfoil consisted of measurements of the section lift, drag, and quarter-chord pitching moment at Reynolds numbers of 2.0×10^6, 1.5×10^6, 1.0×10^6, and 0.7×10^6. In none of these tests did the Mach number exceed 0.15. With the exception of the NACA 64_1A212 airfoil section, lift and pitching-moment measurements at each of the four Reynolds numbers were also made for the smooth airfoils equipped with 0.20c simulated split flaps deflected 60°. In addition, all of the measurements except those of the pitching moment were repeated with standard roughness applied to the leading edges of the airfoils. The standard roughness employed was the same as that used in previous investigations (references 1 to 3) and consisted of 0.011-inch-diameter carborundum grains spread over a surface length of 8 percent of the chord measured from the leading edge on the upper and lower surfaces of the airfoils. The grains were thinly spread to cover from 5 to 10 percent of this area.

In order that comparative data should be available for all the airfoils in the range of Reynolds number from 9.0×10^6 to 0.7×10^6, it was necessary to make standard tests (reference 1) in the Langley two-dimensional low-turbulence pressure tunnel of the NACA 64-409 and NACA 64_1-612 airfoils at Reynolds numbers of 3.0×10^6, 6.0×10^6, and 9.0×10^6 since these data had not previously been obtained. In addition, supplementary tests were made in the Langley two-dimensional low-turbulence pressure tunnel at a Reynolds number of 6.0×10^6 of the NACA 23012 and NACA 23015 sections equipped with split flaps. Such data are available in references 1 to 3 for the other airfoils tested in the present investigation (with exceptions as already noted) and were considered necessary for the NACA 23012 and NACA 23015 sections in order to compare adequately the type of scale effect shown by those sections with that of the other sections tested.

RESULTS

The results are presented (figs. 1 to 15) in the form of standard aerodynamic coefficients representing the lift, drag, and quarter-chord pitching moment. Each figure is in three parts. The lift data for the plain airfoils and the airfoils with split flaps are contained in parts (a) and (b), respectively, together with the appropriate quarter-chord pitching-moment data; the drag results and data on the aerodynamic center and the moment coefficient about this point are contained in part (c).

The Reynolds number range for which the plain, smooth airfoil characteristics are presented extends from 9.0×10^6 to 0.7×10^6. Data are presented for each of the plain airfoils with roughened leading edges and for most of the airfoils with split flaps in both the smooth and rough surface conditions at five Reynolds numbers from 6.0×10^6 to 0.7×10^6. The characteristics at a Reynolds number of 6.0×10^6 of the NACA 4412 and NACA 4415 sections with split flaps are not available in reference 1 for the rough surface condition, nor were these data obtained in the present investigation. From the quarter-chord pitching-moment data, the position of the aerodynamic center and the variation of the moment about this point were calculated and are presented for each of the plain, smooth airfoils (figs. 1 to 15, part (c)).

The influence of the tunnel boundaries has been removed from the aerodynamic data for all the airfoil sections. The following equations (developed in reference 4) which contain the correction factors for the NACA 64_2-415 airfoil show the order of magnitude of the boundary effect:

$$c_d = 0.991c_d'$$

$$c_l = 0.976c_l'$$

$$c_{m_{c/4}} = 0.991\, c_{m_{c/4}}'$$

$$\alpha_o = 1.015\alpha_o'$$

where the primed quantities represent the coefficients measured in the tunnel.

DISCUSSION

A detailed evaluation of the comparative merits of a large number of airfoils is given in reference 1 for a Reynolds number of 6.0×10^6. In the present paper such a detailed evaluation is not attempted for each of the seven Reynolds numbers investigated, but, rather, the data are analyzed to show the effects of several airfoil design parameters upon the manner in which the more important aerodynamic characteristics of the airfoils vary with Reynolds number. As an aid to this study, cross plots (figs. 16 to 22) are used to show some of the important aerodynamic characteristics of the airfoils as functions of Reynolds number. The aerodynamic characteristics discussed concern the drag, the lift, and the pitching moment.

Drag

The general form of the drag polars corresponding to the various Reynolds numbers may be seen in figures 1 to 15. The principal effects on the drag of decreasing the Reynolds number from 9.0×10^6 to 0.7×10^6 appear to be a variation in width of the flat portion of the polars, an increase in value of the minimum drag coefficient, and a steepening of the drag curves beyond the flat portion of the polars.

Low-drag range.- The extent of the lift-coefficient range over which the 10 NACA 6-series airfoils in the smooth condition have low drag, which corresponds to extensive laminar flow, generally increases as the Reynolds number is lowered, with the greatest increase usually occurring as the Reynolds number is lowered below 3.0×10^6 (figs. 1 to 15). The magnitude of the effect is greatest for the airfoils of greatest thickness, highest design lift coefficient, and farthest rearward position of minimum pressure. It is of interest to note that the actual low-drag range is considerably greater than the theoretical low-drag range for all the airfoils at the lower Reynolds numbers. Hence, for these Reynolds numbers, the first small pressure peaks which form near the leading edge as the lift coefficient is increased do not cause transition from laminar to turbulent flow. For most Reynolds numbers, the data show that thick airfoils with the position of minimum pressure far forward tend to have the widest low-drag ranges.

The increase in drag with increasing lift coefficient within the low-drag region shown for some of the airfoils at the lower Reynolds numbers (particularly pronounced for the NACA 64_2-415 section, fig. 3(a)) is believed to be associated with the formation of a laminar separation bubble behind the position of minimum pressure. The exact behavior of this bubble as the lift coefficient and Reynolds number are varied, however, is not entirely clear at the present time.

Although the comparatively high values of the minimum drag coefficient shown by the five NACA 4- and 5-digit-series airfoil sections (figs. 11 to 15) preclude the possibility of a low-drag range corresponding to extensive laminar layers on the airfoil surfaces, there is a range of lift coefficient through which the drag of these airfoils changes very little. Although the manner in which this range varies with Reynolds number for the different airfoils is not very well defined, there does seem to be a tendency, which is especially marked in the cases of the NACA 4412 and NACA 23012 airfoil sections, toward a decrease in the extent of this range as the Reynolds number is decreased. This effect is believed to be associated with the formation and behavior of a laminar separation bubble a short distance behind the leading edge on the suction side of the airfoil. As previously stated, however, the details of the mechanics of the laminar separation bubble are not completely understood.

The drag polars for the airfoils tested with roughened leading edges do not generally have a range of lift coefficient over which the drag is essentially constant but, rather, are of parabolic form. The lower portions of the parabolas, over which the drag variation with lift coefficient is the least, appear to become narrower for most of the airfoils as the Reynolds number is reduced, except at the lowest Reynolds number (0.7×10^6). The behavior of the drag polars at a Reynolds number of 0.7×10^6 probably results from the fact that the leading-edge roughness employed was not sufficiently large to cause fully developed turbulent boundary layers at this low value of the Reynolds number. In most cases, airfoil thickness and camber do not appear to have a very pronounced or consistent effect upon the manner in which the lift-coefficient range corresponding to the lower portion of the drag polars of the rough NACA 6-series sections varies with the Reynolds number, or upon the actual width of the range itself. Movement of the position of minimum pressure on the basic thickness form at zero lift from 40 percent to 60 percent of the chord does, however, seem to reduce the width of the range at most Reynolds numbers. The data for the NACA 4- and 5-digit-series sections (figs. 11 to 15, part (c)) show that the range of lift coefficient corresponding to the lower portion of the drag polars for these airfoils in the rough condition does not differ greatly at most Reynolds numbers from that shown by most of the NACA 6-series sections.

Minimum drag.- The Reynolds number has a very important effect upon the minimum drag (figs. 1 to 15, part (c)) of the airfoils, both in the smooth condition and with roughened leading edges. In order to show more clearly the magnitude and trend of the effect, the drag coefficient corresponding to the measured design lift coefficient (designated minimum drag coefficient) has been plotted in figure 16 as a function of Reynolds number for each of the 15 airfoils tested. For convenience in comparing the drag variation of the different airfoils, the data for the NACA 6-series airfoils are arranged in this plot in three groups according to systematic variations of thickness, camber, and thickness distribution. The data for the NACA 4- and 5-digit-series sections are plotted in one group. The drag coefficient at the experimental design lift coefficient is seen to increase with decreasing Reynolds number for all the airfoils in the smooth condition (fig. 16(a)) and, except at the lowest Reynolds number, for the airfoils with roughened leading edges (fig. 16(b)). The previously mentioned effect of roughness size is probably responsible for the drag reduction shown by the results for the rough airfoils at a Reynolds number of 0.7×10^6.

For the smooth NACA 6-series airfoils, the amount by which the minimum drag coefficient increases as the Reynolds number is lowered appears to become larger as the thickness ratio of the sections is increased and as the position of minimum pressure is moved rearward along

the chord (fig. 16(a)). Variation of camber seems to produce only slight, inconsistent changes in slope of the curve of drag against Reynolds number. These trends indicate that the advantage in drag reduction to be derived from the use of thin airfoil sections increases as the Reynolds number is lowered and that relatively far forward positions of minimum pressure are desirable at low values of the Reynolds number. It is interesting to note that, although the purpose of moving the position of minimum pressure rearward to 60 percent of the chord is to decrease the drag by increasing the relative extent of laminar flow, the section with minimum pressure farthest forward actually has more favorable drag characteristics at the two lowest Reynolds numbers. The fact that regions of laminar separation probably exist behind the position of minimum pressure and increase in extent as the airfoil thickness is increased and as the position of minimum pressure is moved rearward is believed to be responsible for the observed effect of airfoil thickness and thickness distribution on the drag at the lower Reynolds numbers.

The drag data for the NACA 4-digit-series and 5-digit-series airfoils in the smooth surface condition (fig. 16(a)) generally do not show as much variation with Reynolds number as do those for the NACA 6-series sections. Because of the differences in scale effect, the advantage in drag reduction derived from employing a smooth NACA 6-series section as compared with one of the smooth NACA 4- or 5-digit-series sections diminishes as the Reynolds number is lowered. At a Reynolds number of 0.7×10^6, the drag values for the smooth condition of the NACA 6-series airfoils and the NACA 4- and 5-digit-series sections are of about the same order of magnitude. The fact that the scale effect on the minimum drag of the NACA 4-digit- and 5-digit-series sections is smaller than that shown by the NACA 6-series sections may possibly be attributed to the following two effects: first, from some preliminary studies there is reason to believe that there exists on the NACA 6-series sections a region of laminar separation behind the position of minimum pressure which increases in extent as the Reynolds number is lowered and causes the drag to increase rapidly. Within the same range of Reynolds number, however, the transition point on the NACA 4-digit- and 5-digit-series sections is ahead of the incipient laminar separation point so that no regions of separated flow exist. Second, the transition point on the NACA 4- and 5-digit-series sections probably moves rearward as the Reynolds number is reduced so that the relative extent of laminar flow increases as the Reynolds number is decreased. The extent of laminar flow on the NACA 6-series sections is limited at the position of laminar separation which, of course, does not vary with Reynolds number. If the Reynolds number were sufficiently low so that the transition point on the NACA 4-digit- and 5-digit-series sections were to occur behind the incipient separation point, regions of laminar separation

and, consequently, higher drags and more pronounced scale effect would be expected for these airfoils.

In the rough surface condition, the minimum drag coefficients of the NACA 6-series and 4- and 5-digit-series airfoil sections vary with Reynolds number in about the same manner. The values of the drag of comparable NACA 6-series, 00-series, and 230-series sections are also about the same at most Reynolds numbers; whereas the drag values of the NACA 44-series sections are, comparatively, appreciably higher. In general, increases in the airfoil thickness ratio and camber cause rather consistent increases in the drag throughout the Reynolds number range; whereas variations in thickness form seem to have a relatively small effect.

Drag outside the low-drag range.- From an inspection of the data of figures 1 to 15, it can be seen that the drag outside of the relatively flat portion of the polar increases for all the airfoils in the smooth and rough surface conditions as the Reynolds number is lowered from 9.0×10^6 to 0.7×10^6. The magnitude of the scale effect is generally largest for the smooth surface condition. Variations in airfoil-design parameters have some influence upon the magnitude and character of the scale effect; however, consistent trends are difficult to distinguish.

Lift

The lift parameters which are usually considered to be of most importance are the lift-curve slope, the angle of zero lift, and the maximum lift coefficient. From the lift data presented in figures 1 to 15, the values of these parameters have been determined at each Reynolds number for the airfoils tested and are plotted as functions of Reynolds number in figures 17 to 22.

Lift-curve slope.- According to reference 1, the slope of the lift curve is considered to be defined by a straight line tangent to the lift curve at the design lift coefficient. The lift-curve slopes for a Reynolds number of 6.0×10^6, presented in reference 1, could be determined quite easily in accordance with this definition since the lift data corresponding to the higher Reynolds numbers generally show only a small amount of dispersion and are characterized by a nearly linear variation with angle of attack within the low lift-coefficient range. In the present experiments at Reynolds numbers below 3.0×10^6, however, the necessarily low dynamic pressures reduced the accuracy of the measuring apparatus so that some scatter is present in the lift data. For this reason, and because some of the lift curves tended to have slight jogs and variations in slope near the design lift coefficient,

comparable measurements of the lift-curve slope for different Reynolds numbers did not appear feasible by the method employed in reference 1. The lift-curve slopes were therefore considered to be defined by the best straight line through the experimental points between zero lift and the design lift coefficient for the cambered airfoils. For the two symmetrical sections, the lift-curve slopes were determined by the best fairing of the data from zero lift to a few tenths in lift coefficient above and below zero lift. The lift-curve slopes corresponding to all the Reynolds numbers from 9.0×10^6 to 0.7×10^6 were measured according to this procedure and are presented for the 15 airfoils in the smooth and rough surface conditions in figure 17.

An examination of the data of figure 17 indicates that the value of the slope of the lift curve for the smooth airfoils decreases as the Reynolds number is lowered from 9.0×10^6 to 0.7×10^6. The magnitude and character of the scale effect vary somewhat for the different airfoils; however, these variations in scale effect do not form any consistent trends with systematic changes in the design parameters of the airfoils. In most instances, for the smooth airfoils, the decrease in lift-curve slope which accompanies reductions in Reynolds number is greatest between Reynolds numbers of 3.0×10^6 and 0.7×10^6, with variations in Reynolds number from 9.0×10^6 to 3.0×10^6 usually having an almost imperceptible effect on the slope of the lift curve (fig. 17(a)). In comparison with the data for the NACA 6-series airfoils, the lift-curve slope of the NACA 64_1A212 airfoil is seen to be rather low at all Reynolds numbers. As pointed out in reference 3, the trailing-edge angles of the NACA 6A-series sections, which are larger than the trailing-edge angles of the NACA 6-series sections, cause reductions in the lift-curve slope.

The addition of roughness to the leading edge usually results in lower lift-curve slopes for all the airfoils (fig. 17(b)). In general, however, for any particular airfoil, the decrement in lift-curve slope due to roughness does not seem to vary to any large extent with the Reynolds number.

Angle of zero lift.- The data presented in figure 18 indicate that the angle of zero lift of most of the airfoils changes to some small extent with Reynolds number, but in most cases the scale effect is relatively insignificant. The addition of standard leading-edge roughness (fig. 18(b)) causes a change in the magnitude of the angle of zero lift of most of the airfoils.

Maximum lift coefficient.- The lift parameter which is most affected by variations in the Reynolds number is the maximum lift coefficient (figs. 1 to 15). A discussion of the flow phenomena associated with the occurrence of maximum lift and the relationship between these phenomena and the Reynolds number is given in reference 5.

The plot of maximum lift against Reynolds number for the different airfoils (figs. 19 to 22) shows that, in all cases, decreasing the Reynolds number from the highest value to 0.7×10^6 effects reductions in the maximum lift of the airfoils, with and without split flaps, in both the smooth and rough surface conditions. The manner in which the maximum lift of the airfoils varies with Reynolds number and the magnitude of this variation are seen to depend upon the airfoil design, surface condition, and whether a split flap is employed. Unfortunately, the data also show that the type and magnitude of the scale effect on the maximum lift do not vary in any very consistent manner with the airfoil-design parameters investigated. It is not possible, therefore, to predict from the comparative values of the maximum lift of a group of airfoils at one Reynolds number the advantage one airfoil will have over another at any other Reynolds number.

As an example of the manner in which the merits of different airfoils change with Reynolds number consider the manner in which the comparative values of the maximum lift of the NACA 64-409 and NACA 64_3-418 airfoils in the smooth condition change as the Reynolds number is lowered from 9.0×10^6 to 0.7×10^6 (fig. 19). Notice also that the rather large advantage of the NACA 23012 airfoil in the smooth, plain condition as compared with the NACA 64_1-412 and NACA 4412 sections decreases and finally vanishes as the Reynolds number is progressively reduced from 9.0×10^6 to 0.7×10^6 (figs. 20 and 22). In general, there is less scale effect on the maximum lift of the airfoils with rough leading edges than on the airfoils with smooth surfaces. Surface roughness, nevertheless, has a large effect upon the comparison of some of the airfoils for the different Reynolds numbers. Again consider the data for the NACA 23012 section which show that the maximum lift of this plain airfoil with roughness becomes progressively less favorable relative to that of comparable NACA 6-series sections (NACA 64_1A212 and NACA 64_1-412) as the Reynolds number is reduced and is actually less than that of the NACA 64-409 section below 2.0×10^6; whereas at practically all Reynolds numbers, the plain NACA 23012 section with smooth surface has maximum lift coefficients as high as or higher than those of comparable 6-series airfoils. With split flaps deflected 60°, the data show that the amount and type of maximum-lift variation with Reynolds number are not necessarily the same as indicated by the results for the plain airfoils; and again, the comparative values of the maximum lift of the various airfoils with split flaps are seen to change with the Reynolds number and surface condition. From the viewpoint of the aircraft designer, the most important conclusion to be drawn from these maximum-lift data is that the selection of an airfoil for a given application must be made from data at a Reynolds number corresponding to the Reynolds number of the application.

Stalling characteristics.- In airplane design problems the manner in which the airfoil stalls is frequently of great importance. The lift data in parts (a) and (b) of figures 1 to 15 show that the type of stall depends upon the Reynolds number, airfoil design, surface condition, and whether a split flap is employed. In general, the data for the plain, smooth NACA 6-series sections show that the stall becomes less abrupt as the airfoil thickness and camber are increased and as the Reynolds number is reduced. The favorable effect of a decreasing Reynolds number on the character of the stall is not evident in the data for the NACA 6-series airfoils of 15- and 18-percent thickness and for the airfoil of 0.6 design lift coefficient. These sections, however, show favorable stalling characteristics at all Reynolds numbers as compared with the rather abrupt stalls shown by the thinner sections and sections of smaller camber at the higher Reynolds numbers. Variations in thickness form corresponding to positions of minimum pressure on the basic thickness form at zero lift from 30 to 60 percent chord do not appear to have any effect upon the character of the stall of the 15-percent-thick, smooth airfoil sections. Rearward movement of the minimum-pressure point may, however, have some small adverse effect upon the stalling characteristics of airfoils thinner than 15 percent of the chord as indicated by data corresponding to Reynolds numbers from 3.0×10^6 to 9.0×10^6 for 12-percent-thick airfoils having different positions of minimum pressure (reference 1).

In the smooth surface condition the two NACA 230-series sections are seen to possess extremely undesirable stalling characteristics at nearly all Reynolds numbers, whereas both of the NACA 44-series sections have very good stall characteristics throughout the Reynolds number range investigated. The stall of the NACA 0012 section is very acute at the higher Reynolds numbers but, like the NACA 64_1-012 airfoil, reductions in the Reynolds number have a somewhat favorable effect.

In the rough surface condition, nearly all of the plain airfoils have good stalling characteristics at most Reynolds numbers. The NACA 230-series sections, and at the higher Reynolds numbers the NACA 0012 section, are notable exceptions, for even in the rough condition the stalling characteristics of these airfoils are rather undesirable at most Reynolds numbers.

With 0.20c split flaps deflected 60°, the stalling characteristics of the smooth NACA 6-series sections do not vary in an entirely consistent manner with either Reynolds number or airfoil design. In some cases, decreasing the Reynolds number improves the stalling characteristics (examples, NACA 64-409 and NACA 64_1-412 sections); in other cases, decreasing the Reynolds number does not seem to affect the stall (NACA 64_3-418); whereas in still other cases, the stall seems to be affected slightly adversely by reducing the Reynolds number (NACA 63_2-415). It is interesting to note that, whereas increasing thickness improved the stall of the plain

NACA 6-series sections, the NACA 64_2-415 and NACA 64_3-418 sections with flaps have stalling characteristics at Reynolds numbers below 6.0×10^6 generally less desirable than those of the 9-percent-thick section. Neither variations in thickness form nor in amount of camber seem to have a very important effect upon the stall, although the stall of the 66-series section at the different Reynolds numbers may be somewhat more desirable than the stalls of the other airfoils of 15-percent thickness. The smooth NACA 23012, 23015, and 0012 airfoil sections with split flaps are characterized by quite abrupt stalls at all Reynolds numbers. The NACA 44-series sections, when equipped with split flaps, possess stalling properties which are somewhat similar to those of comparable NACA 6-series sections.

Except for the NACA 0012 and NACA 230-series sections, the addition of roughness usually improves to some degree the stalling characteristics of the airfoils with flaps, although this is not always true. (See, for example, the data for the NACA 64_3-418 section, fig. 4(b).)

Pitching Moment and Aerodynamic Center

The values of the quarter-chord pitching-moment coefficient corresponding to the design angles of attack show practically no variation with Reynolds number for any of the plain airfoils (figs. 1 to 15, part (c)). Accompanying changes in the Reynolds number, some change in the slope of the pitching-moment curve against angle of attack is noticeable. Consequently, the chordwise position of the aerodynamic center varies somewhat with Reynolds number; however, these variations do not appear to form any consistent trend with the Reynolds number (figs. 1 to 15).

When the airfoils are equipped with split flaps there is some variation with Reynolds number of the quarter-chord pitching moment corresponding to zero angle of attack for several of the airfoils. This variation usually consists of a decrease in magnitude of the coefficient with decreasing Reynolds number and is most pronounced for the thicker airfoils with far back position of minimum pressure. There is also some change in the shape of the curve of pitching moment plotted against angle of attack with Reynolds number for several of the airfoils. This change of shape usually consists of a decrease in magnitude of the pitching moment with increasing angle of attack which becomes more pronounced as the Reynolds number is reduced. The magnitude of the effect seems to become more pronounced as the airfoil thickness and camber are increased and as the position of minimum pressure is moved rearward.

CONCLUSIONS

From investigations of the two-dimensional aerodynamic characteristics of 10 NACA 6-series and 5 NACA 4- and 5-digit-series airfoil sections at seven Reynolds numbers from 9.0×10^6 to 0.7×10^6, the following conclusions can be drawn:

1. The drag coefficient at the design lift coefficient (designated minimum drag coefficient) of each of the 15 airfoils both in the smooth and rough surface conditions increased as the Reynolds number was lowered from 9.0×10^6 to 0.7×10^6. The magnitude of this increase became larger for the smooth NACA 6-series sections with increasing airfoil thickness and rearward movement of the position of minimum pressure on the basic thickness form at zero lift. In the rough surface condition and at the lower Reynolds numbers in the smooth surface condition, the reduction in minimum drag to be derived from the use of NACA 6-series as compared with NACA 5-digit-series sections disappeared.

2. Reductions in the Reynolds number generally caused some increase in the extent of the low-drag range for the smooth NACA 6-series airfoils. For all the airfoils, the actual extent of the low-drag range was greater than the theoretical value at the lower Reynolds numbers.

3. Decreasing the Reynolds number from 9.0×10^6 to 0.7×10^6 caused reductions in the maximum lift of all the airfoils with and without split flaps, in both the smooth and rough surface conditions. The magnitude and character of this reduction, however, varied rather inconsistently with airfoil design and surface condition so that the comparative merits of the group of airfoils changed markedly and in a rather unpredictable manner with Reynolds number and surface conditions.

4. In general, reductions in the Reynolds number appeared to decrease the sharpness of the stall on those NACA 6-series airfoils for which the lift curves are characterized by rather abrupt losses in lift at the stall. The very undesirable stalling characteristics of the NACA 230-series sections were not improved in either the smooth or rough surface condition by reductions in the Reynolds number.

5. Some decrease in the lift-curve slopes of the smooth and rough airfoils accompanied decreases in the Reynolds number. The type and magnitude of the scale effect changed to a small degree, with variations in the airfoil-design parameters considered. In most cases the angle of zero lift seemed to be almost independent of variations in the Reynolds number.

6. The value of the quarter-chord pitching moment at the design angle of attack did not vary with Reynolds number for the plain airfoils. The chordwise position of the aerodynamic center varied somewhat with Reynolds number, but these variations were, in most cases, relatively small. With 0.20-chord simulated split flaps deflected 60°, the value of the quarter-chord pitching moment at zero angle of attack in many cases varied somewhat in magnitude with Reynolds number.

Langley Aeronautical Laboratory
National Advisory Committee for Aeronautics
Langley Air Force Base, Va., July 6, 1949

REFERENCES

1. Abbott, Ira H., Von Doenhoff, Albert E., and Stivers, Louis S., Jr.: Summary of Airfoil Data. NACA Rep. 824, 1945.

2. Loftin, Laurence K., Jr., and Cohen, Kenneth S.: Aerodynamic Characteristics of a Number of Modified NACA Four-Digit-Series Airfoil Sections. NACA TN 1591, 1948.

3. Loftin, Laurence K., Jr.: Theoretical and Experimental Data for a Number of NACA 6A-Series Airfoil Sections. NACA TN 1368, 1947.

4. Von Doenhoff, Albert E., and Abbott, Frank T., Jr.: The Langley Two-Dimensional Low-Turbulence Pressure Tunnel. NACA TN 1283, 1947.

5. Loftin, Laurence K., Jr., and Bursnall, William J.: The Effects of Variations in Reynolds Number between 3.0×10^6 and 25.0×10^6 upon the Aerodynamic Characteristics of a Number of NACA 6-Series Airfoil Sections. NACA TN 1773, 1948.

TABLE I

ORDINATES OF THE

NACA 64-409 AIRFOIL SECTION

[Stations and ordinates given in percent of airfoil chord]

Upper surface		Lower surface	
Station	Ordinate	Station	Ordinate
0	0	0	0
.377	.829	.623	-.629
.613	1.021	.887	-.741
1.095	1.331	1.405	-.903
2.322	1.895	2.678	-1.151
4.803	2.732	5.197	-1.468
7.297	3.383	7.703	-1.687
9.798	3.925	10.202	-1.857
14.810	4.796	15.190	-2.104
19.830	5.456	20.170	-2.272
24.854	5.957	25.146	-2.377
29.882	6.315	30.118	-2.427
34.912	6.538	35.088	-2.418
39.942	6.632	40.058	-2.348
44.972	6.554	45.028	-2.174
50.000	6.342	50.000	-1.930
55.024	6.016	54.976	-1.636
60.045	5.594	59.955	-1.310
65.060	5.085	64.940	-.965
70.069	4.504	69.931	-.616
75.072	3.858	74.928	-.278
80.069	3.154	79.931	.030
85.059	2.413	84.941	.279
90.043	1.644	89.957	.424
95.021	.858	94.979	.406
100.000	0	100.000	0

L.E. radius: 0.579
Slope of radius through L.E.: 0.168

TABLE II

ORDINATES OF THE

NACA 64_1-412 AIRFOIL SECTION

[Stations and ordinates given in percent of airfoil chord]

Upper surface		Lower surface	
Station	Ordinate	Station	Ordinate
0	0	0	0
.338	1.064	.662	-.864
.569	1.305	.931	-1.025
1.045	1.690	1.455	-1.262
2.264	2.393	2.736	-1.649
4.738	3.430	5.262	-2.166
7.229	4.231	7.771	-2.535
9.730	4.896	10.270	-2.828
14.745	5.959	15.255	-3.267
19.772	6.760	20.228	-3.576
24.805	7.363	25.195	-3.783
29.842	7.786	30.158	-3.898
34.882	8.037	35.118	-3.917
39.923	8.123	40.077	-3.839
44.963	7.988	45.037	-3.608
50.000	7.686	50.000	-3.274
55.032	7.246	54.968	-2.866
60.059	6.690	59.941	-2.406
65.078	6.033	64.922	-1.913
70.090	5.293	69.910	-1.405
75.094	4.483	74.906	-.903
80.089	3.619	79.911	-.435
85.076	2.722	84.924	-.038
90.055	1.818	89.945	.250
95.027	.919	94.973	.345
100.000	0	100.000	0

L.E. radius: 1.040
Slope of radius through L.E.: 0.168

TABLE III

ORDINATES OF THE

NACA 64_2-415 AIRFOIL SECTION

[Stations and ordinates given in percent of airfoil chord]

Upper surface		Lower surface	
Station	Ordinate	Station	Ordinate
0	0	0	0
.299	1.291	.701	-1.091
.526	1.579	.974	-1.299
.996	2.038	1.504	-1.610
2.207	2.883	2.793	-2.139
4.673	4.121	5.327	-2.857
7.162	5.075	7.838	-3.379
9.662	5.864	10.338	-3.796
14.681	7.122	15.319	-4.430
19.714	8.066	20.286	-4.882
24.756	8.771	25.244	-5.191
29.803	9.260	30.197	-5.372
34.853	9.541	35.147	-5.421
39.904	9.614	40.096	-5.330
44.954	9.414	45.046	-5.034
50.000	9.016	50.000	-4.604
55.040	8.456	54.960	-4.076
60.072	7.762	59.928	-3.478
65.096	6.954	64.904	-2.834
70.111	6.055	69.889	-2.167
75.115	5.084	74.885	-1.504
80.109	4.062	79.891	-.878
85.092	3.020	84.908	-.328
90.066	1.982	89.934	.086
95.032	.976	94.968	.288
100.000	0	100.000	0

L.E. radius: 1.590
Slope of radius through L.E.: 0.168

TABLE IV

ORDINATES OF THE

NACA 64_3-418 AIRFOIL SECTION

[Stations and ordinates given in percent of airfoil chord]

Upper surface		Lower surface	
Station	Ordinate	Station	Ordinate
0	0	0	0
.263	1.508	.737	-1.308
.486	1.840	1.014	-1.560
.950	2.370	1.550	-1.942
2.152	3.357	2.848	-2.613
4.609	4.800	5.391	-3.536
7.095	5.908	7.905	-4.212
9.595	6.823	10.405	-4.755
14.617	8.277	15.383	-5.585
19.657	9.366	20.343	-6.182
24.707	10.176	25.293	-6.596
29.763	10.730	30.237	-6.842
34.823	11.037	35.177	-6.917
39.885	11.093	40.115	-6.809
44.945	10.820	45.055	-6.440
50.000	10.320	50.000	-5.908
55.047	9.635	54.953	-5.255
60.086	8.799	59.914	-4.515
65.114	7.841	64.886	-3.721
70.131	6.784	69.869	-2.896
75.135	5.654	74.865	-2.074
80.127	4.477	79.873	-1.293
85.108	3.294	84.892	-.602
90.077	2.132	89.923	-.064
95.037	1.030	94.963	.234
100.000	0	100.000	0

L.E. radius: 1.590
Slope of radius through L.E.: 0.168

TABLE V

ORDINATES OF THE

NACA 64_1-012 AIRFOIL SECTION

[Stations and ordinates given in percent of airfoil chord]

Upper surface		Lower surface	
Station	Ordinate	Station	Ordinate
0	0	0	0
.5	.978	.5	-.978
.75	1.179	.75	-1.179
1.25	1.490	1.25	-1.490
2.5	2.035	2.5	-2.035
5	2.810	5	-2.810
7.5	3.394	7.5	-3.394
10	3.871	10	-3.871
15	4.620	15	-4.620
20	5.173	20	-5.173
25	5.576	25	-5.576
30	5.844	30	-5.844
35	5.978	35	-5.978
40	5.981	40	-5.981
45	5.798	45	-5.798
50	5.480	50	-5.480
55	5.056	55	-5.056
60	4.548	60	-4.548
65	3.974	65	-3.974
70	3.350	70	-3.350
75	2.695	75	-2.695
80	2.029	80	-2.029
85	1.382	85	-1.382
90	.786	90	-.786
95	.288	95	-.288
100	0	100	0

L.E. radius: 1.040

TABLE VI

ORDINATES OF THE

NACA 64_1A212 AIRFOIL SECTION

[Stations and ordinates given in percent of airfoil chord]

Upper Surface		Lower Surface	
Station	Ordinate	Station	Ordinate
0	0	0	0
.409	1.013	.591	-.901
.648	1.233	.852	-1.075
1.135	1.580	1.365	-1.338
2.365	2.225	2.635	-1.803
4.849	3.145	5.151	-2.423
7.343	3.846	7.657	-2.874
9.842	4.432	10.158	-3.240
14.849	5.358	15.151	-3.796
19.862	6.060	20.138	-4.200
24.880	6.584	25.120	-4.482
29.900	6.956	30.100	-4.660
34.922	7.189	35.078	-4.741
39.946	7.272	40.054	-4.714
44.970	7.177	45.030	-4.549
49.993	6.935	50.007	-4.275
55.015	6.570	54.985	-3.918
60.034	6.103	59.966	-3.499
65.050	5.544	64.950	-3.034
70.064	4.903	69.936	-2.537
75.075	4.197	74.925	-2.037
80.090	3.433	79.910	-1.563
85.088	2.601	84.912	-1.159
90.062	1.751	89.938	-.771
95.032	.888	94.968	-.398
100.000	.025	100.000	-.025

L.E. radius: 0.994
T.E. radius: 0.028
Slope of radius through L.E.: 0.095

TABLE VII

ORDINATES OF THE

NACA 64_1-612 AIRFOIL SECTION

[Stations and ordinates given in percent of airfoil chord]

Upper surface		Lower surface	
Station	Ordinate	Station	Ordinate
0	0	0	0
.260	1.098	.740	-.798
.482	1.358	1.018	-.938
.946	1.780	1.554	-1.138
2.149	2.563	2.851	-1.447
4.609	3.731	5.391	-1.835
7.096	4.642	7.904	-2.098
9.596	5.401	10.404	-2.299
14.619	6.623	15.381	-2.585
19.658	7.550	20.341	-2.774
24.708	8.253	25.292	-2.883
29.764	8.755	30.236	-2.923
34.823	9.065	35.177	-2.885
39.884	9.193	40.116	-2.767
44.945	9.083	45.055	-2.513
50.000	8.789	50.000	-2.171
55.048	8.341	54.952	-1.771
60.088	7.760	59.912	-1.334
65.117	7.062	64.883	-.882
70.135	6.263	69.865	-.431
75.141	5.376	74.859	-.006
80.134	4.413	79.866	.363
85.114	3.396	84.886	.642
90.082	2.333	89.918	.769
95.040	1.233	94.960	.663
100.000	0	100.000	0

L.E. radius: 1.040
Slope of radius through L.E.: 0.2527

TABLE VIII

ORDINATES OF THE

NACA 63_2-415 AIRFOIL SECTION

[Stations and ordinates given in percent of airfoil chord]

Upper surface		Lower surface	
Station	Ordinate	Station	Ordinate
0	0	0	0
.300	1.287	.700	-1.087
.525	1.585	.975	-1.305
.991	2.074	1.509	-1.646
2.198	2.964	2.802	-2.220
4.660	4.264	5.340	-3.000
7.147	5.261	7.853	-3.565
9.647	6.077	10.353	-4.009
14.669	7.348	15.331	-4.656
19.705	8.279	20.295	-5.095
24.750	8.941	25.250	-5.361
29.800	9.362	30.200	-5.474
34.852	9.559	35.148	-5.439
39.905	9.527	40.095	-5.243
44.955	9.289	45.045	-4.909
50.000	8.871	50.000	-4.459
55.039	8.298	54.961	-3.918
60.070	7.595	59.930	-3.311
65.093	6.780	64.907	-2.660
70.106	5.877	69.894	-1.989
75.109	4.907	74.891	-1.327
80.102	3.900	79.898	-.716
85.085	2.885	84.915	-.193
90.059	1.884	89.941	.184
95.028	.931	94.972	.333
100.000	0	100.000	0

L.E. radius: 1.594
Slope of radius through L.E.: 0.168

TABLE IX

ORDINATES OF THE

NACA 65_2-415 AIRFOIL SECTION

[Stations and ordinates given in percent of airfoil chord]

Upper surface		Lower surface	
Station	Ordinate	Station	Ordinate
0	0	0	0
.313	1.208	.687	-1.008
.542	1.480	.958	-1.200
1.016	1.900	1.484	-1.472
2.231	2.680	2.769	-1.936
4.697	3.863	5.303	-2.599
7.184	4.794	7.816	-3.098
9.682	5.578	10.318	-3.510
14.697	6.842	15.303	-4.150
19.726	7.809	20.274	-4.625
24.764	8.550	25.236	-4.970
29.807	9.093	30.193	-5.205
34.854	9.455	35.146	-5.335
39.903	9.639	40.097	-5.355
44.953	9.617	45.047	-5.237
50.000	9.374	50.000	-4.982
55.043	8.910	54.957	-4.530
60.079	8.260	59.921	-3.976
65.106	7.462	64.894	-3.342
70.124	6.542	69.876	-2.654
75.131	5.532	74.869	-1.952
80.126	4.447	79.874	-1.263
85.109	3.320	84.891	-.628
90.080	2.175	89.920	-.107
95.040	1.058	94.960	.206
100.000	0	100.000	0

L.E. radius: 1.505
Slope of radius through L.E.: 0.168

TABLE X

ORDINATES OF THE

NACA 66_2-415 AIRFOIL SECTION

[Stations and ordinates given in percent of airfoil chord]

Upper surface		Lower surface	
Station	Ordinate	Station	Ordinate
0	0	0	0
.314	1.206	.686	-1.006
.544	1.467	.956	-1.187
1.019	1.873	1.481	-1.445
2.241	2.592	2.759	-1.848
4.711	3.718	5.289	-2.454
7.199	4.617	7.801	-2.921
9.696	5.381	10.304	-3.313
14.709	6.624	15.291	-3.932
19.736	7.581	20.264	-4.397
24.771	8.329	25.229	-4.749
29.812	8.897	30.188	-5.009
34.857	9.309	35.143	-5.189
39.904	9.571	40.096	-5.287
44.952	9.685	45.048	-5.305
50.000	9.656	50.000	-5.244
55.046	9.473	54.954	-5.093
60.090	9.100	59.910	-4.816
65.126	8.431	64.874	-4.311
70.150	7.518	69.850	-3.630
75.162	6.419	74.838	-2.839
80.159	5.187	79.841	-2.003
85.139	3.872	84.861	-1.180
90.104	2.519	89.896	-.451
95.053	1.196	94.947	.068
100.000	0	100.000	0

L.E. radius: 1.435
Slope of radius through L.E.: 0.168

TABLE XI

ORDINATES OF THE

NACA 0012 AIRFOIL SECTION

[Stations and ordinates given in percent of airfoil chord]

Upper surface		Lower surface	
Station	Ordinate	Station	Ordinate
0	0	0	0
.5	-----	.5	-----
1.25	1.894	1.25	-1.894
2.5	2.615	2.5	-2.615
5	3.555	5	-3.555
7.5	4.200	7.5	-4.200
10	4.683	10	-4.683
15	5.345	15	-5.345
20	5.738	20	-5.738
25	5.941	25	-5.941
30	6.002	30	-6.002
40	5.803	40	-5.803
50	5.294	50	-5.294
60	4.565	60	-4.565
70	3.664	70	-3.664
80	2.623	80	-2.623
90	1.448	90	-1.448
95	.807	95	-.807
100	.126	100	-.126

L.E. radius: 1.58

TABLE XII

ORDINATES OF THE

NACA 4412 AIRFOIL SECTION

[Stations and ordinates given in percent of airfoil chord]

Upper surface		Lower surface	
Station	Ordinate	Station	Ordinate
0	0	0	0
1.25	2.44	1.25	-1.43
2.5	3.39	2.5	-1.95
5	4.73	5	-2.49
7.5	5.76	7.5	-2.74
10	6.59	10	-2.82
15	7.89	15	-2.88
20	8.80	20	-2.74
25	9.41	25	-2.50
30	9.76	30	-2.26
40	9.80	40	-1.80
50	9.19	50	-1.40
60	8.14	60	-1.00
70	6.69	70	-.65
80	4.89	80	-.39
90	2.71	90	-.22
95	1.47	95	-.16
100	(.13)	100	(-.13)
100	-----	100	0

L.E. radius: 1.58
Slope of radius through L.E.: 0.20

TABLE XIII

ORDINATES OF THE

NACA 4415 AIRFOIL SECTION

[Stations and ordinates given in percent of airfoil chord]

Upper surface		Lower surface	
Station	Ordinate	Station	Ordinate
0	-----	0	0
1.25	3.07	1.25	-1.79
2.5	4.17	2.5	-2.48
5	5.74	5	-3.27
7.5	6.91	7.5	-3.71
10	7.84	10	-3.98
15	9.27	15	-4.18
20	10.25	20	-4.15
25	10.92	25	-3.98
30	11.25	30	-3.75
40	11.25	40	-3.25
50	10.53	50	-2.72
60	9.30	60	-2.14
70	7.63	70	-1.55
80	5.55	80	-1.03
90	3.08	90	-.57
95	1.67	95	-.36
100	(.16)	100	(-.16)
100	-----	100	0

L.E. radius: 2.48
Slope of radius through L.E.: 0.20

TABLE XIV

ORDINATES OF THE

NACA 23012 AIRFOIL SECTION

[Stations and ordinates given in percent of airfoil chord]

Upper surface		Lower surface	
Station	Ordinate	Station	Ordinate
0	-----	0	0
1.25	2.67	1.25	-1.23
2.5	3.61	2.5	-1.71
5	4.91	5	-2.26
7.5	5.80	7.5	-2.61
10	6.43	10	-2.92
15	7.19	15	-3.50
20	7.50	20	-3.97
25	7.60	25	-4.28
30	7.55	30	-4.46
40	7.14	40	-4.48
50	6.41	50	-4.17
60	5.47	60	-3.67
70	4.36	70	-3.00
80	3.08	80	-2.16
90	1.68	90	-1.23
95	.92	95	-.70
100	(.13)	100	(-.13)
100	-----	100	0

L.E. radius: 1.58
Slope of radius through L.E.: 0.305

TABLE XV

ORDINATES OF THE

NACA 23015 AIRFOIL SECTION

[Stations and ordinates given in percent of airfoil chord]

Upper surface		Lower surface	
Station	Ordinate	Station	Ordinate
0	-----	0	0
1.25	3.34	1.25	-1.54
2.5	4.44	2.5	-2.25
5	5.89	5	-3.04
7.5	6.90	7.5	-3.61
10	7.64	10	-4.09
15	8.52	15	-4.84
20	8.92	20	-5.41
25	9.08	25	-5.78
30	9.05	30	-5.96
40	8.59	40	-5.92
50	7.74	50	-5.50
60	6.61	60	-4.81
70	5.25	70	-3.91
80	3.73	80	-2.83
90	2.04	90	-1.59
95	1.12	95	-.90
100	(.16)	100	(-.16)
100	-----	100	0

L.E. radius: 2.48
Slope of radius through L.E.: 0.305

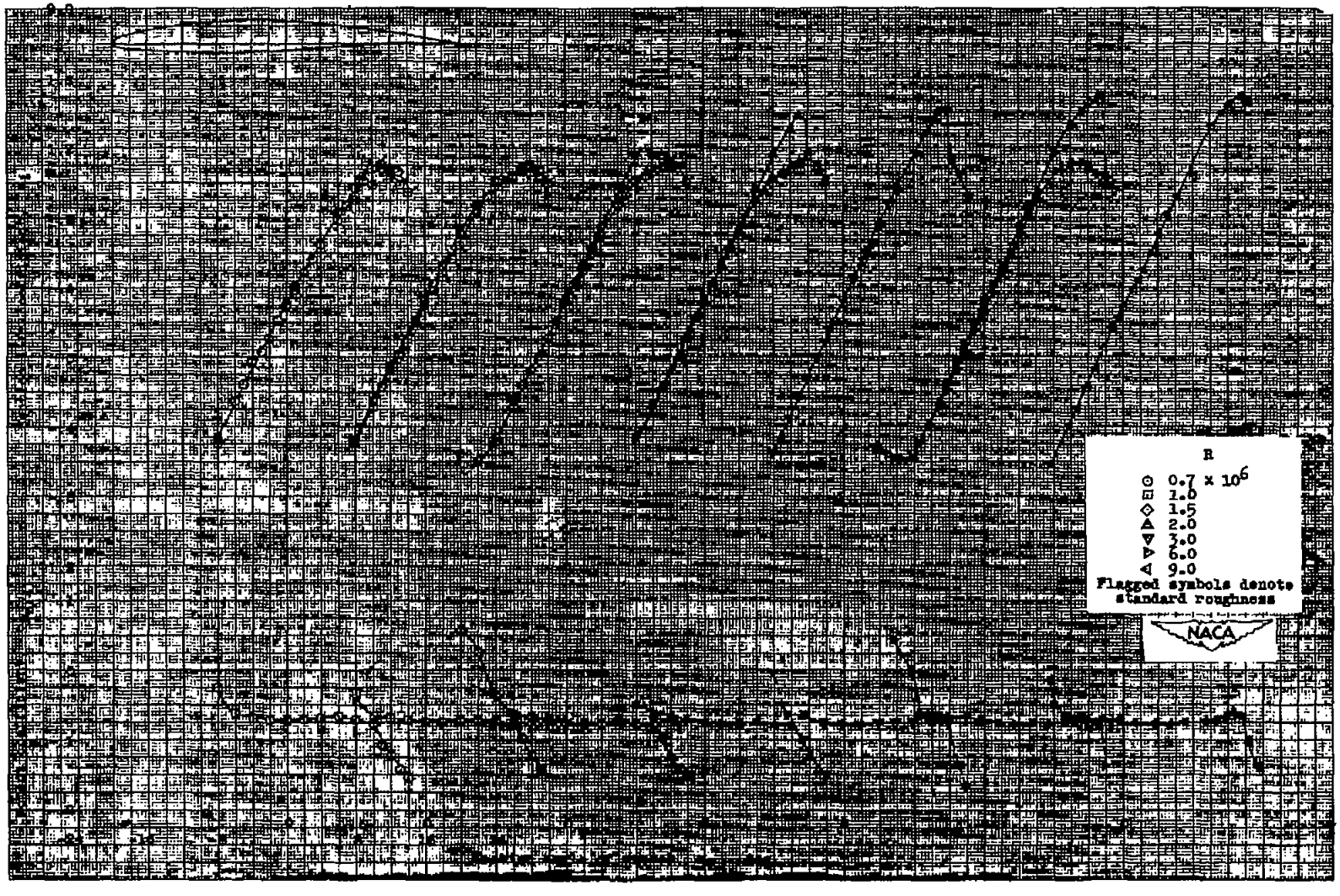

(a) Section lift and pitching-moment characteristics of the plain airfoil section.

Figure 1.- Aerodynamic characteristics of the NACA 64-409 airfoil section, 24-inch chord.

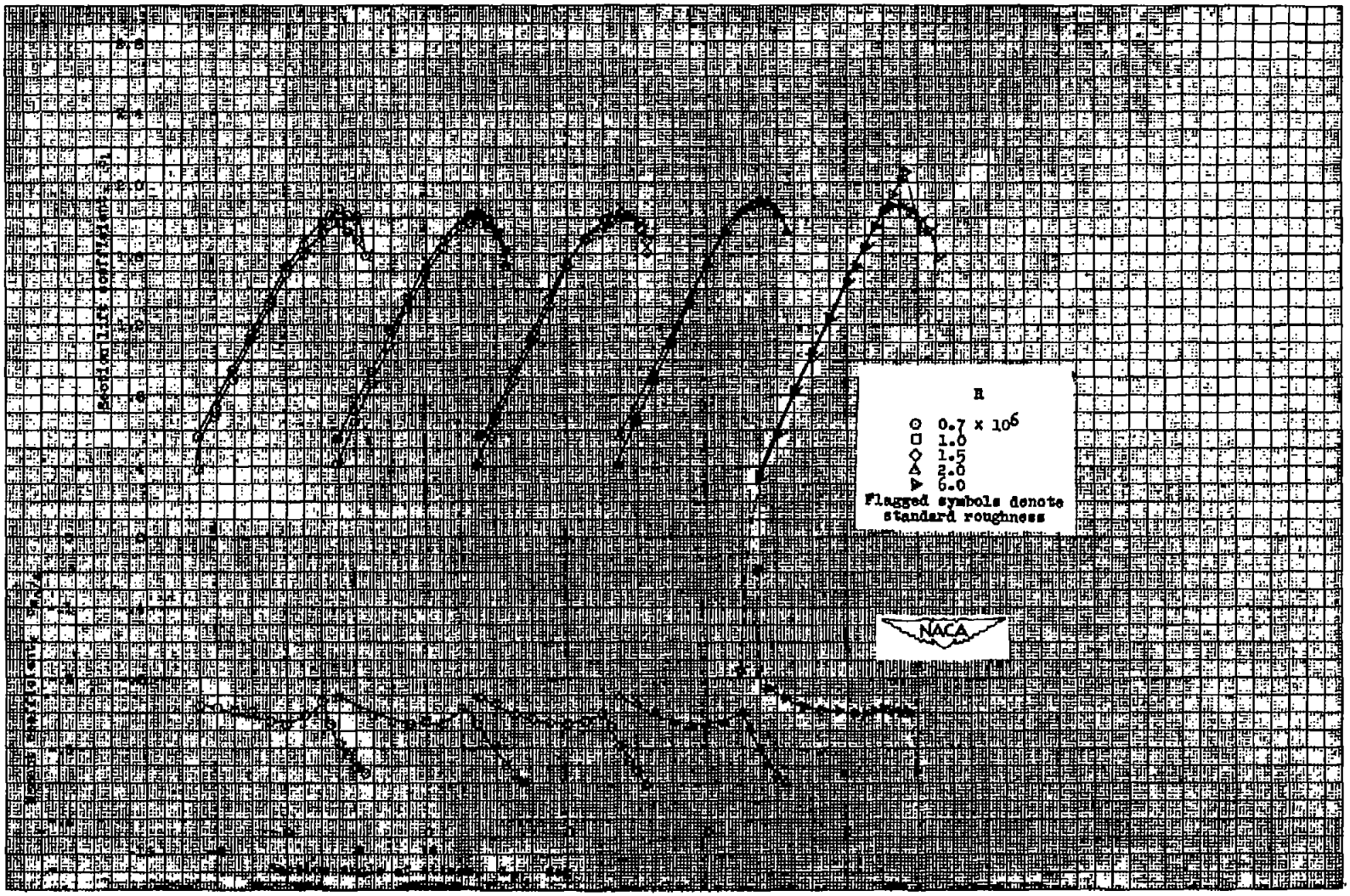

(b) Section lift and pitching-moment characteristics of the NACA 64-409 airfoil section with a 0.20c simulated split flap deflected 60°.

Figure 1.- Continued.

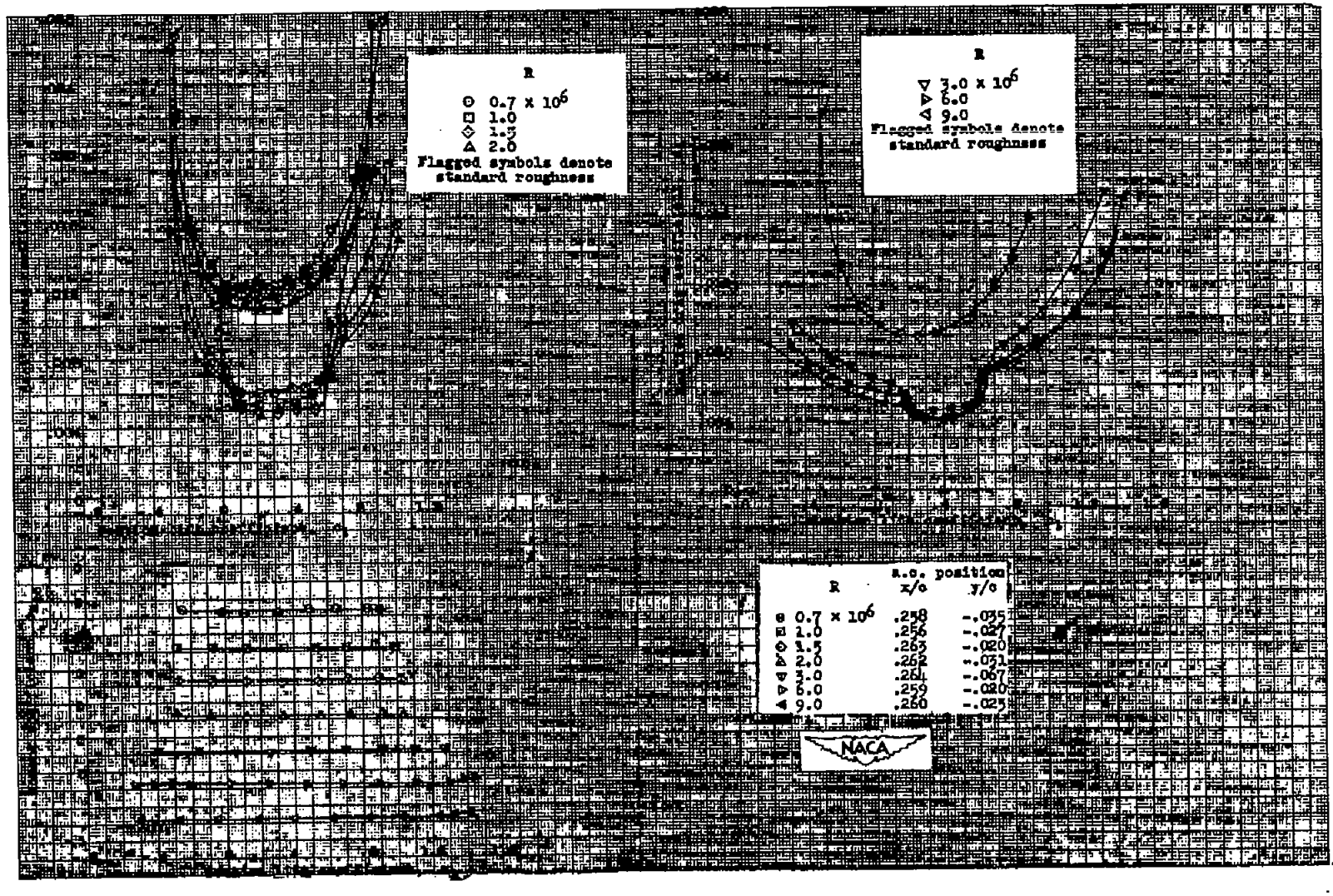

(c) Section drag characteristics and section pitching-moment characteristics about the aerodynamic center of the plain NACA 64-409 airfoil section.

Figure 1.- Concluded.

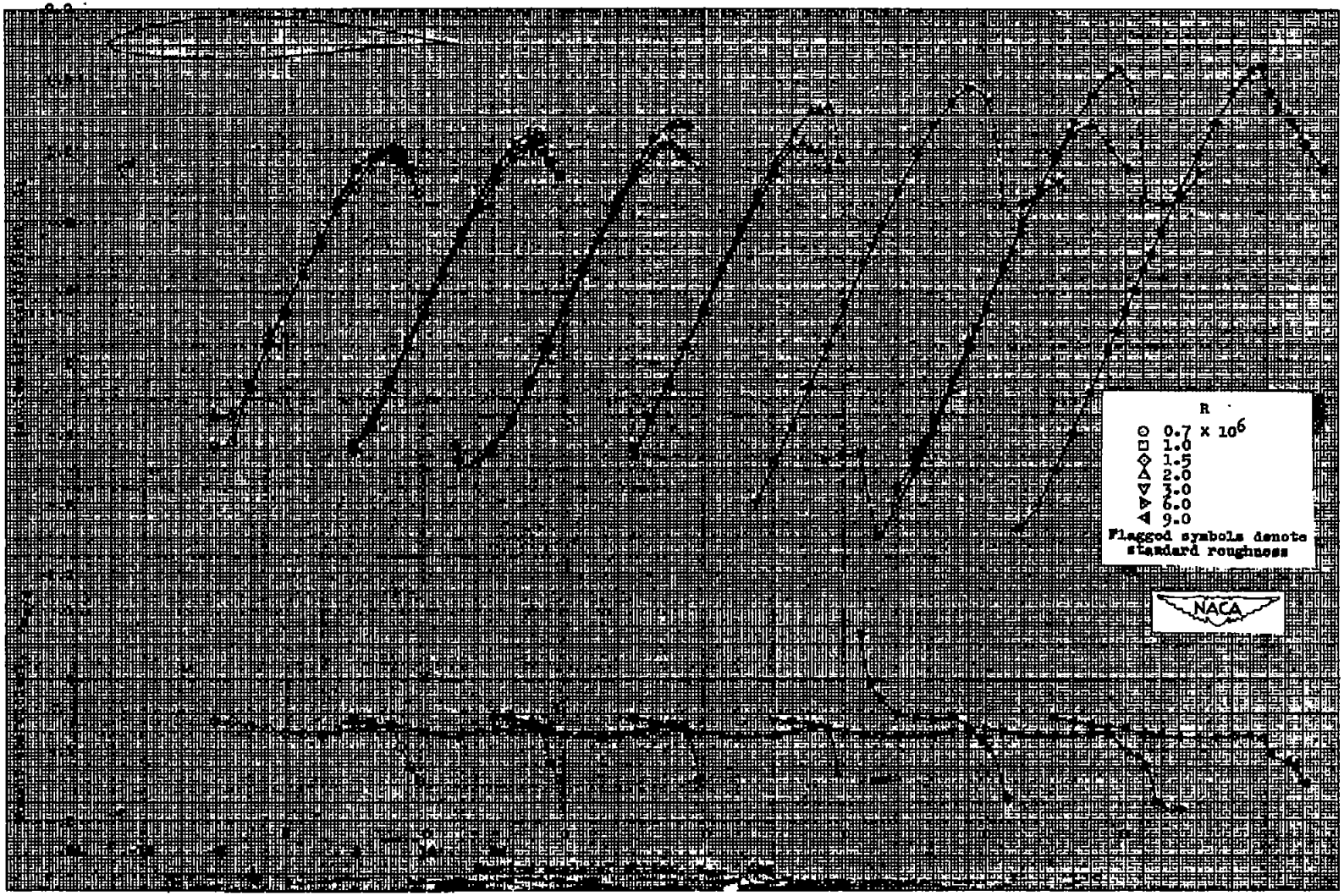

(a) Section lift and pitching-moment characteristics of the plain airfoil section.

Figure 2.- Aerodynamic characteristics of the NACA 64_1-412 airfoil section, 24-inch chord.

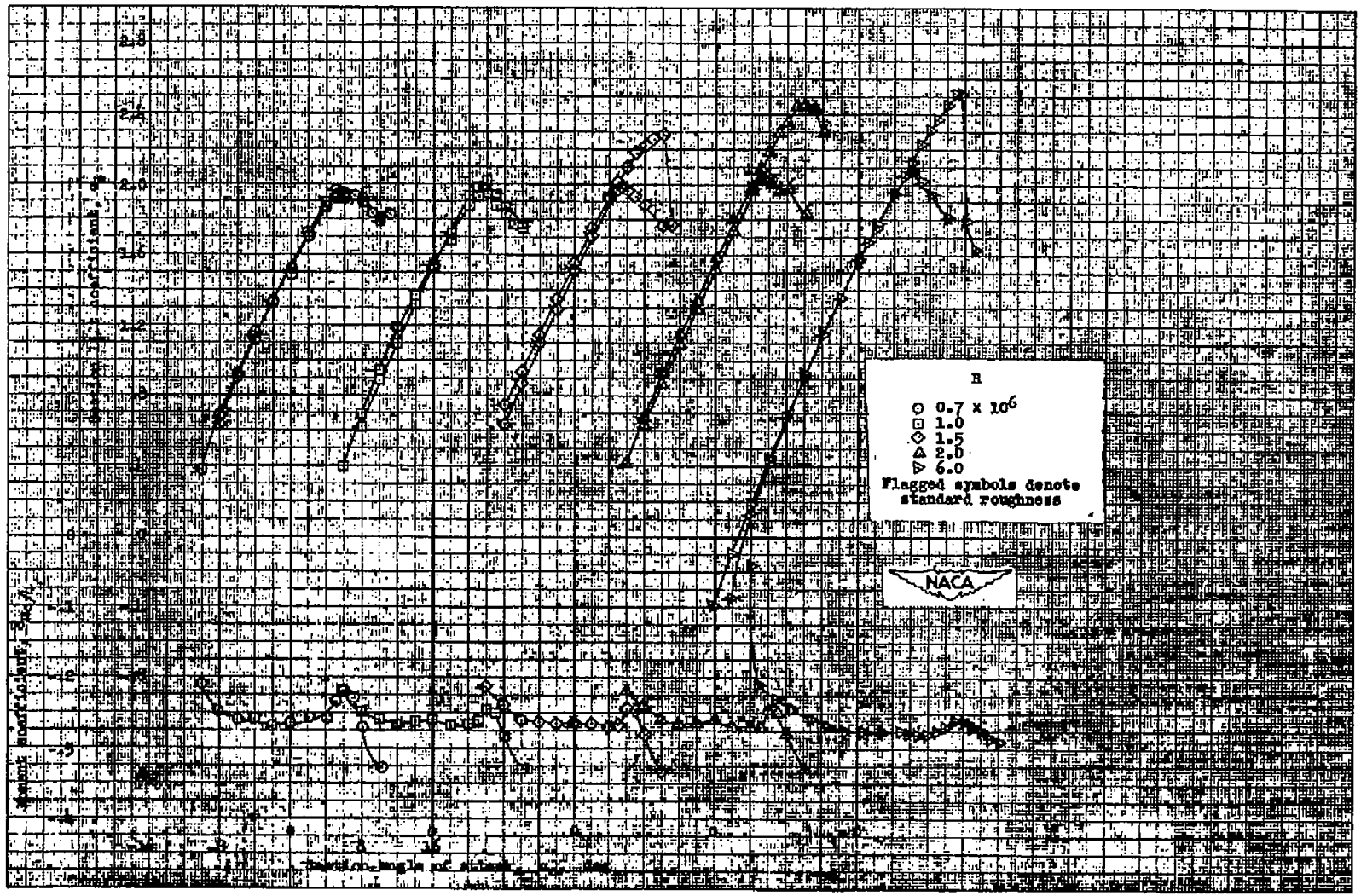

(b) Section lift and pitching-moment characteristics of the NACA 64_1-412 airfoil section with a 0.20c simulated split flap deflected 60°.

Figure 2.- Continued.

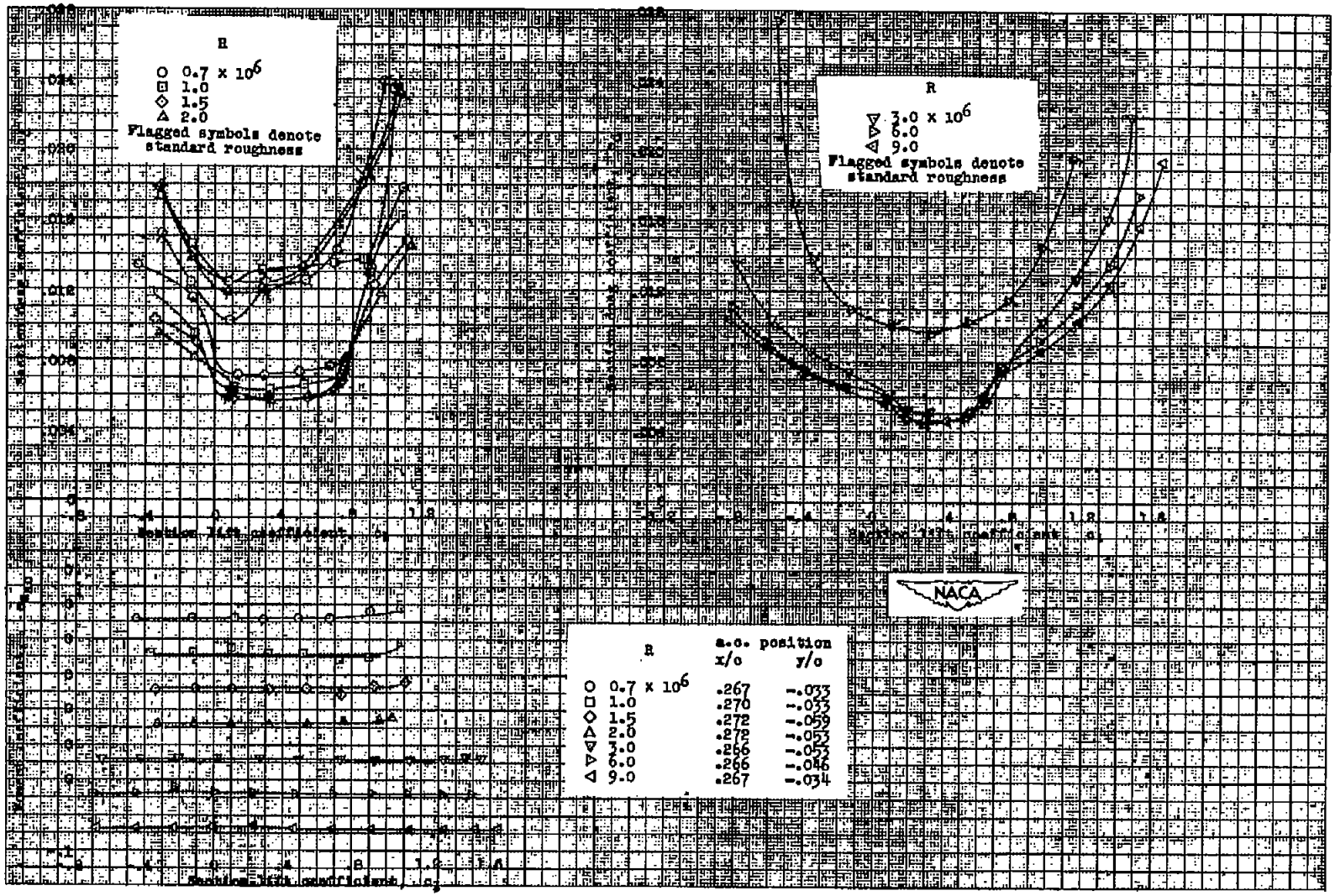

(c) Section drag characteristics and section pitching-moment characteristics about the aerodynamic center of the plain NACA 64$_1$-412 airfoil section.

Figure 2.- Concluded.

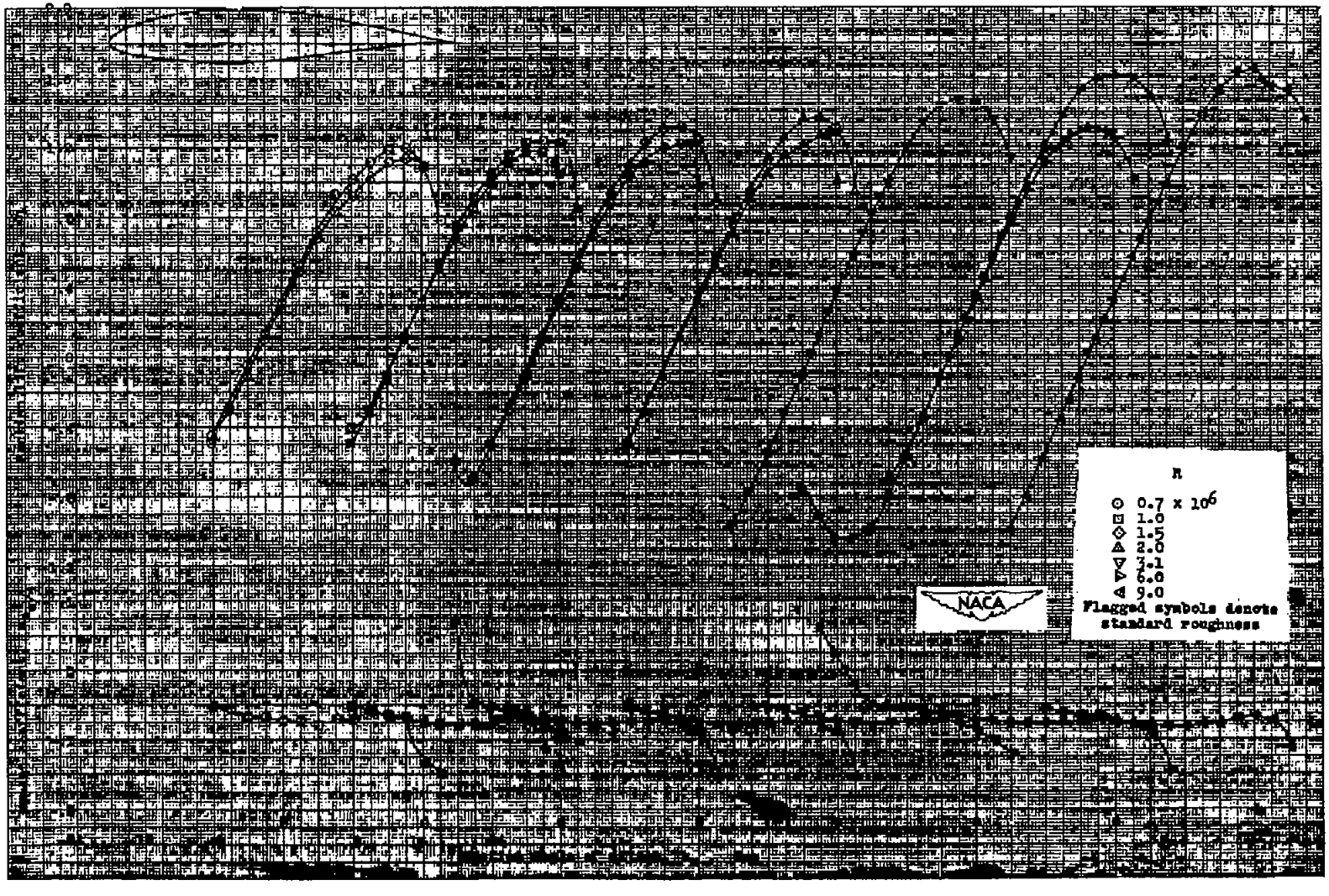

(a) Section lift and pitching-moment characteristics of the plain airfoil section.

Figure 3.– Aerodynamic characteristics of the NACA 64_2–415 airfoil section, 24–inch chord.

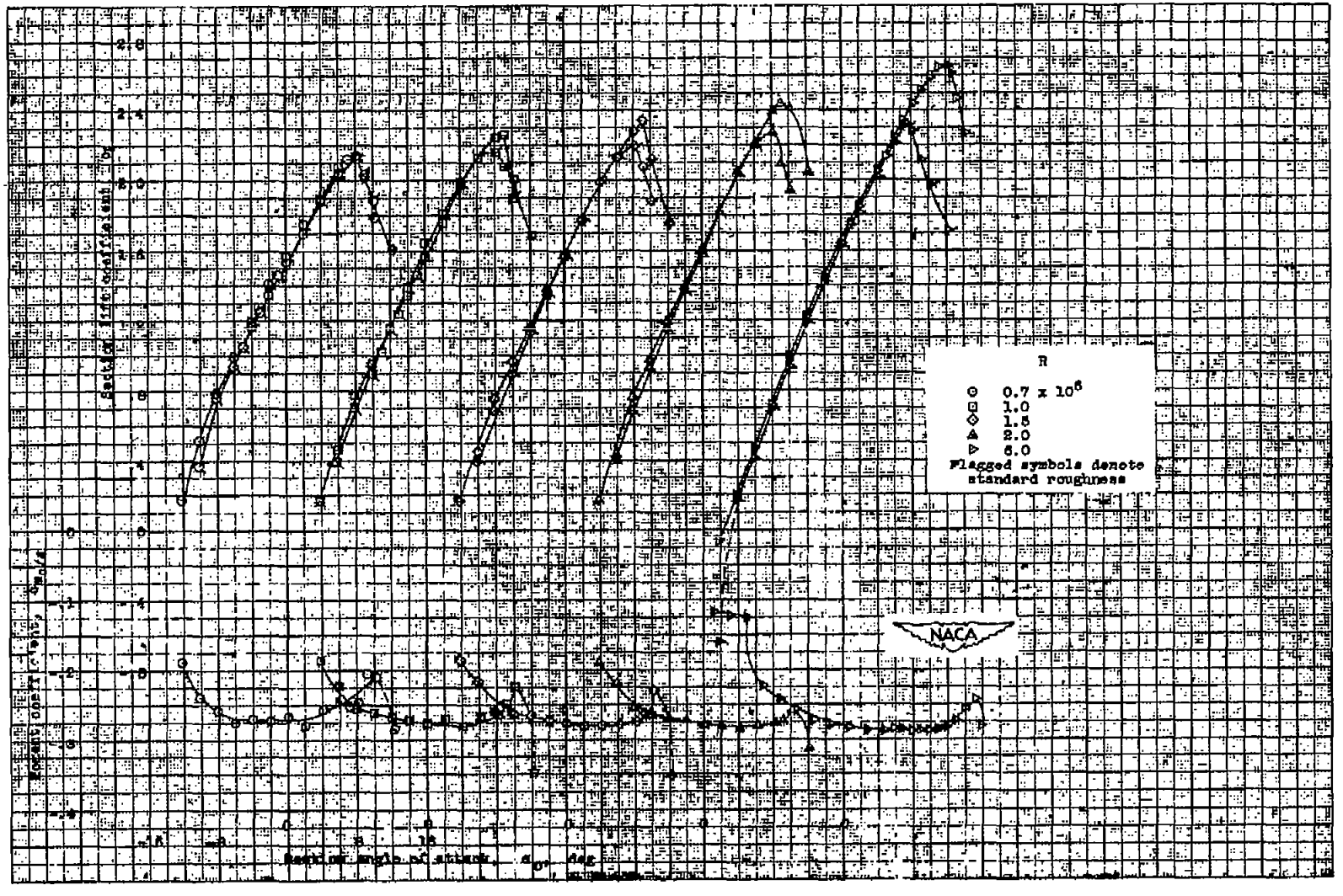

(b) Section lift and pitching-moment characteristics of the NACA 64_2-415 airfoil section with a 0.20c simulated split flap deflected 60°.

Figure 3.- Continued.

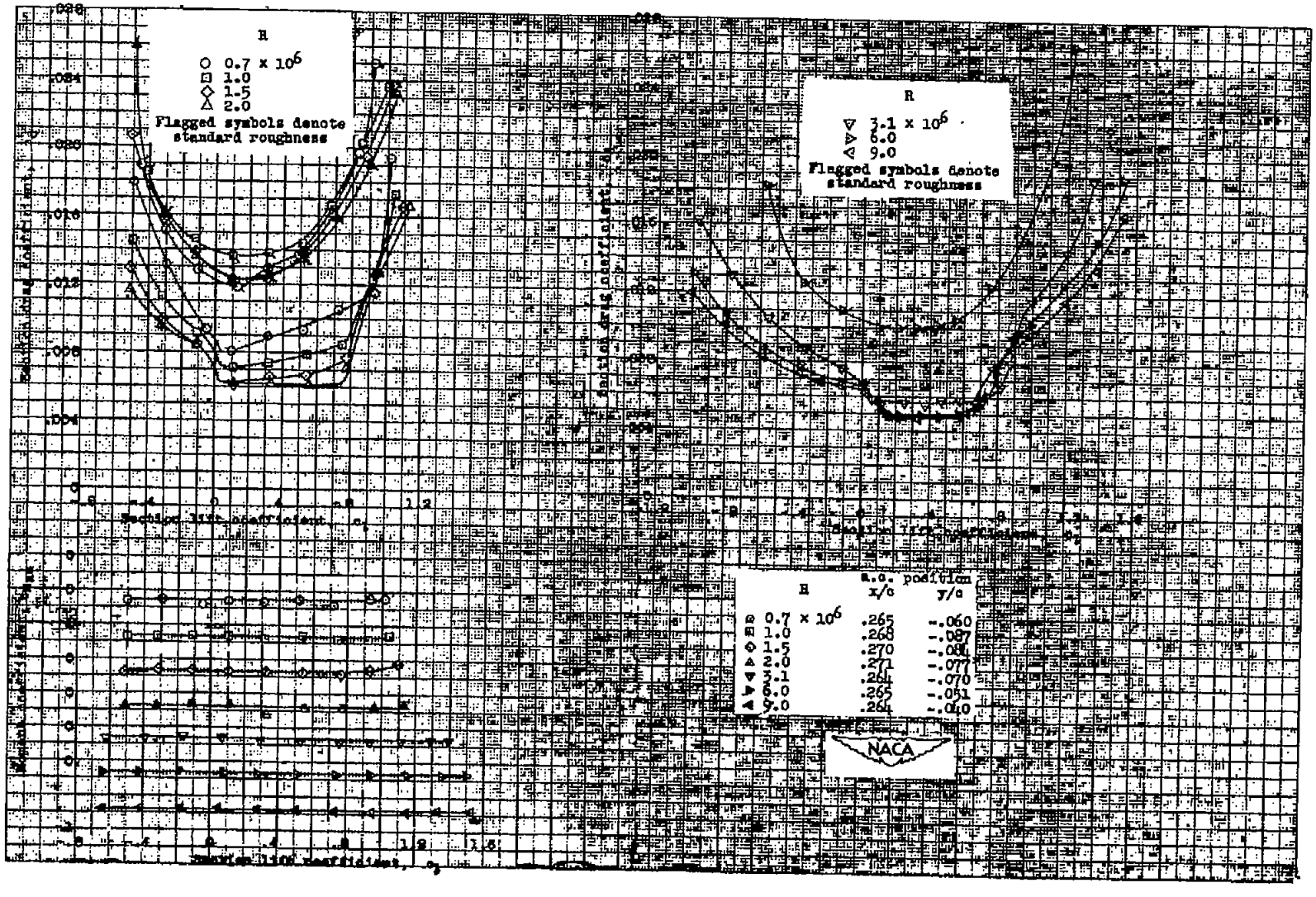

(c) Section drag characteristics and section pitching-moment characteristics about the aerodynamic center of the plain NACA 64$_2$-415 airfoil section.

Figure 3.- Concluded.

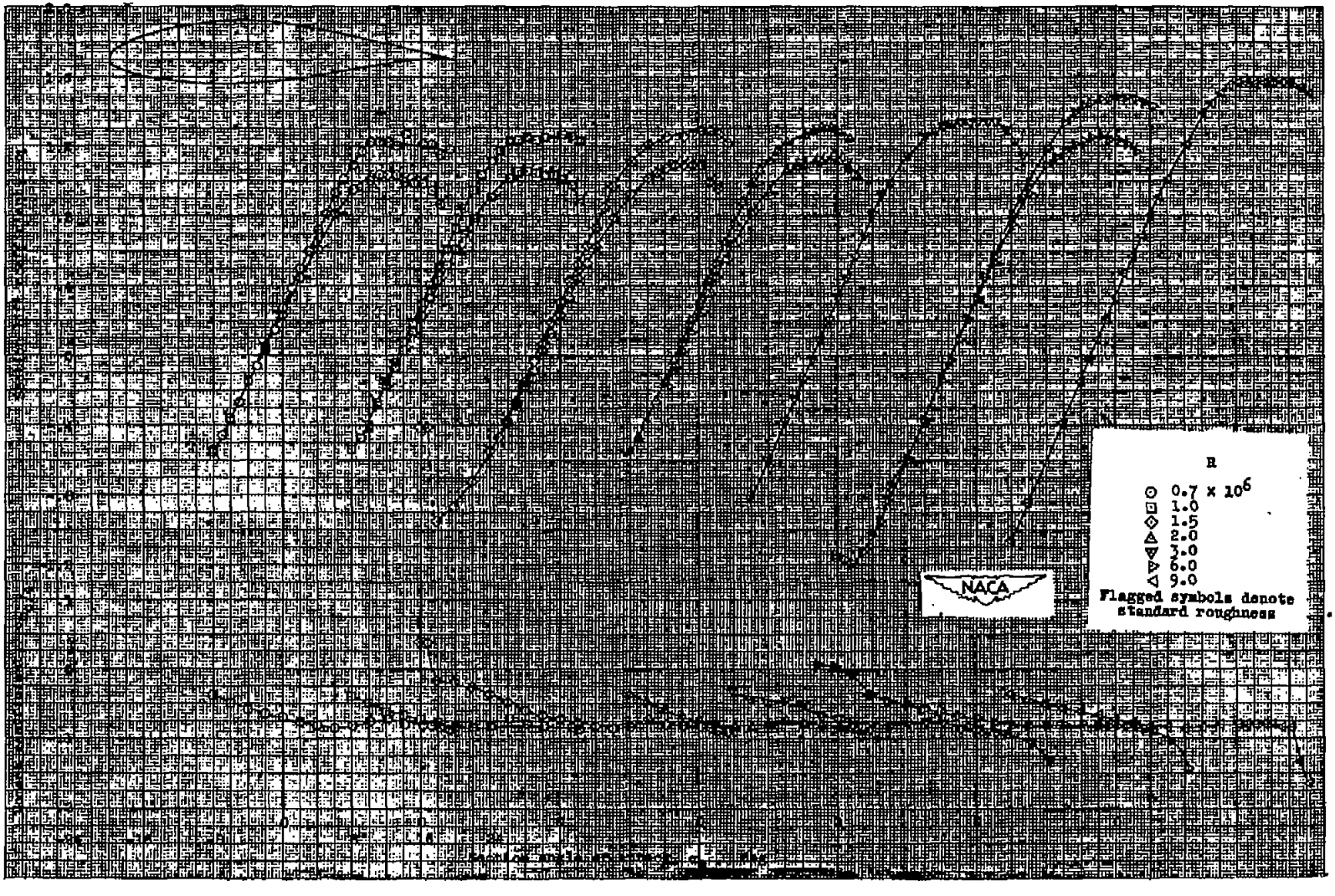

(a) Section lift and pitching-moment characteristics of the plain airfoil section.

Figure 4.- Aerodynamic characteristics of the NACA 64_3-418 airfoil section, 24-inch chord.

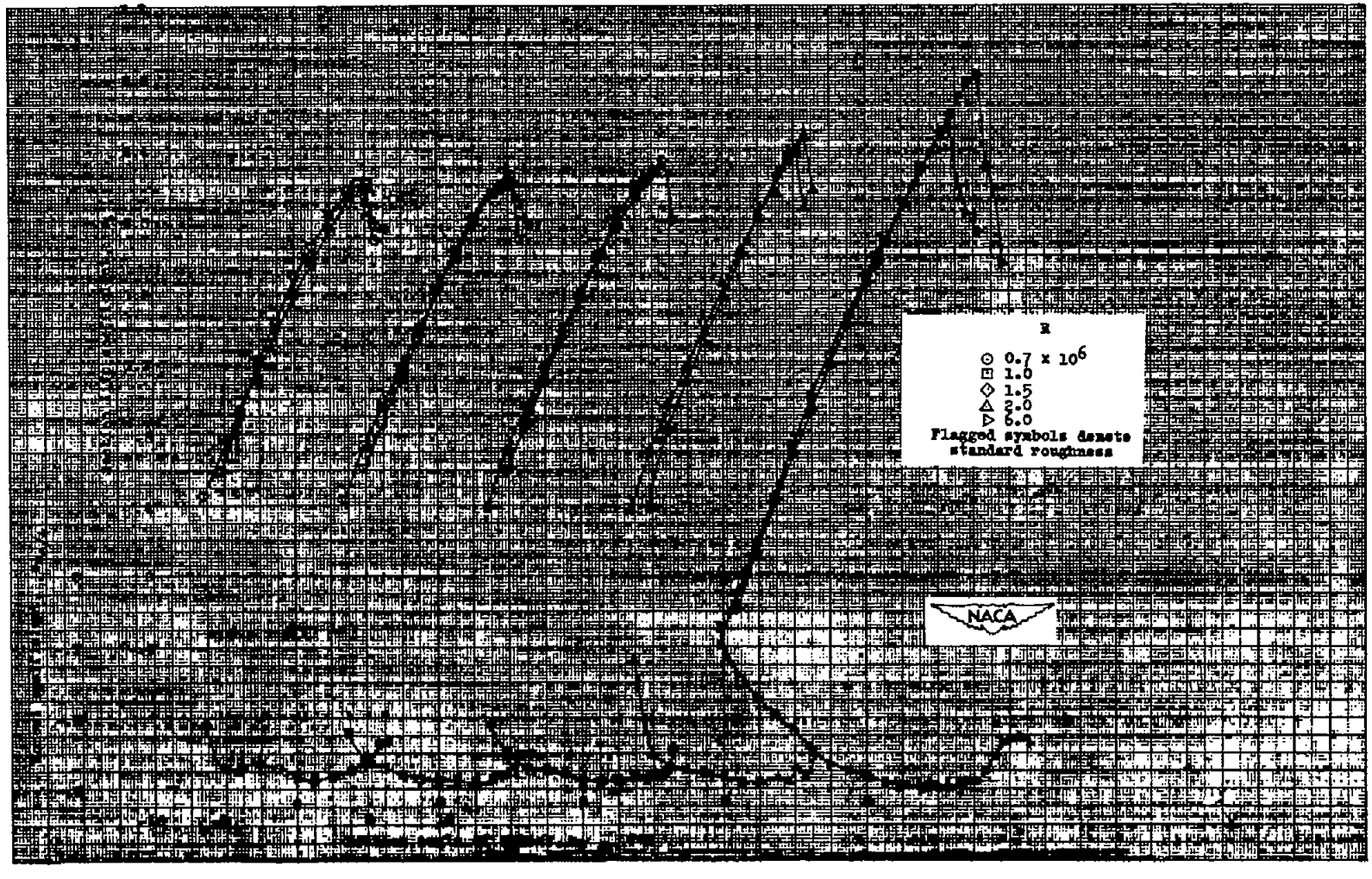

(b) Section lift and pitching-moment characteristics of the NACA 64_3-418 airfoil section with a 0.20c simulated split flap deflected 60°.

Figure 4.- Continued.

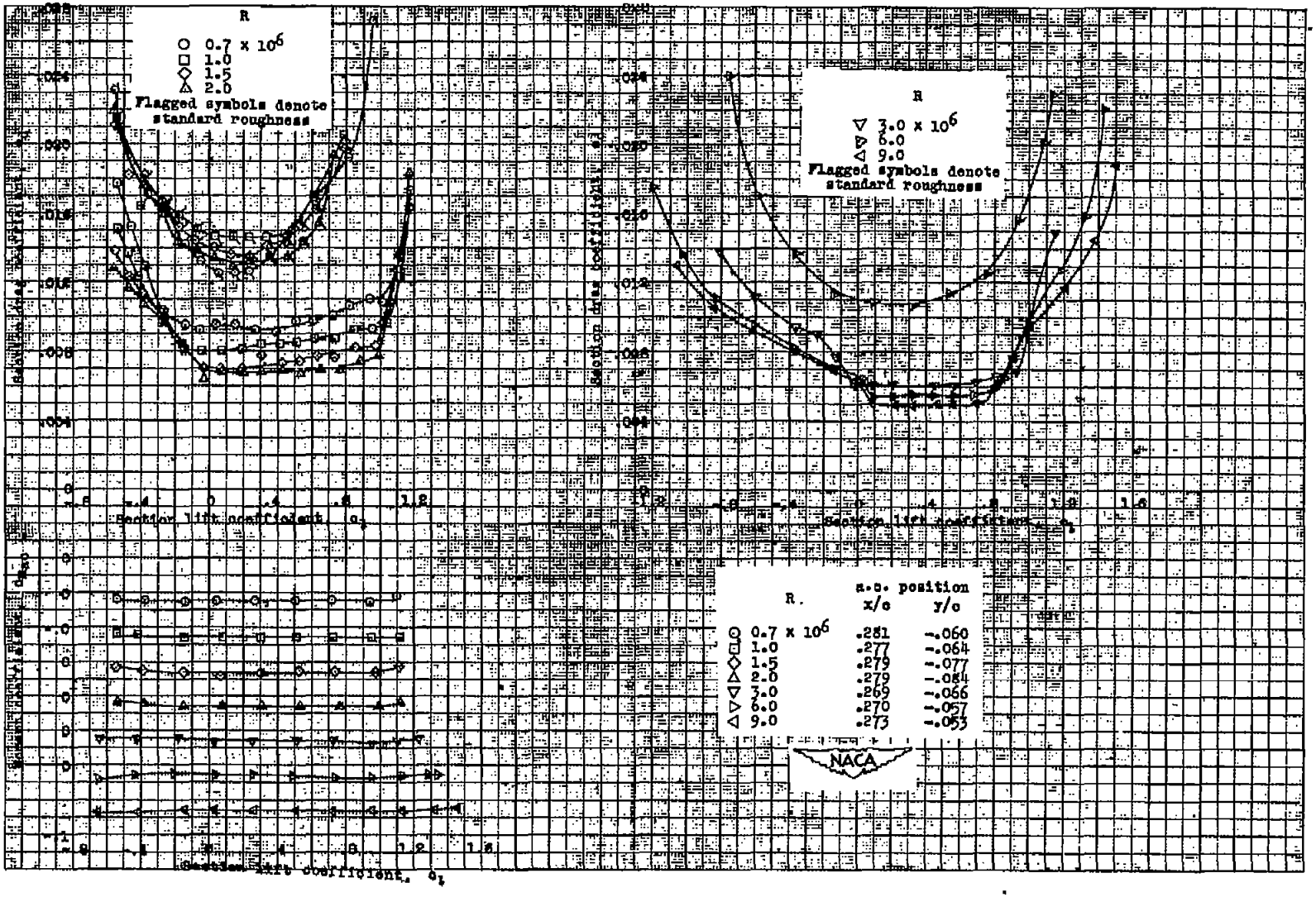

(c) Section drag characteristics and section pitching-moment characteristics about the aerodynamic center of the plain NACA 64_3-418 airfoil section.

Figure 4.– Concluded.

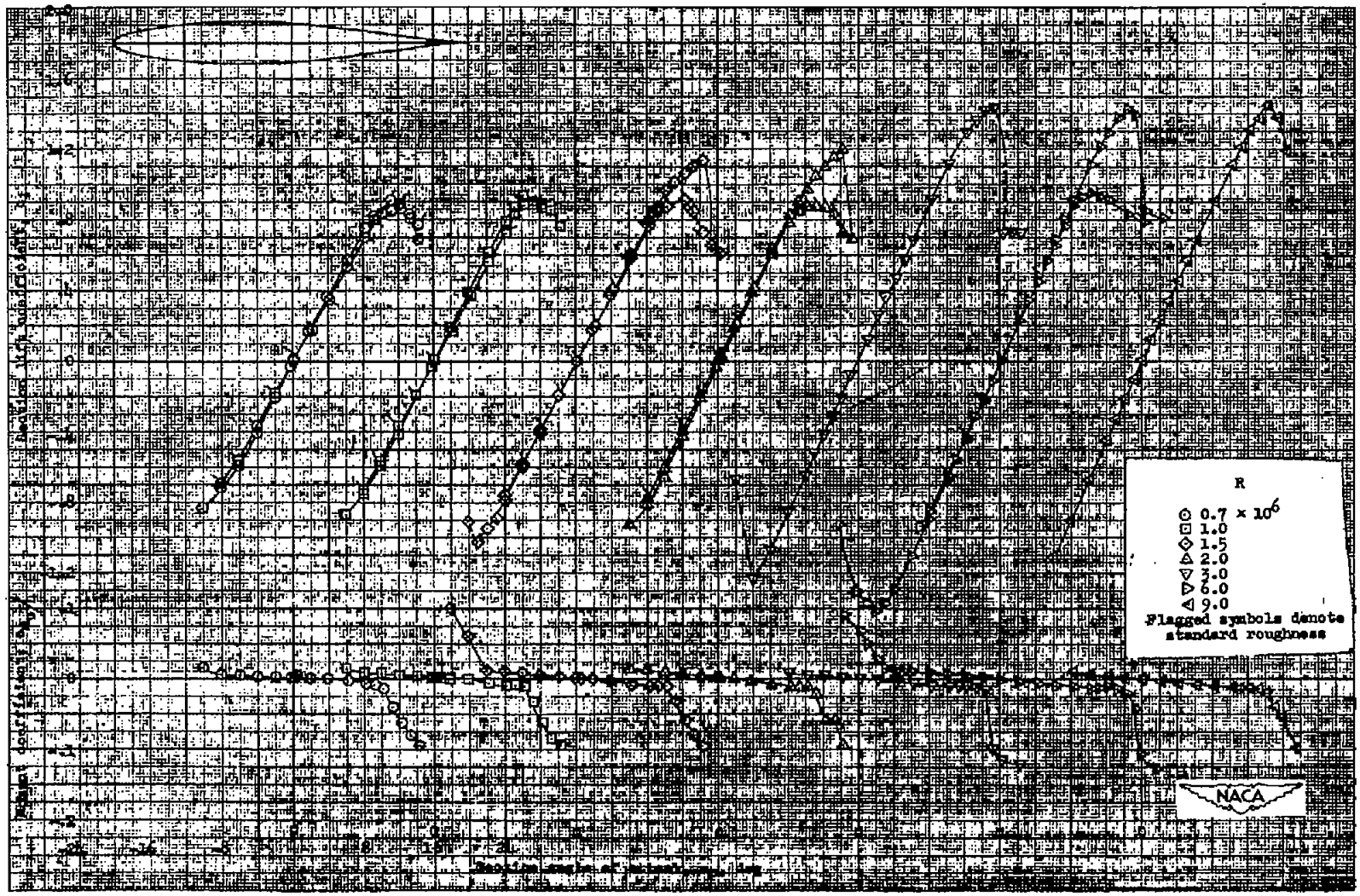

(a) Section lift and pitching-moment characteristics of the plain airfoil section.

Figure 5.– Aerodynamic characteristics of the NACA 64_1-012 airfoil section, .24-inch chord.

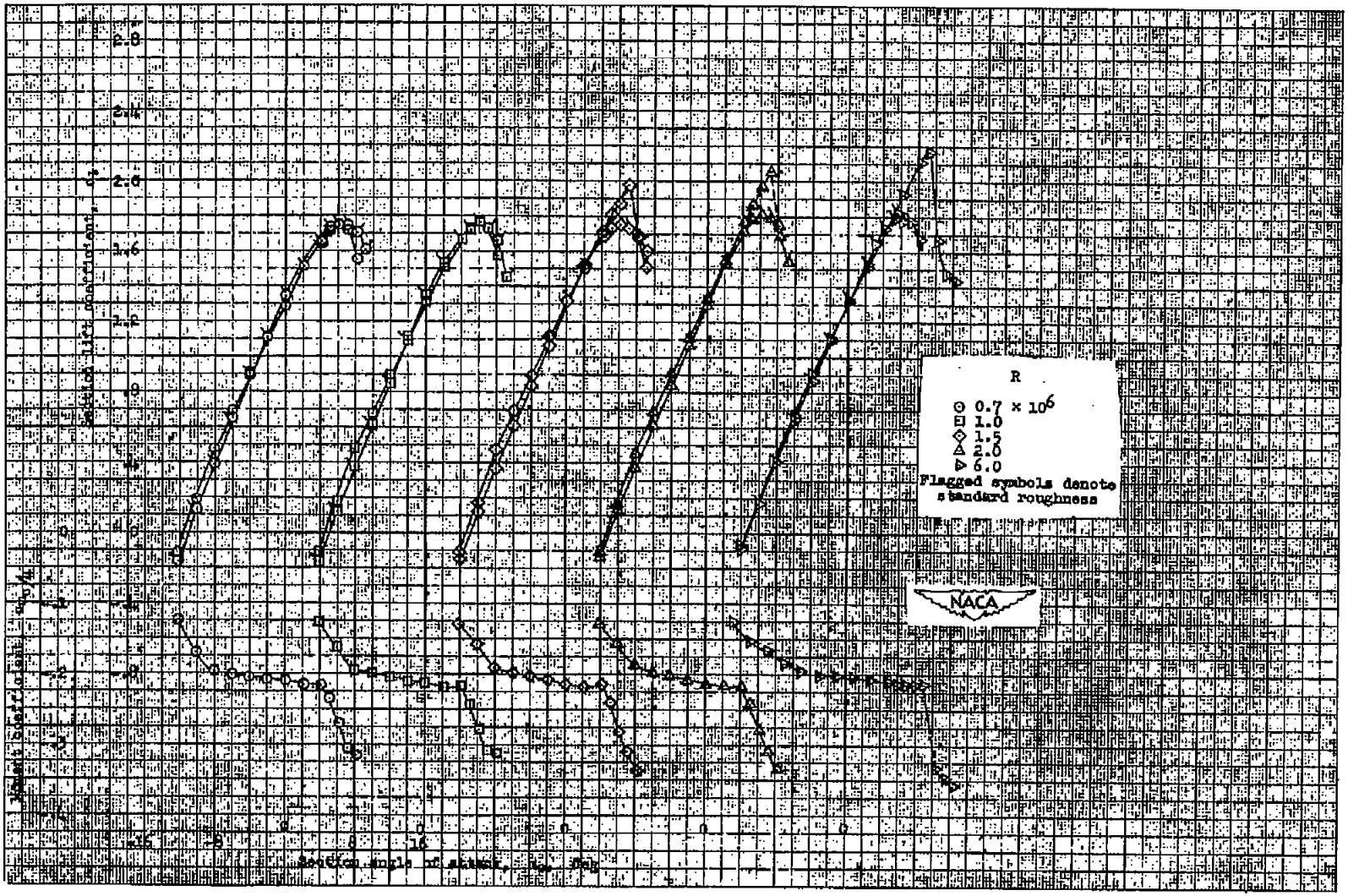

(b) Section lift and pitching-moment characteristics of the NACA 64_1-012 airfoil section with a 0.20c simulated split flap deflected 60°.

Figure 5.- Continued.

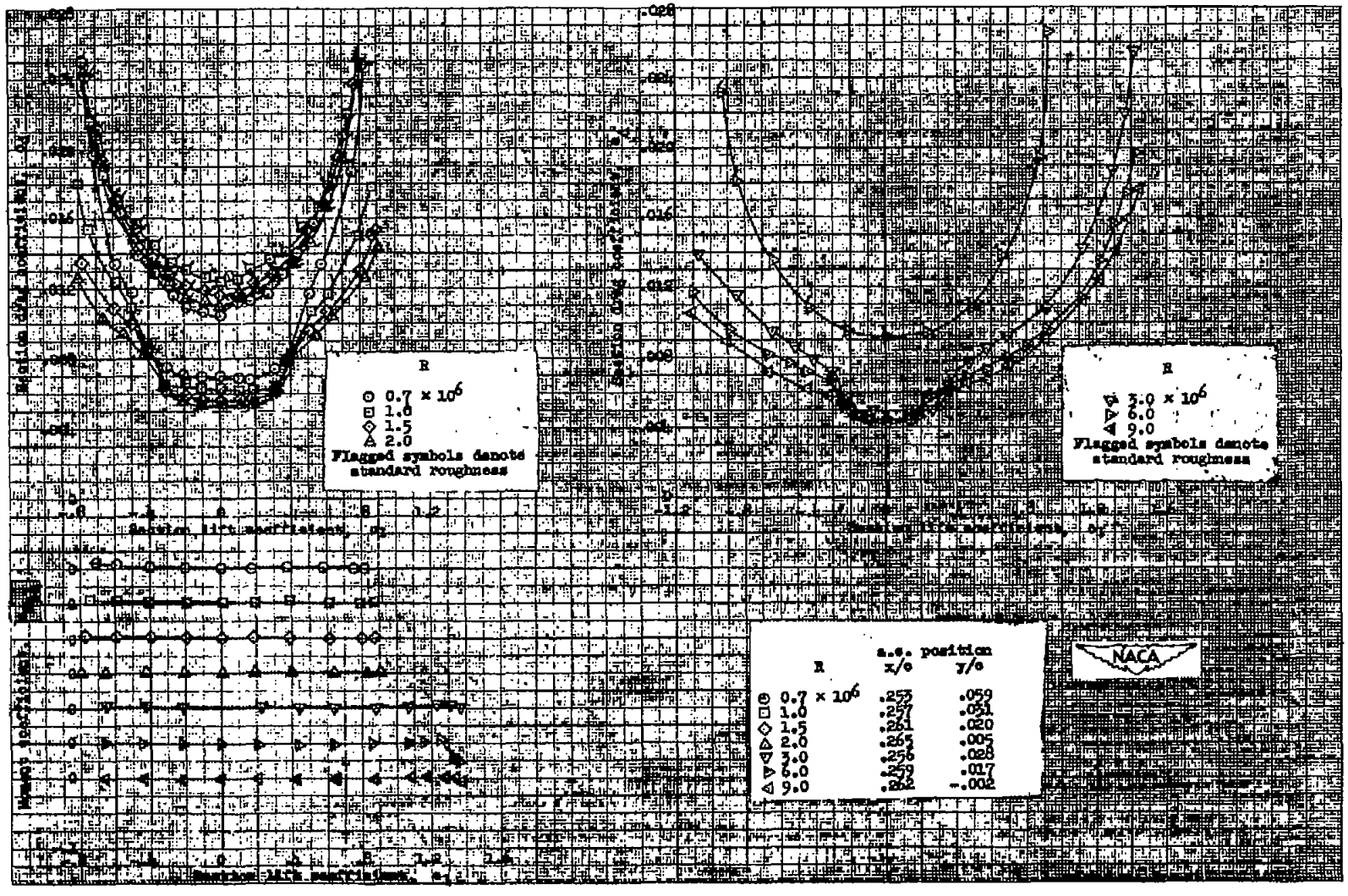

(c) Section drag characteristics and section pitching-moment characteristics about the aerodynamic center of the plain NACA 64_1-012 airfoil section.

Figure 5.- Concluded.

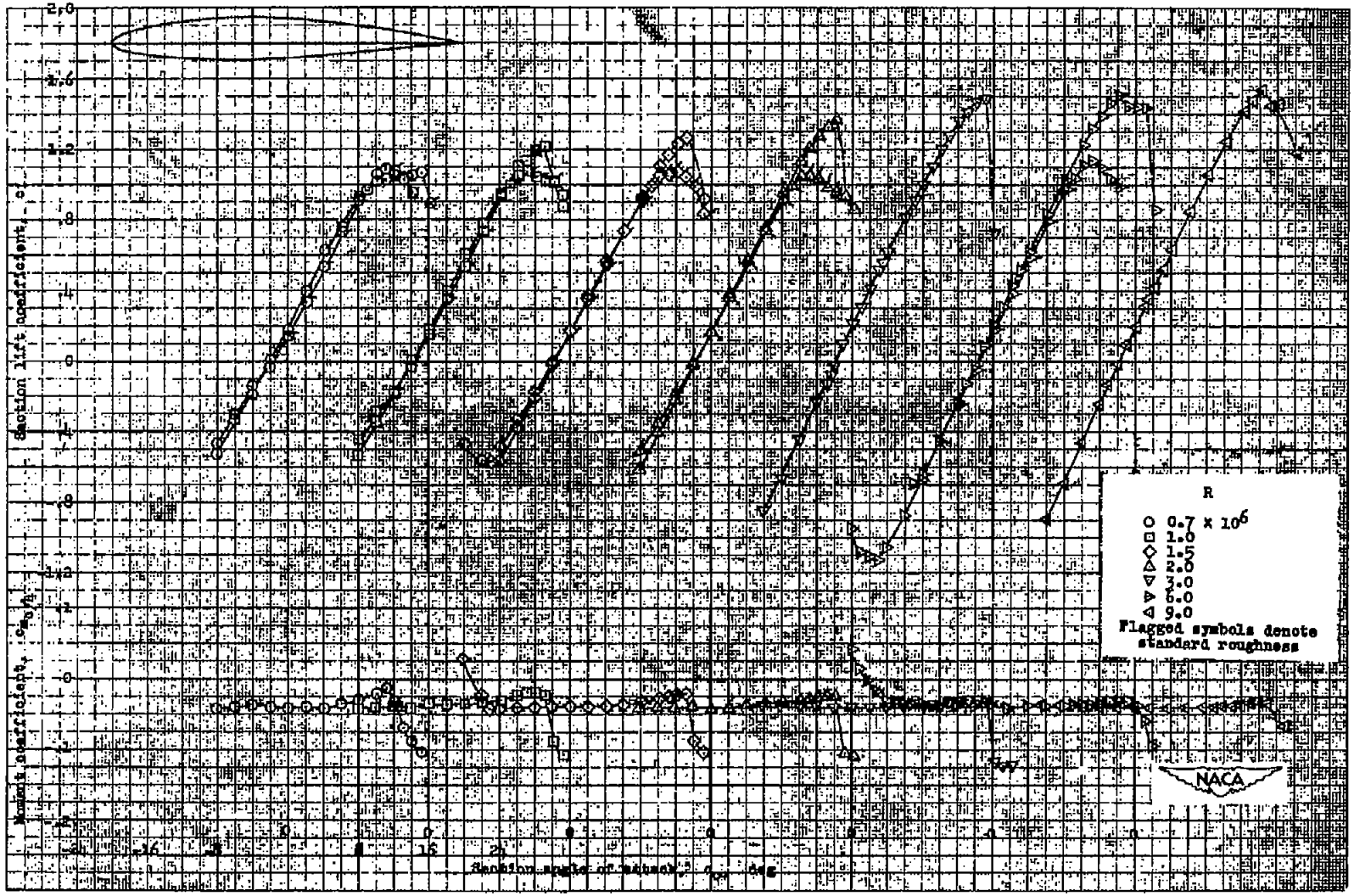

(a) Section lift and pitching-moment characteristics of the plain airfoil section.

Figure 6.- Aerodynamic characteristics of the NACA 64_1A212 airfoil section, 24-inch chord.

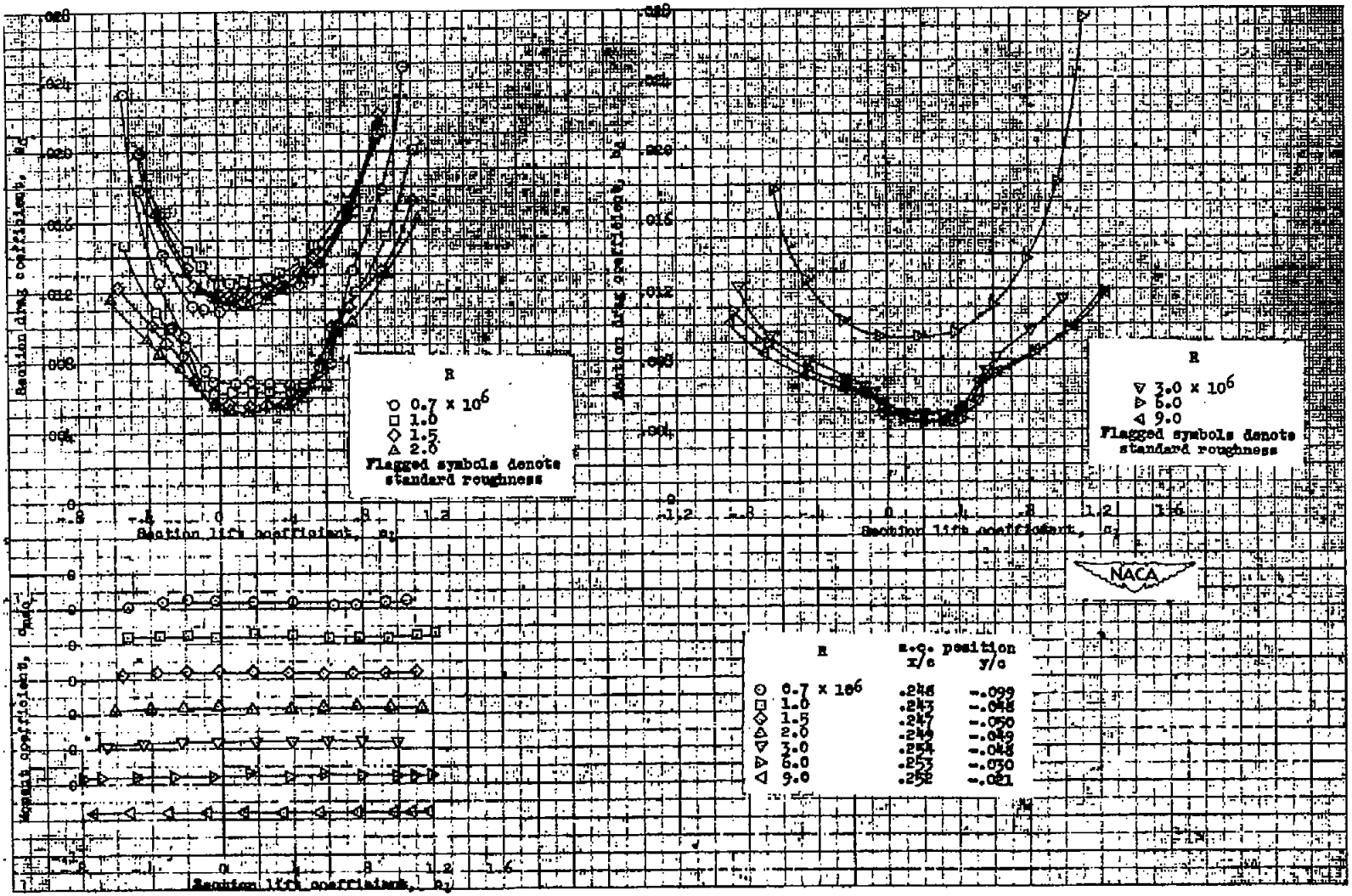

(b) Section drag characteristics and section pitching-moment characteristics about the aerodynamic center of the plain NACA 64_1A212 airfoil section.

Figure 6.– Concluded.

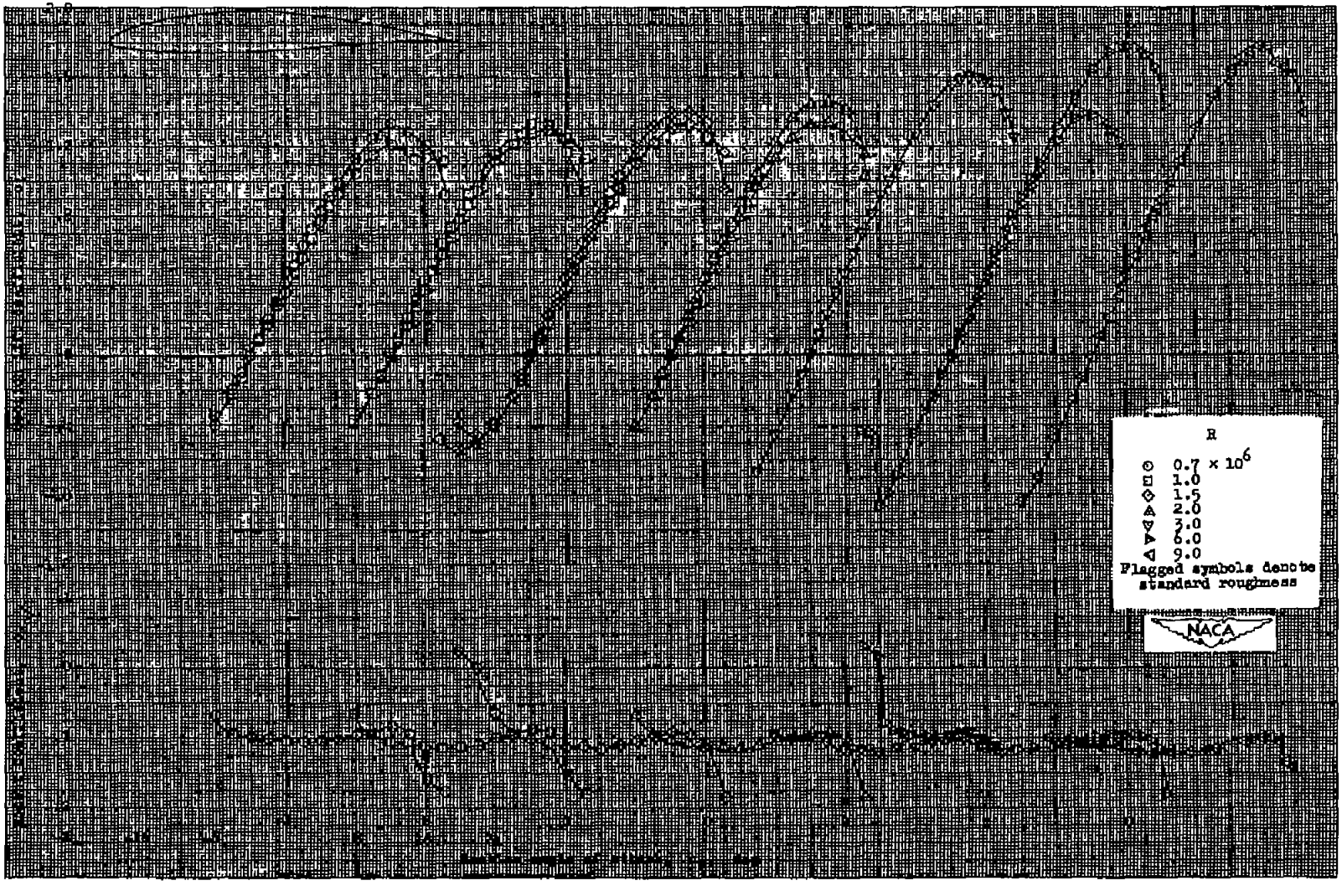

(a) Section lift and pitching-moment characteristics of the plain airfoil section.

Figure 7.– Aerodynamic characteristics of the NACA 64_1-612 airfoil section, 24-inch chord.

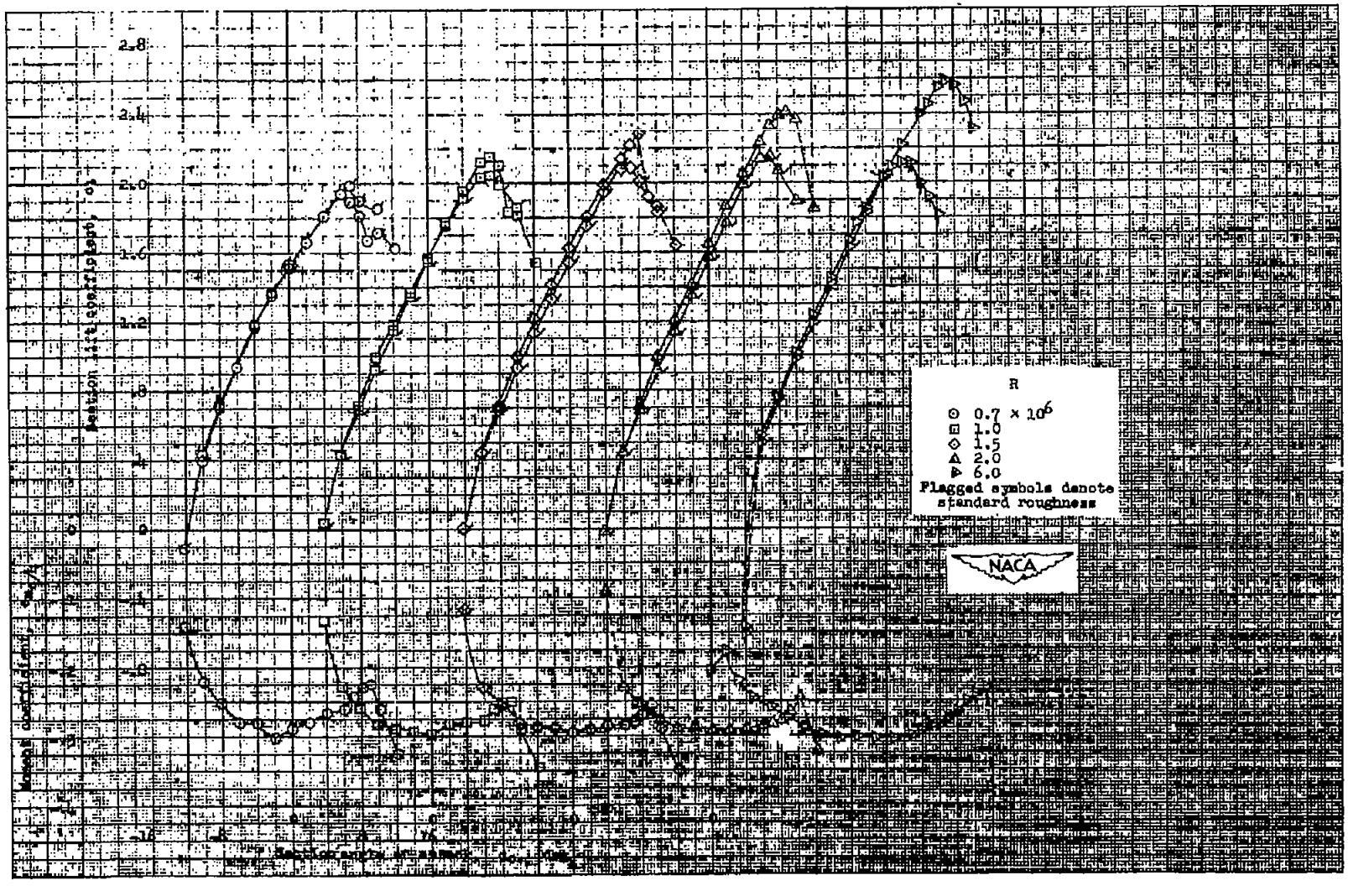

(b) Section lift and pitching-moment characteristics of the NACA 64_1-612 airfoil section with a 0.20c simulated split flap deflected 60°.

Figure 7.– Continued.

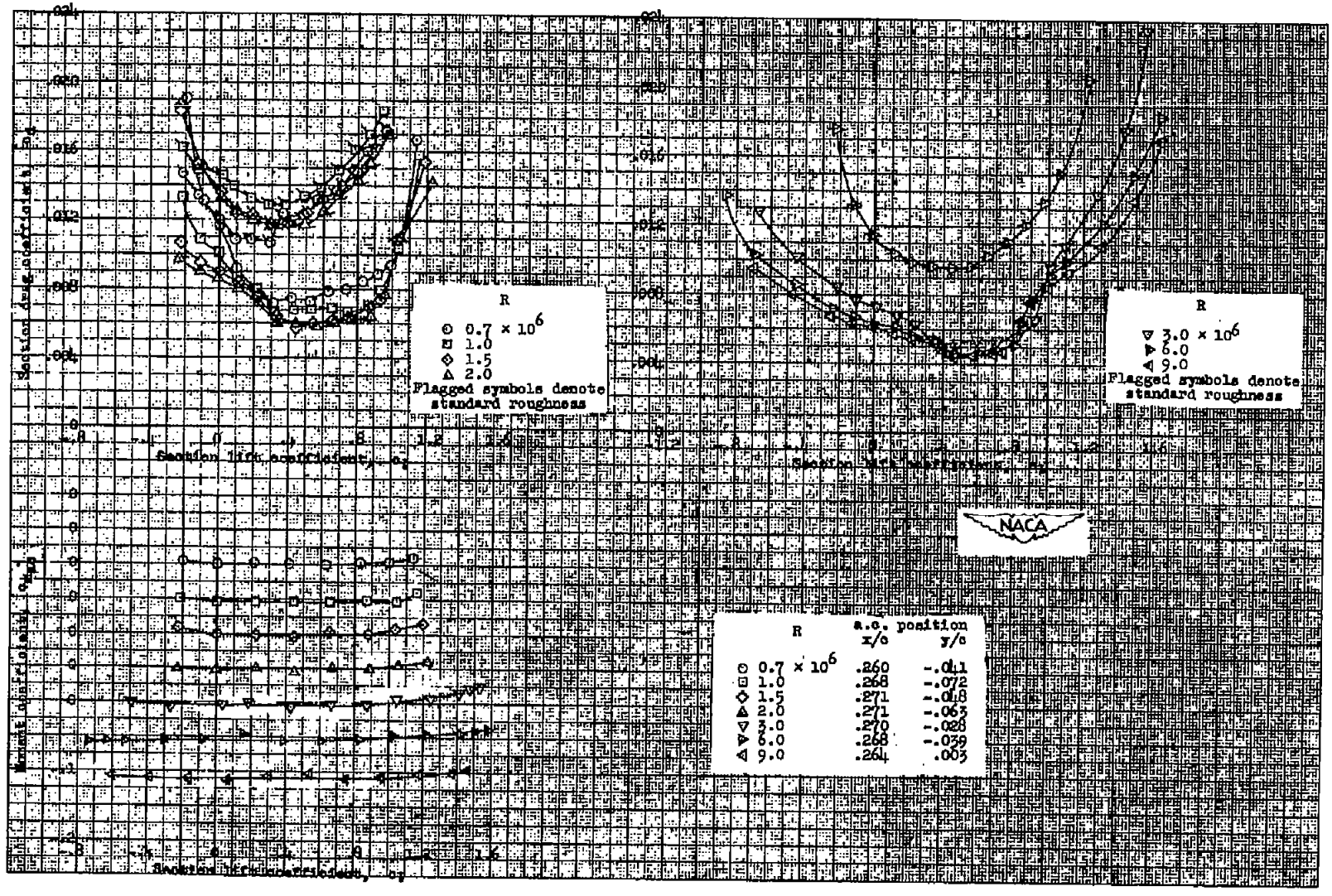

(c) Section drag characteristics and section pitching-moment characteristics about the aerodynamic center of the plain NACA 64_1-612 airfoil section.

Figure 7.- Concluded.

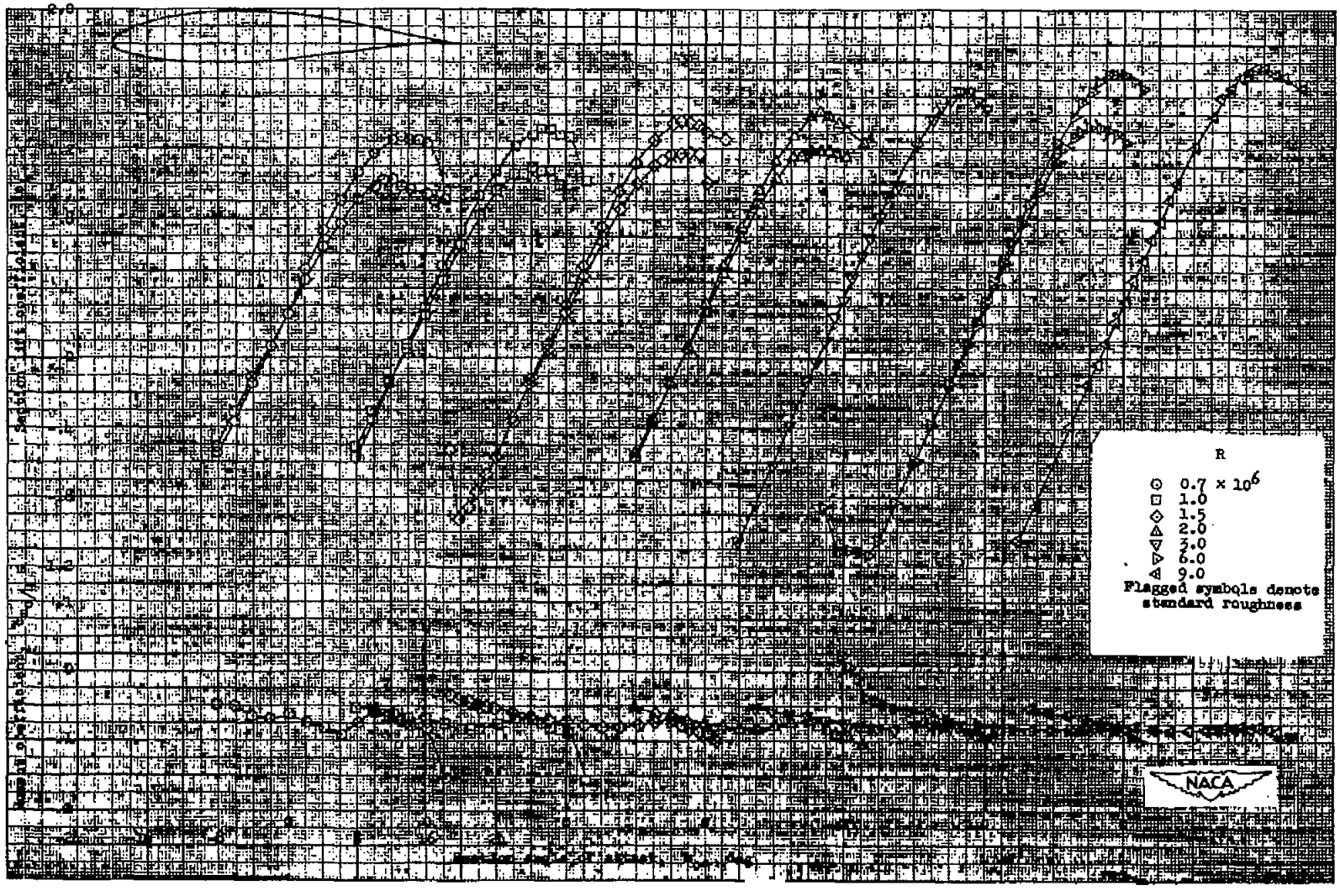

(a) Section lift and pitching-moment characteristics of the plain airfoil section.

Figure 8.— Aerodynamic characteristics of the NACA 63_2-415 airfoil section, 24-inch chord.

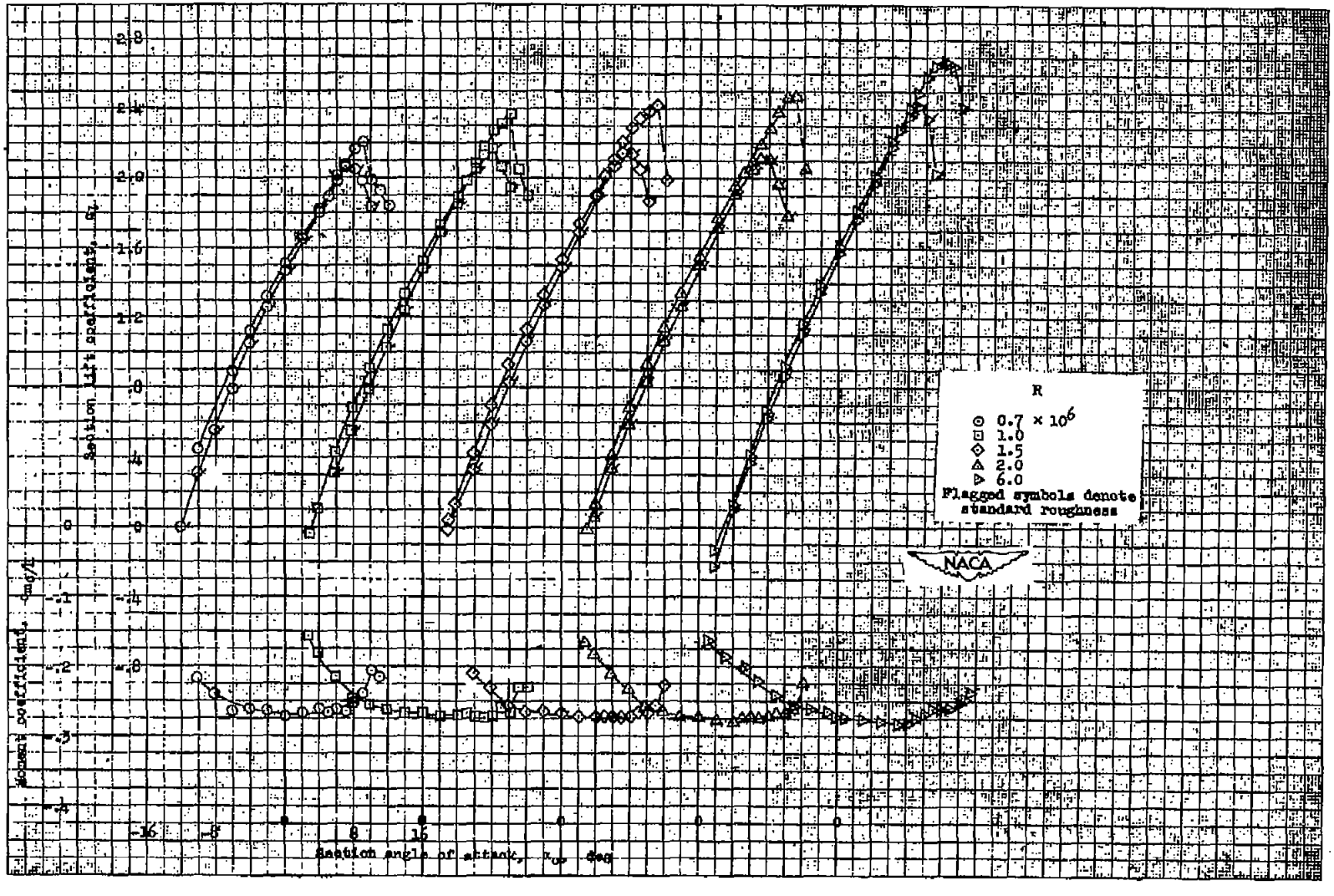

(b) Section lift and pitching-moment characteristics of the NACA 63_2-415 airfoil section with a 0.20c simulated split flap deflected 60°.

Figure 8.– Continued.

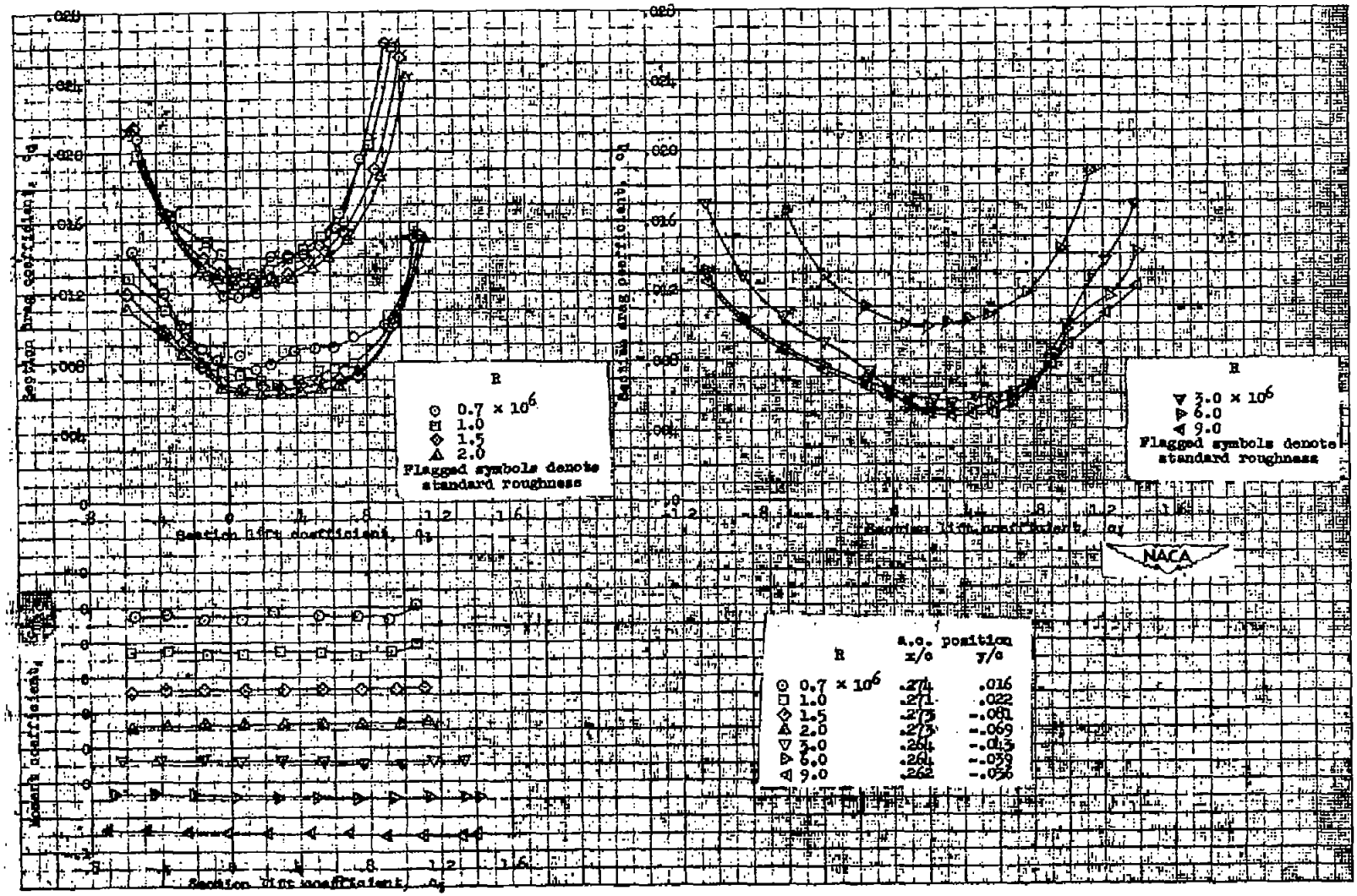

(c) Section drag characteristics and section pitching-moment characteristics about the aerodynamic center of the plain NACA 63_2-415 airfoil section.

Figure 8.- Concluded.

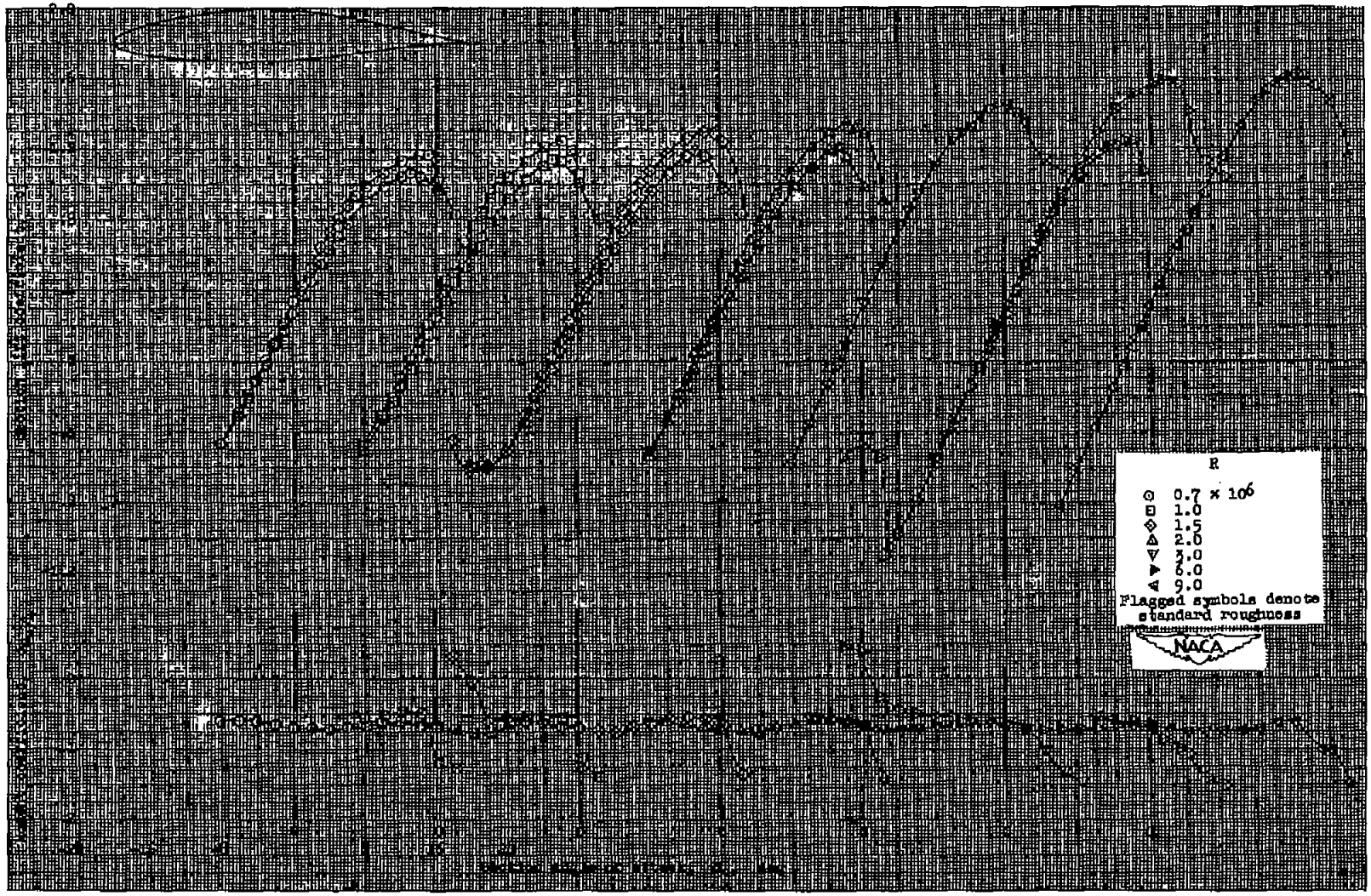

(a) Section lift and pitching-moment characteristics of the plain airfoil section.

Figure 9.- Aerodynamic characteristics of the NACA 65_2-415 airfoil section, 24-inch chord.

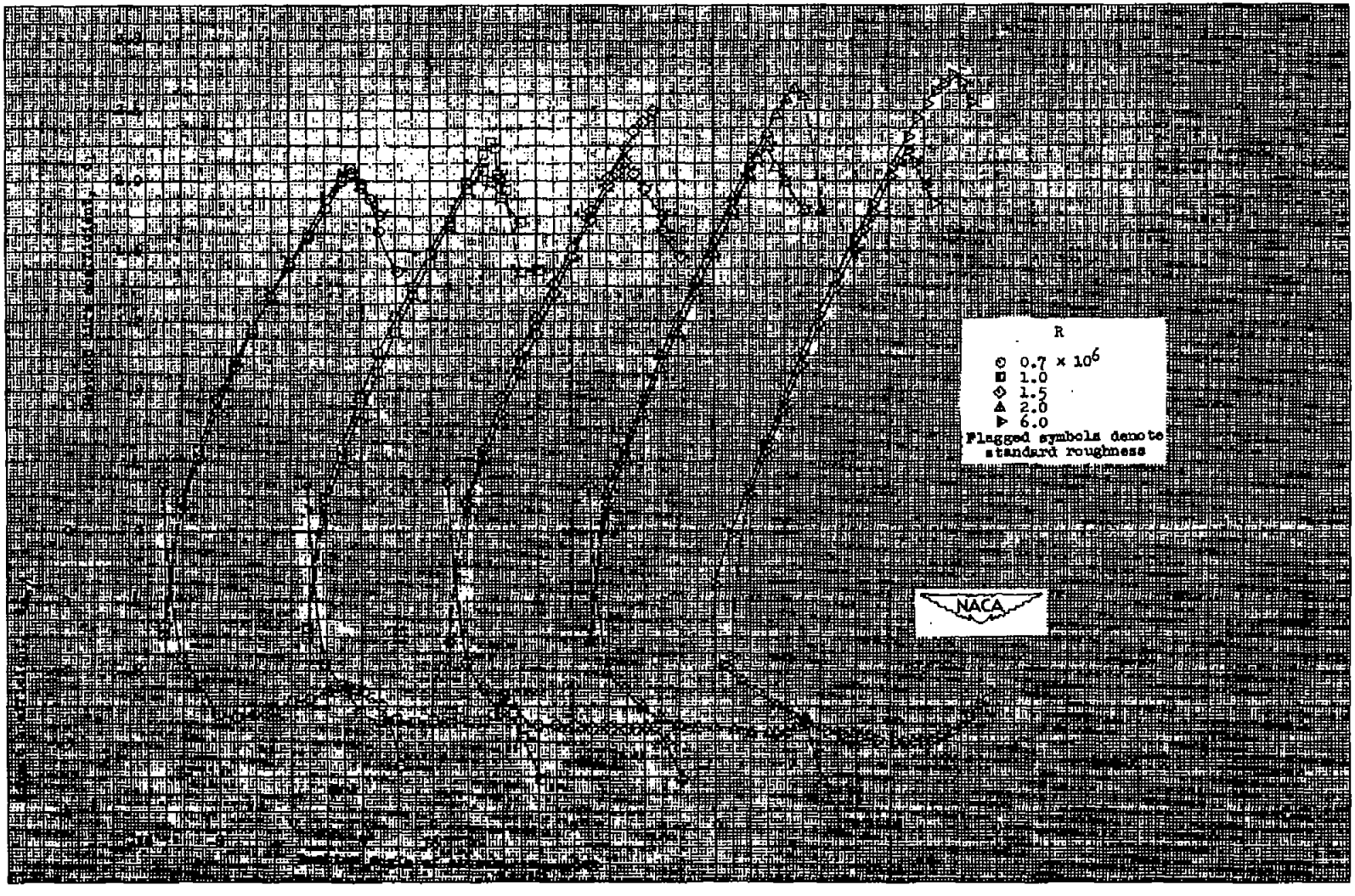

(b) Section lift and pitching-moment characteristics of the NACA 65_2-415 airfoil section with a 0.20c simulated split flap deflected 60°.

Figure 9.- Continued.

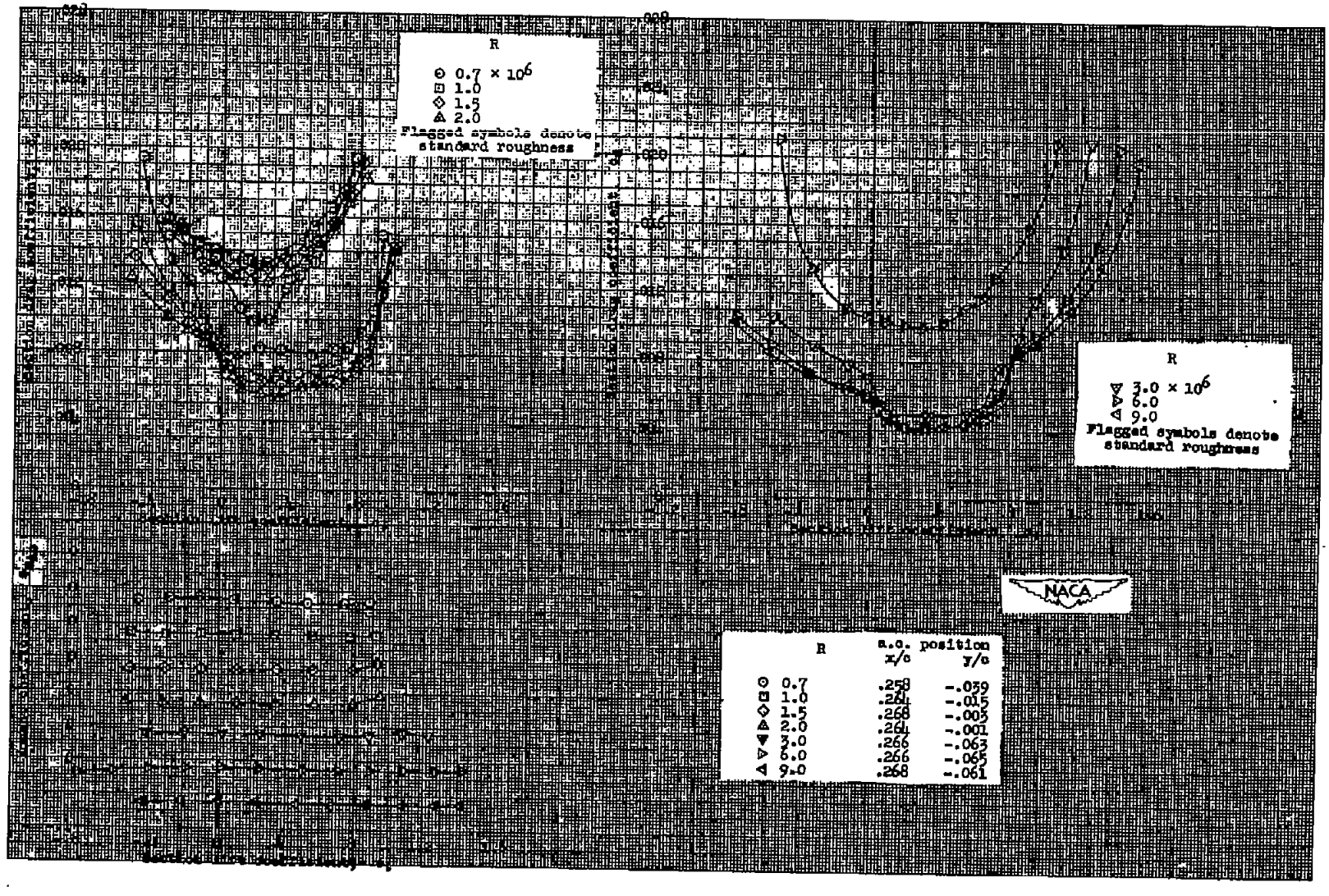

(c) Section drag characteristics and section pitching-moment characteristics about the aerodynamic center of the plain NACA 65_2-415 airfoil section.

Figure 9.- Concluded.

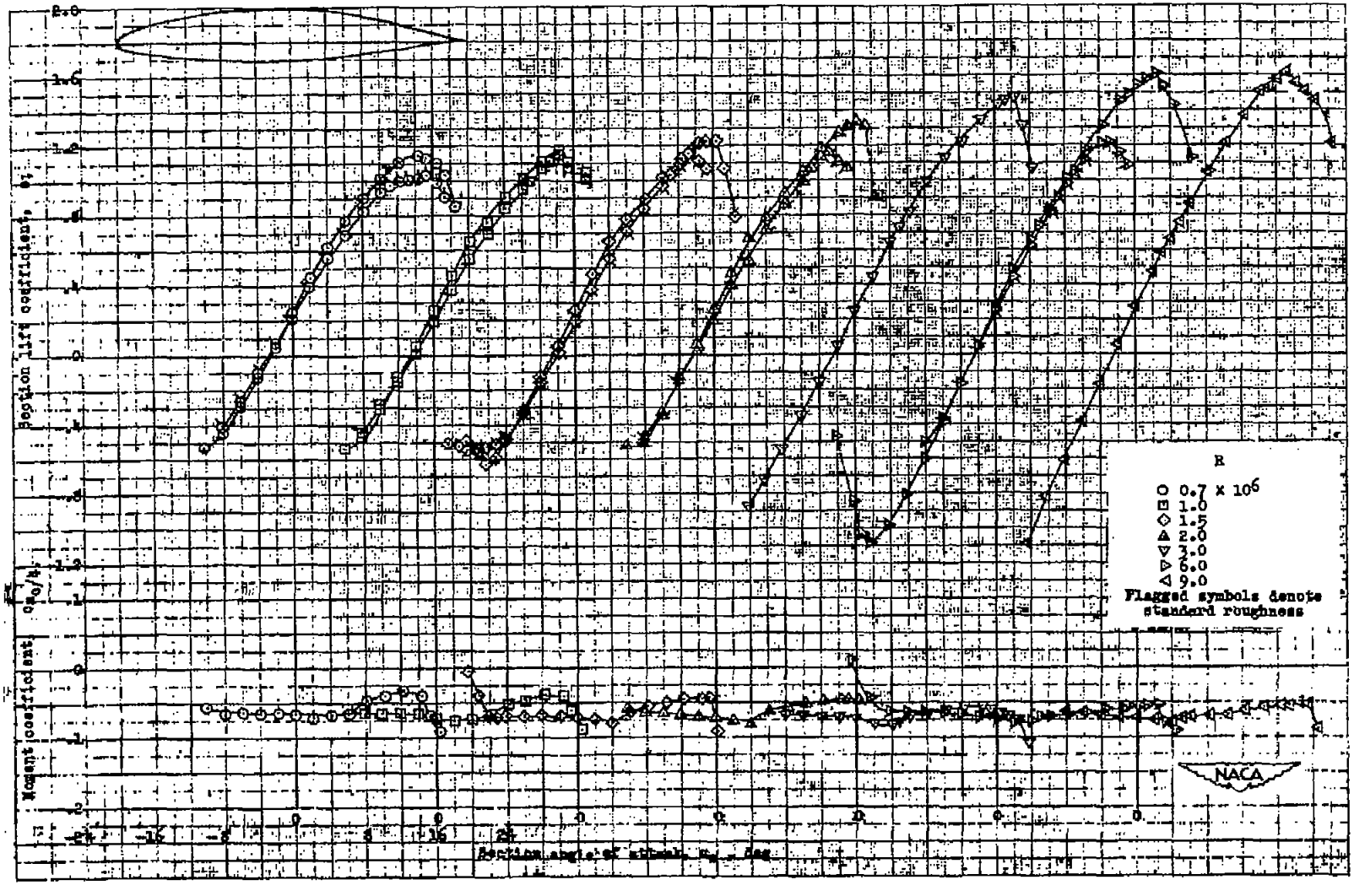

(a) Section lift and pitching-moment characteristics of the plain airfoil section.

Figure 10.- Aerodynamic characteristics of the NACA 66_2-415 airfoil section, 24-inch chord.

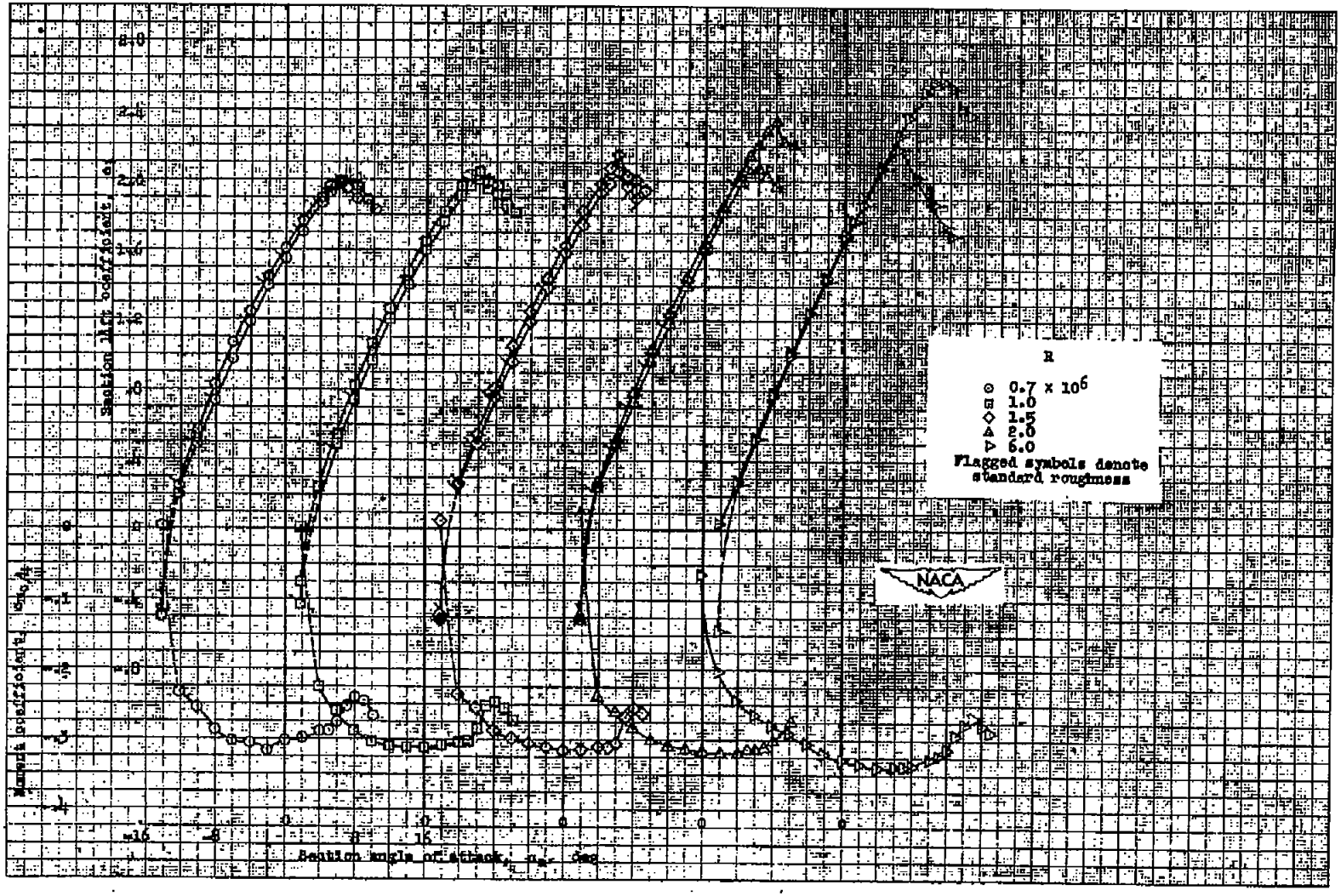

(b) Section lift and pitching-moment characteristics of the NACA 66_2-415 airfoil section with a 0.20c simulated split flap deflected 60°.

Figure 10.– Continued.

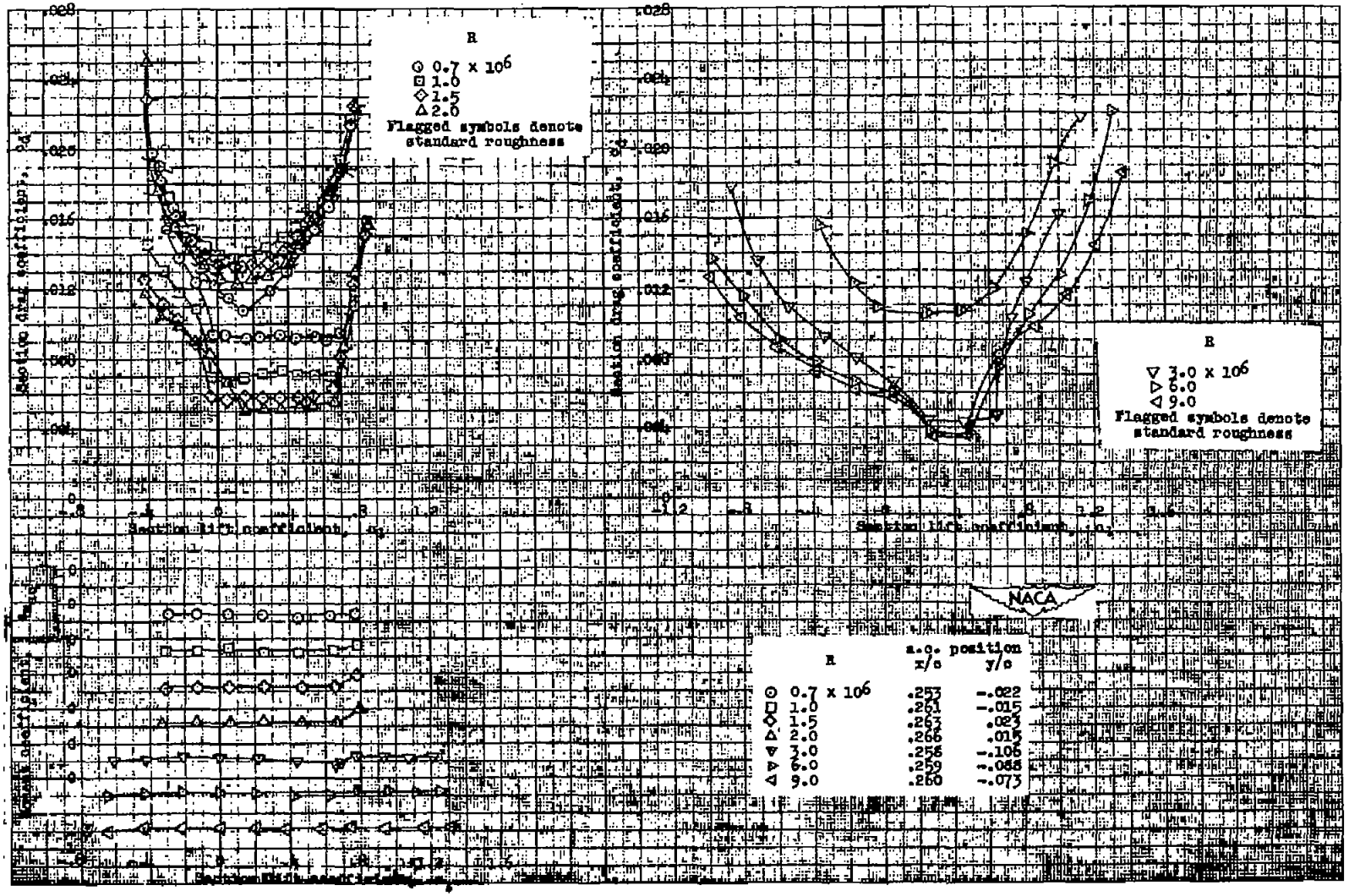

(c) Section drag characteristics and section pitching-moment characteristics about the aerodynamic center of the plain NACA 662-415 airfoil section.

Figure 10.- Concluded.

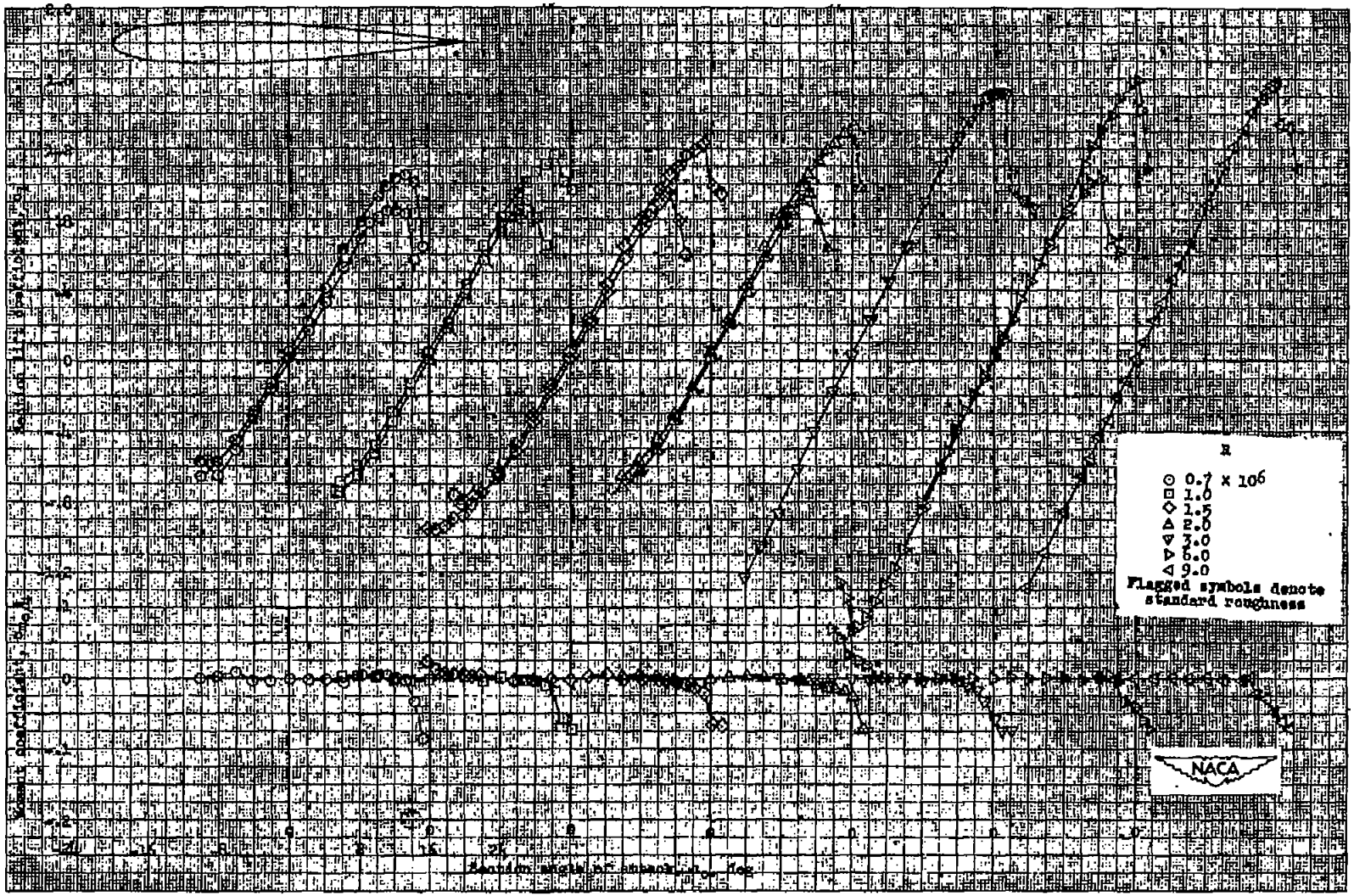

(a) Section lift and pitching-moment characteristics of the plain airfoil section.

Figure 11.- Aerodynamic characteristics of the NACA 0012 airfoil section, 24-inch chord.

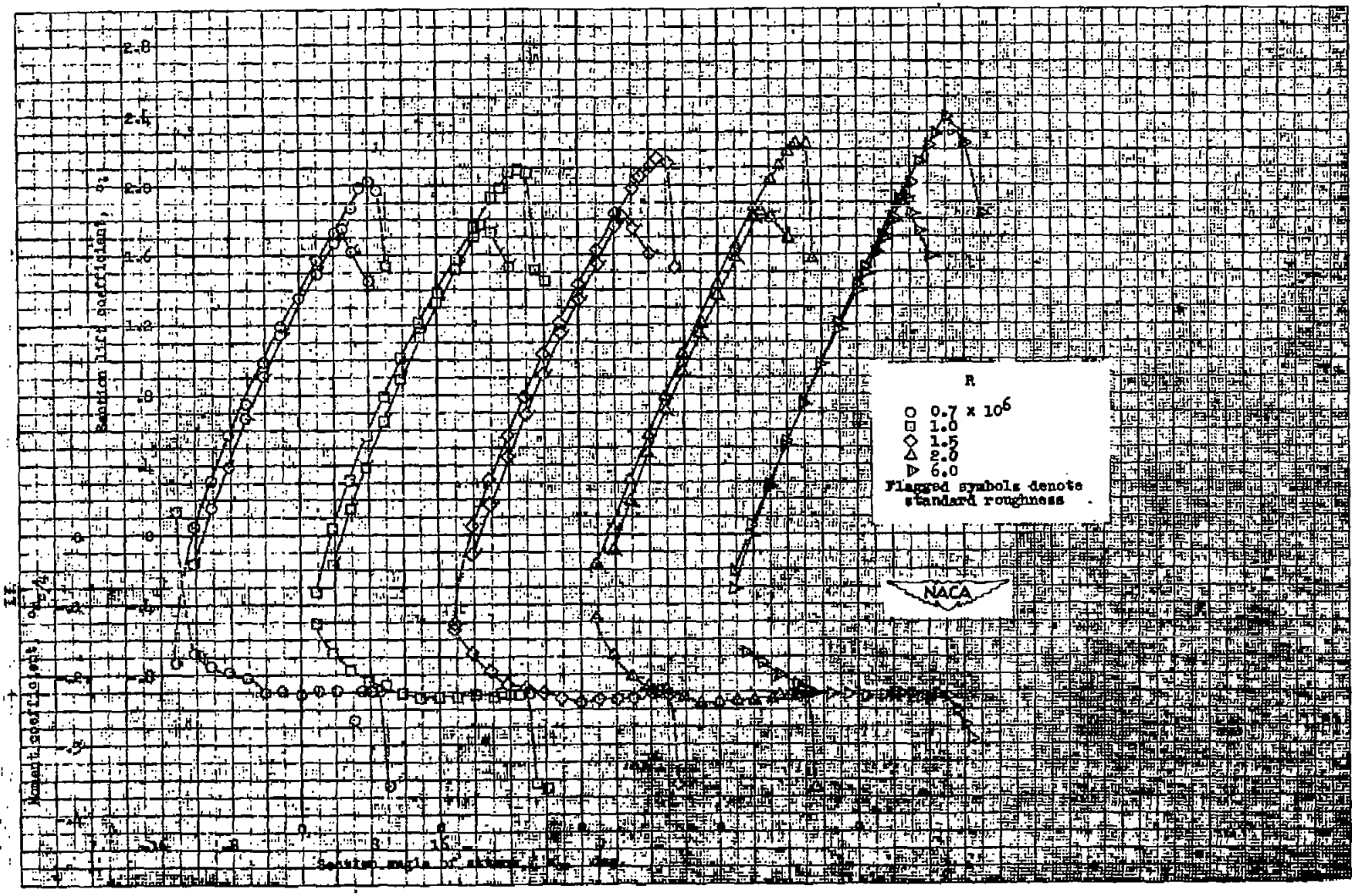

(b) Section lift and pitching-moment characteristics of the NACA 0012 airfoil section with a 0.20c simulated split flap deflected 60°.

Figure 11.— Continued.

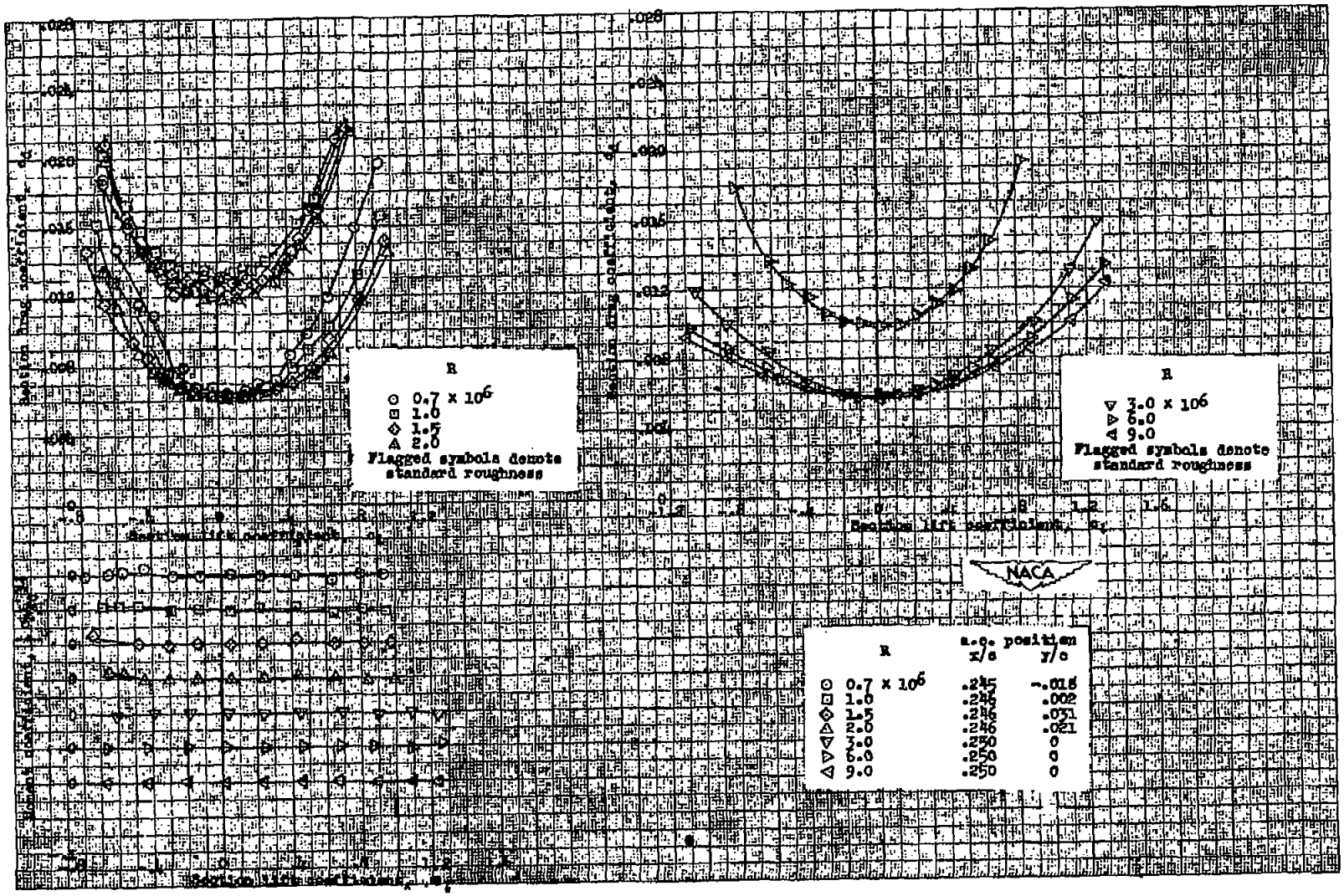

(c) Section drag characteristics and section pitching-moment characteristics about the aerodynamic center of the plain NACA 0012 airfoil section.

Figure 11.– Concluded.

(a) Section lift and pitching-moment characteristics of the plain airfoil section.

Figure 12.- Aerodynamic characteristics of the NACA 4412 airfoil section, 24-inch chord.

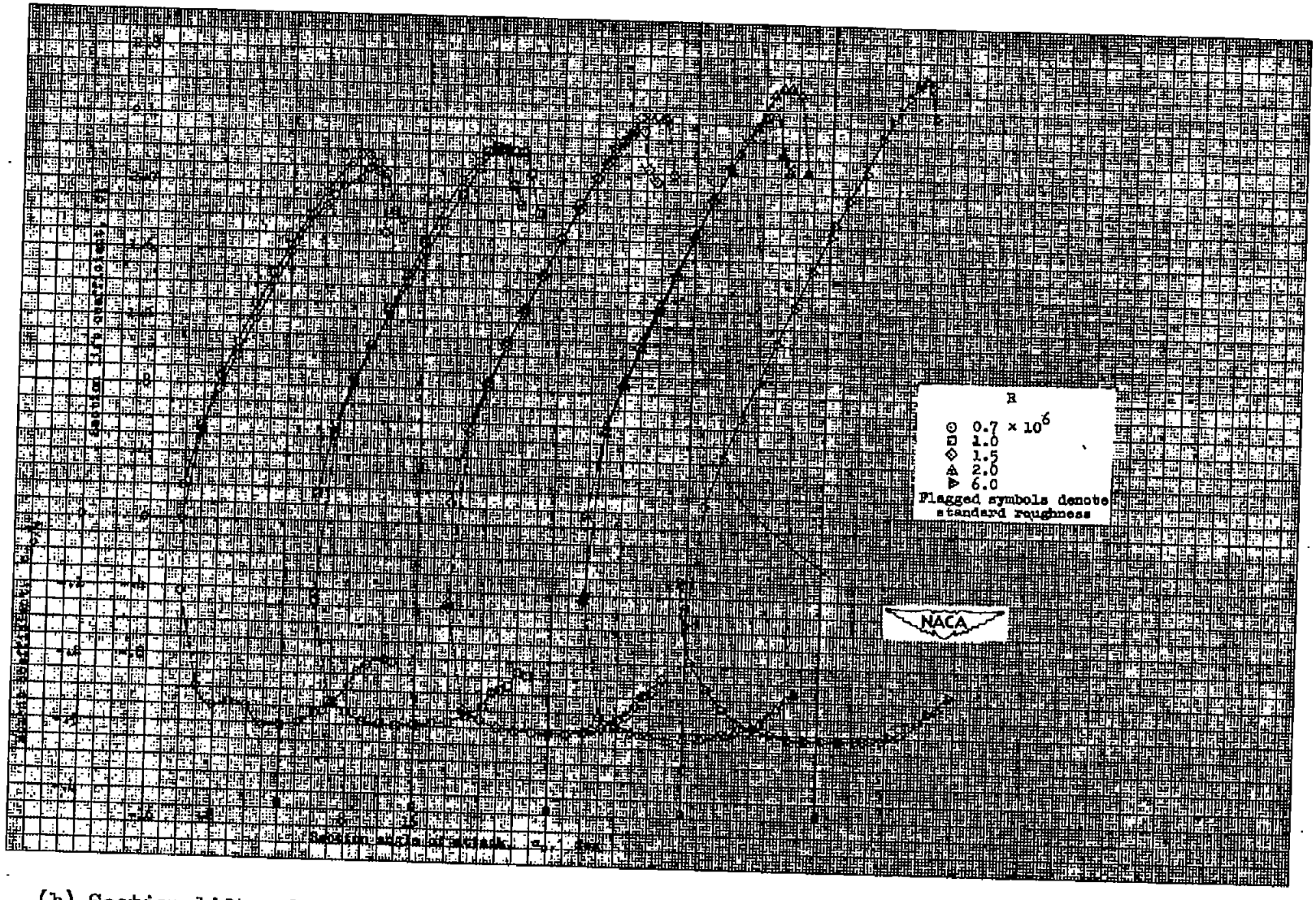

(b) Section lift and pitching-moment characteristics of the NACA 4412 airfoil section with a 0.20c simulated split flap deflected 60°.

Figure 12.- Continued.

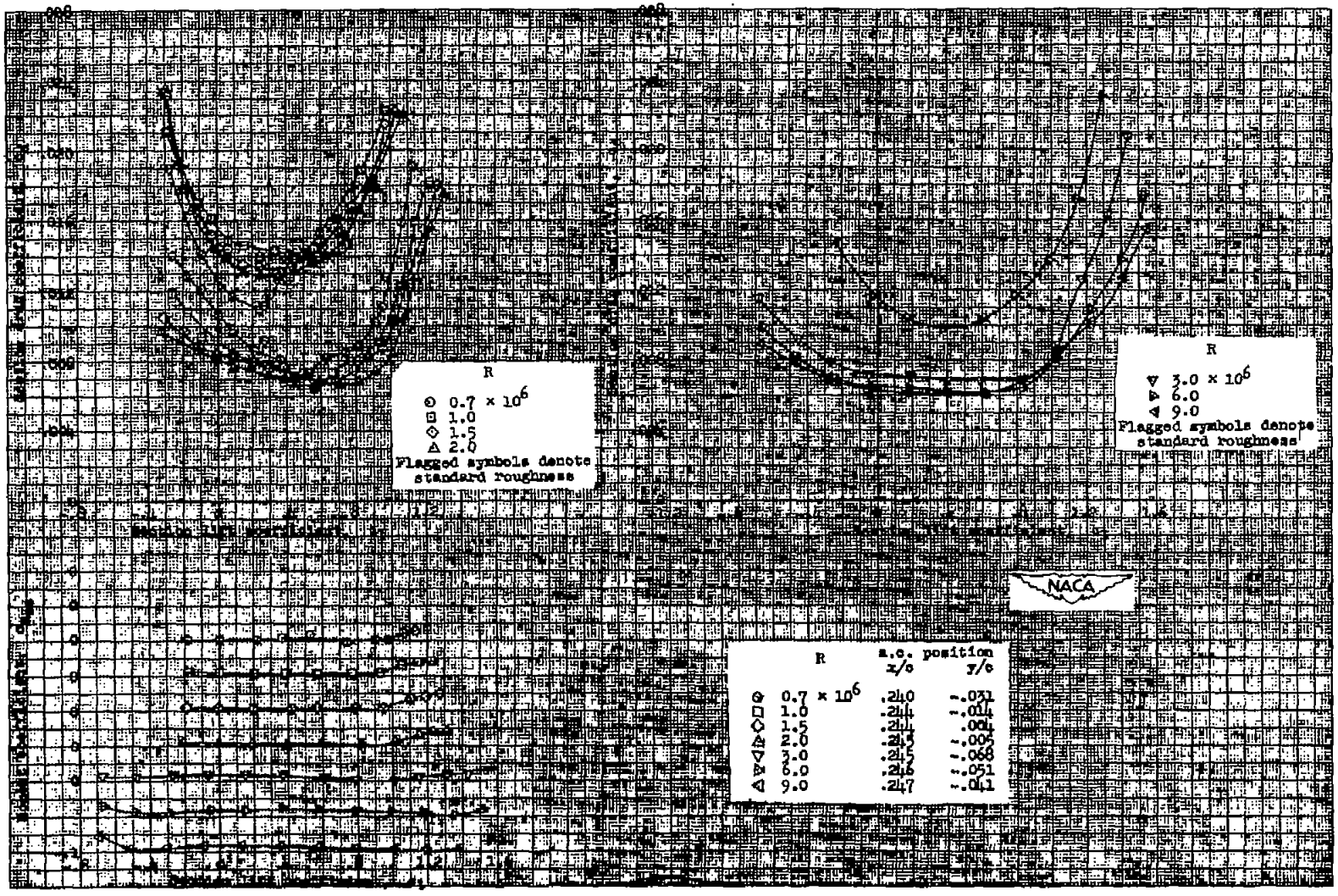

(c) Section drag characteristics and section pitching-moment characteristics about the aerodynamic center of the plain NACA 4412 airfoil section.

Figure 12.- Concluded.

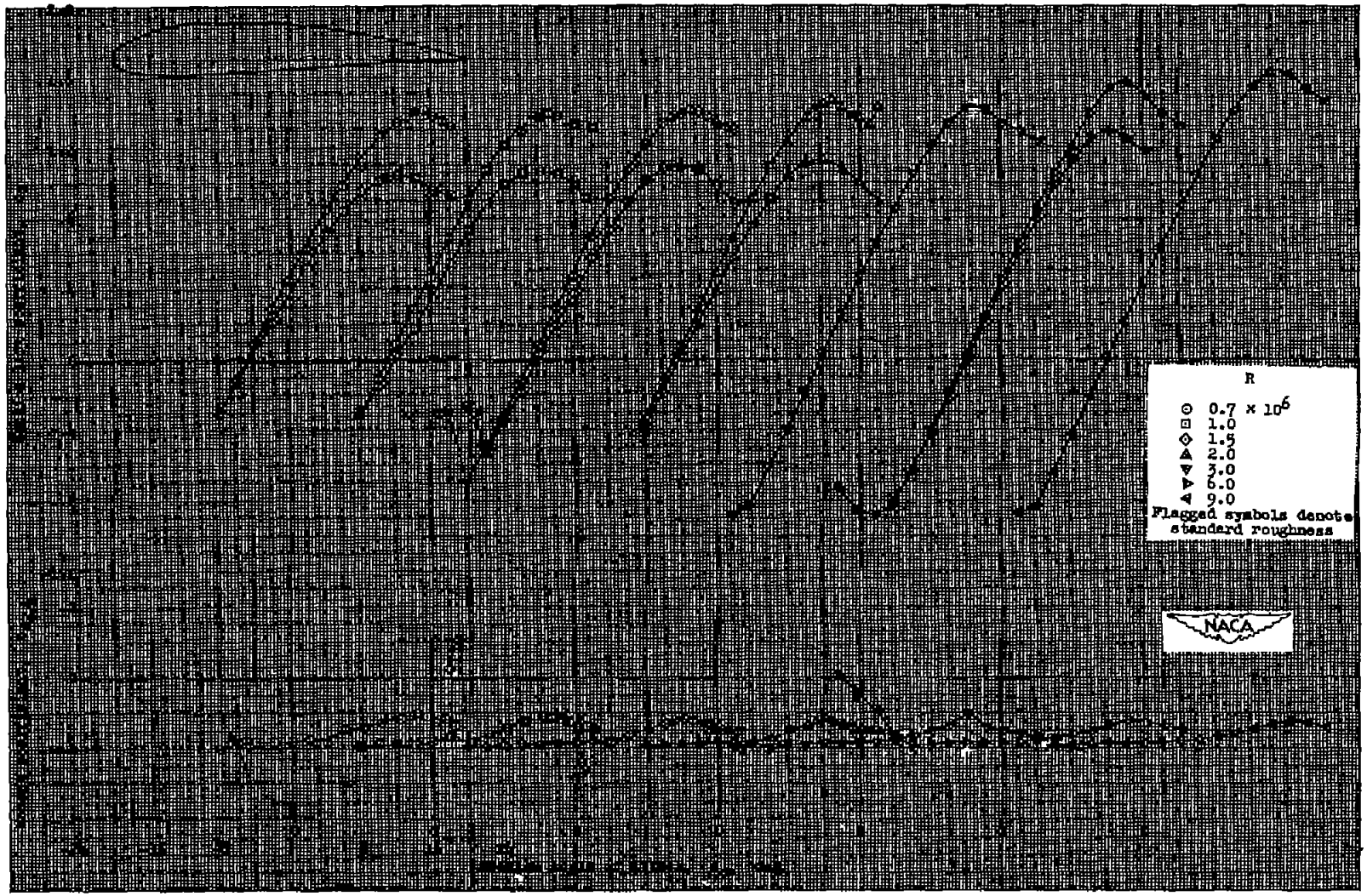

(a) Section lift and pitching-moment characteristics of the plain airfoil section.

Figure 13.- Aerodynamic characteristics of the NACA 4415 airfoil section, 24-inch chord.

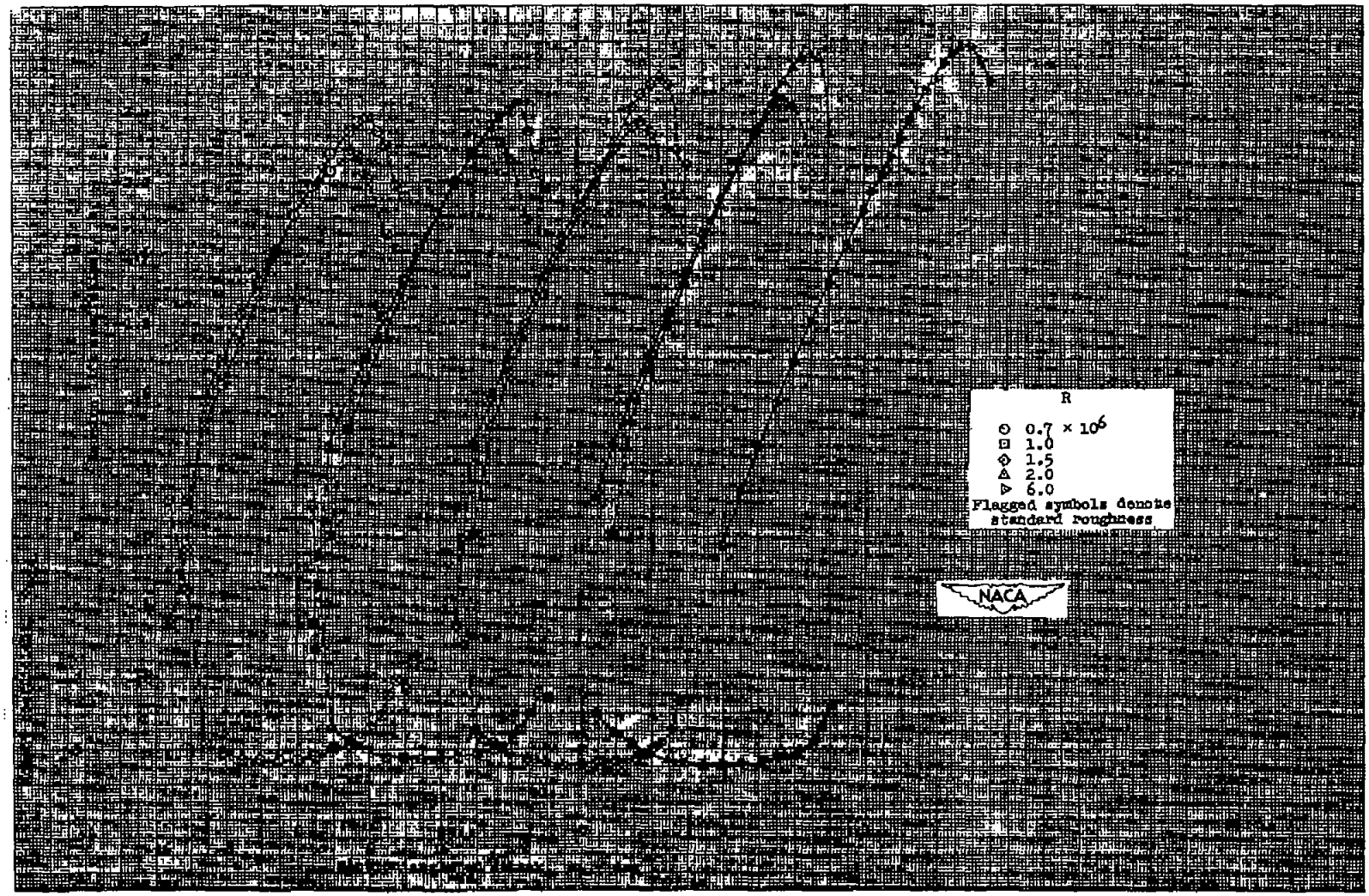

(b) Section lift and pitching-moment characteristics of the NACA 4415 airfoil section with a 0.20c simulated split flap deflected 60°.

Figure 13.– Continued.

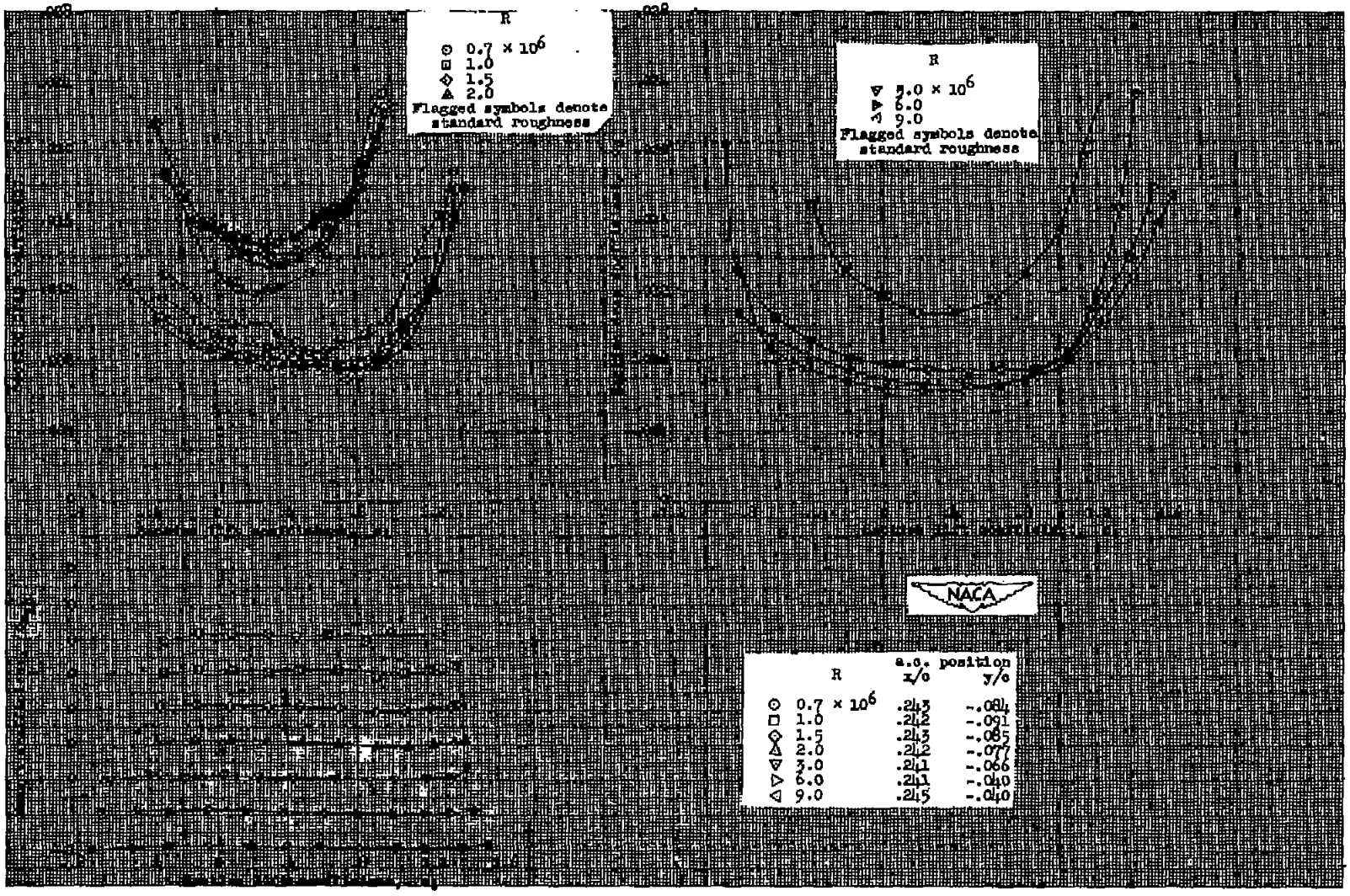

(c) Section drag characteristics and section pitching-moment characteristics about the aerodynamic center of the plain NACA 4415 airfoil section.

Figure 13.- Concluded.

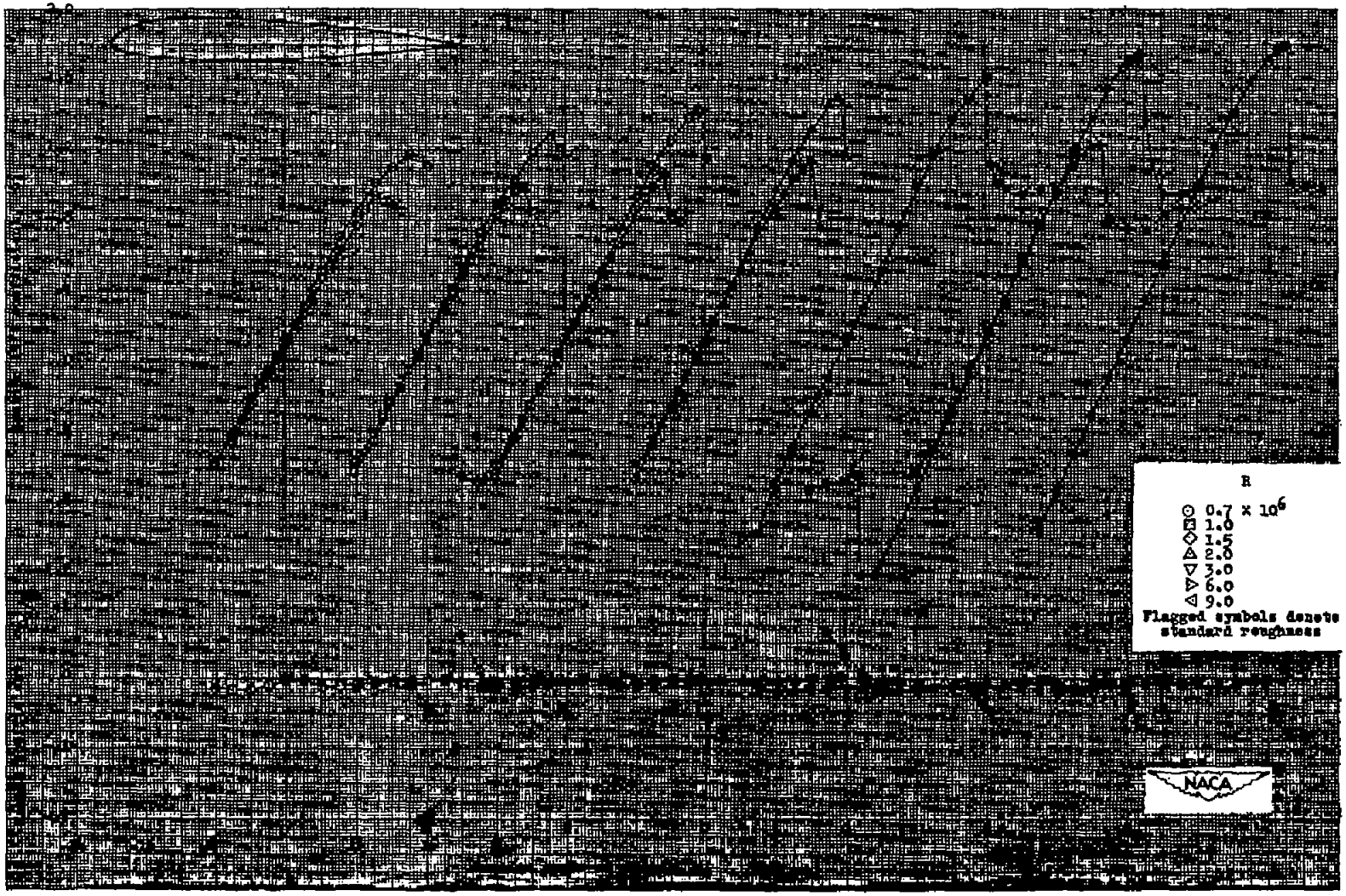

(a) Section lift and pitching-moment characteristics of the plain airfoil section.

Figure 14.- Aerodynamic characteristics of the NACA 23012 airfoil section, 24-inch chord.

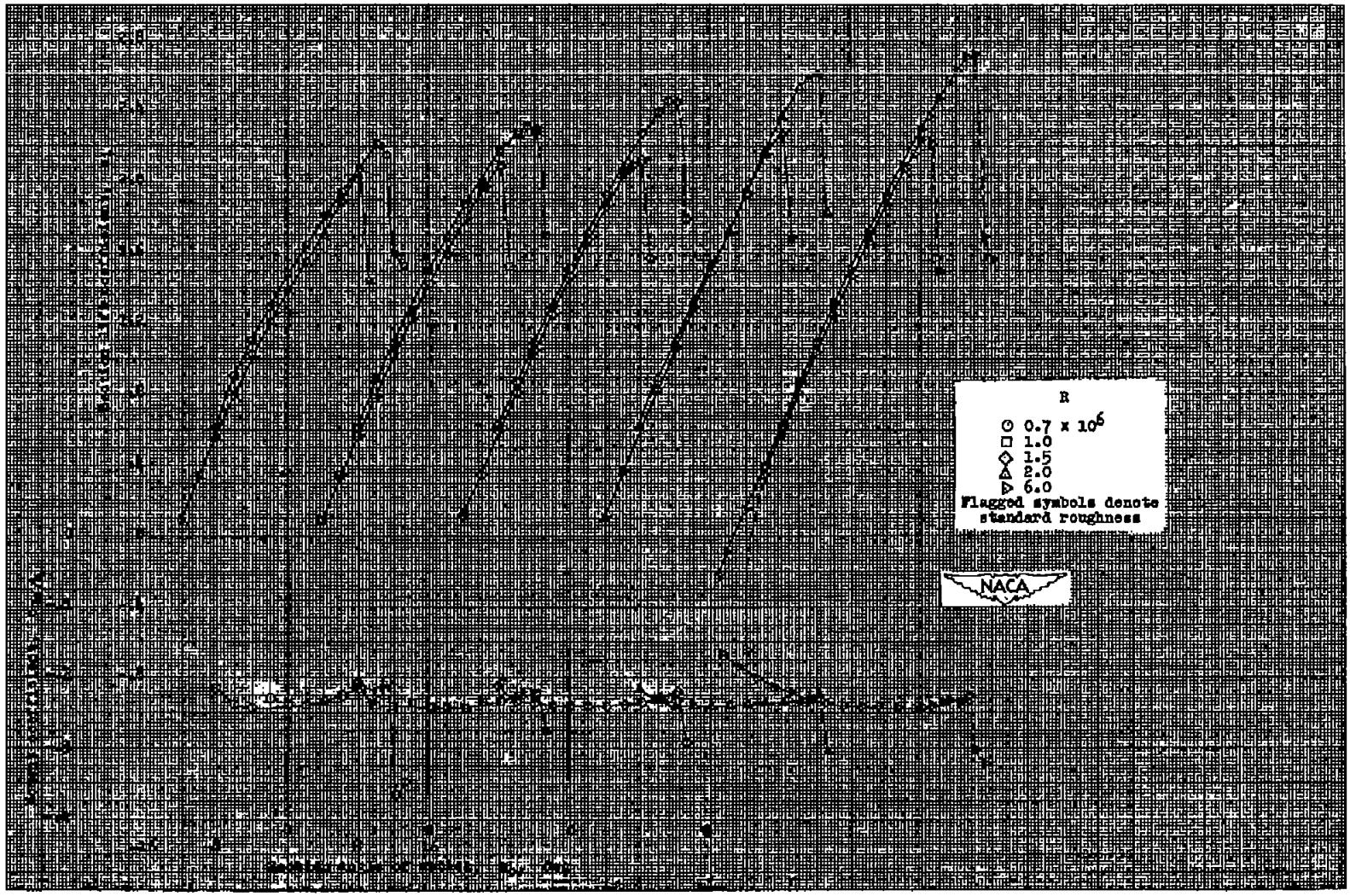

(b) Section lift and pitching-moment characteristics of the NACA 23012 airfoil section with a 0.20c simulated split flap deflected 60°.

Figure 14.— Continued.

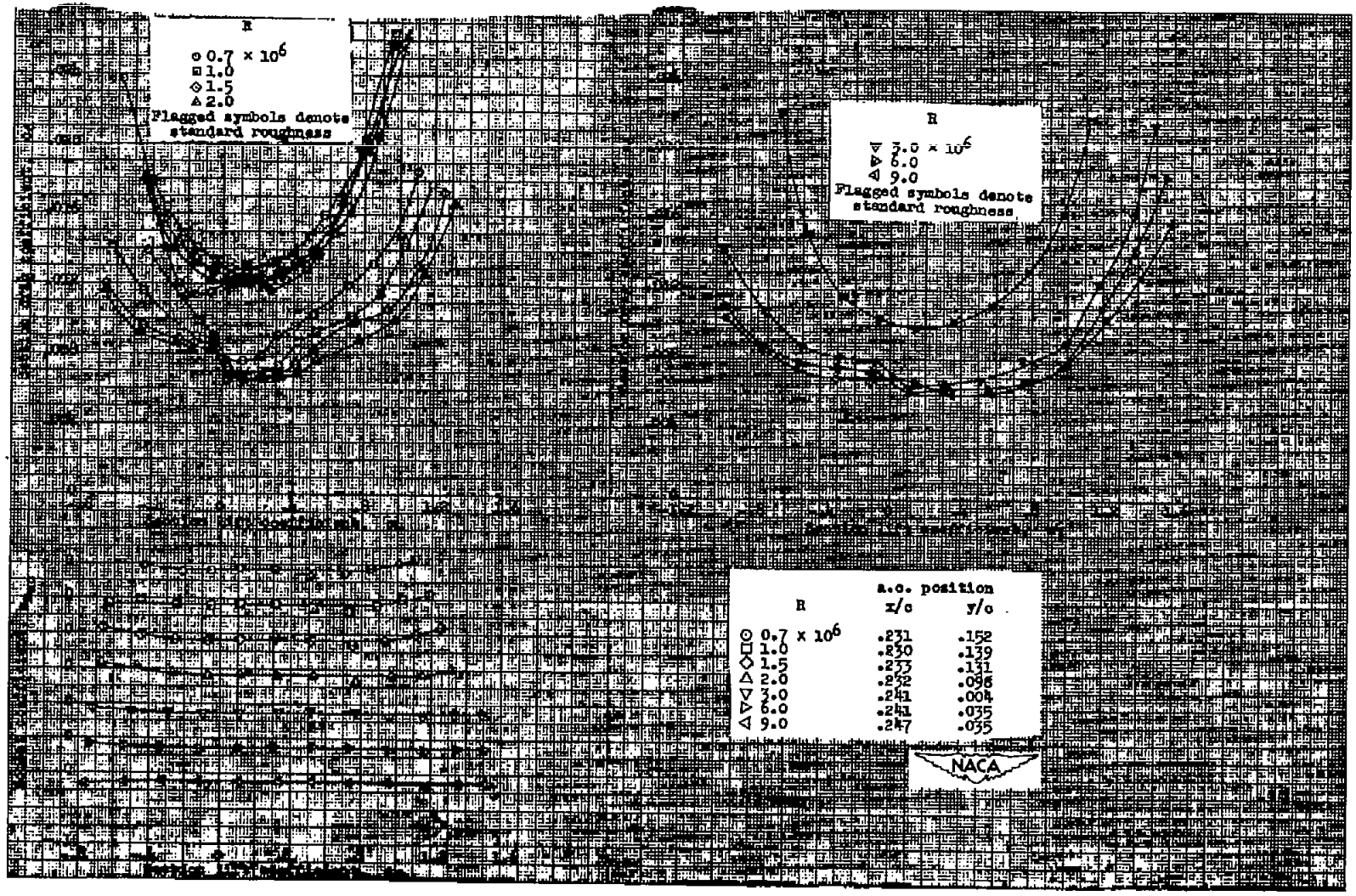

(c) Section drag characteristics and section pitching-moment characteristics about the aerodynamic center of the plain NACA 23012 airfoil section.

Figure 14.— Concluded.

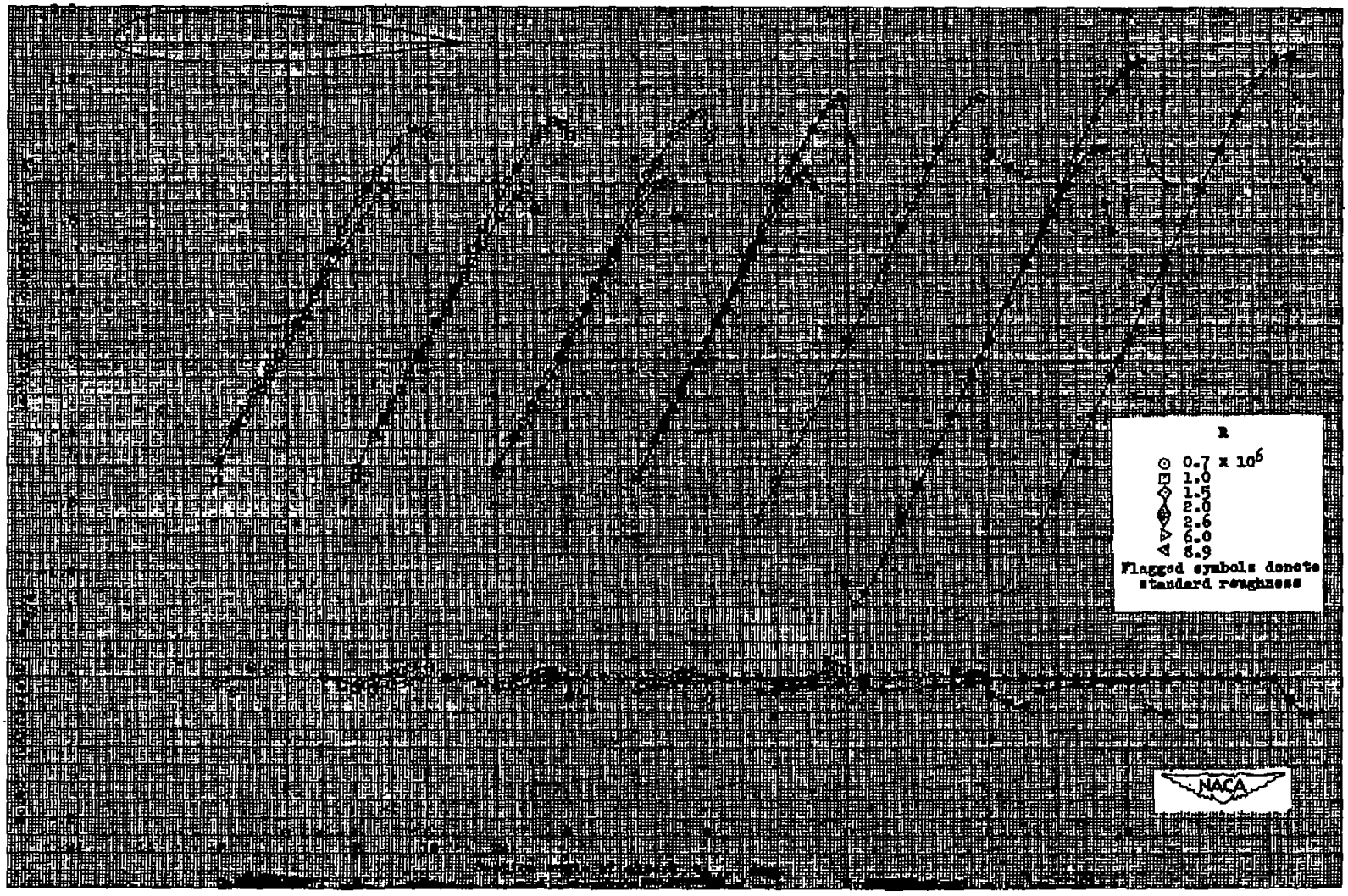

(a) Section lift and pitching-moment characteristics of the plain airfoil section.

Figure 15.- Aerodynamic characteristics of the NACA 23015 airfoil section, 24-inch chord.

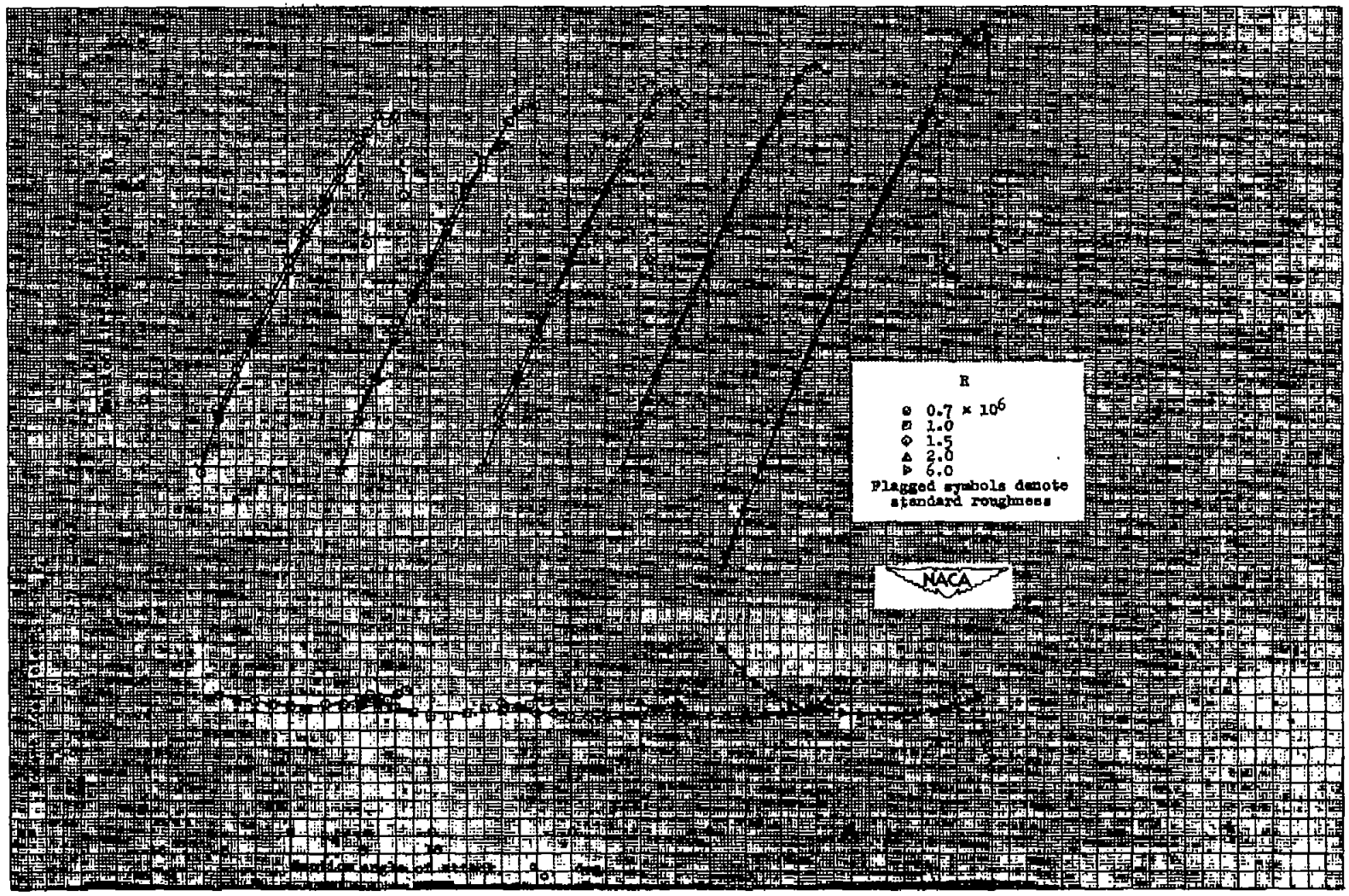

(b) Section lift and pitching-moment characteristics of the NACA 23015 airfoil section with a 0.20c simulated split flap deflected 60°.

Figure 15.- Continued.

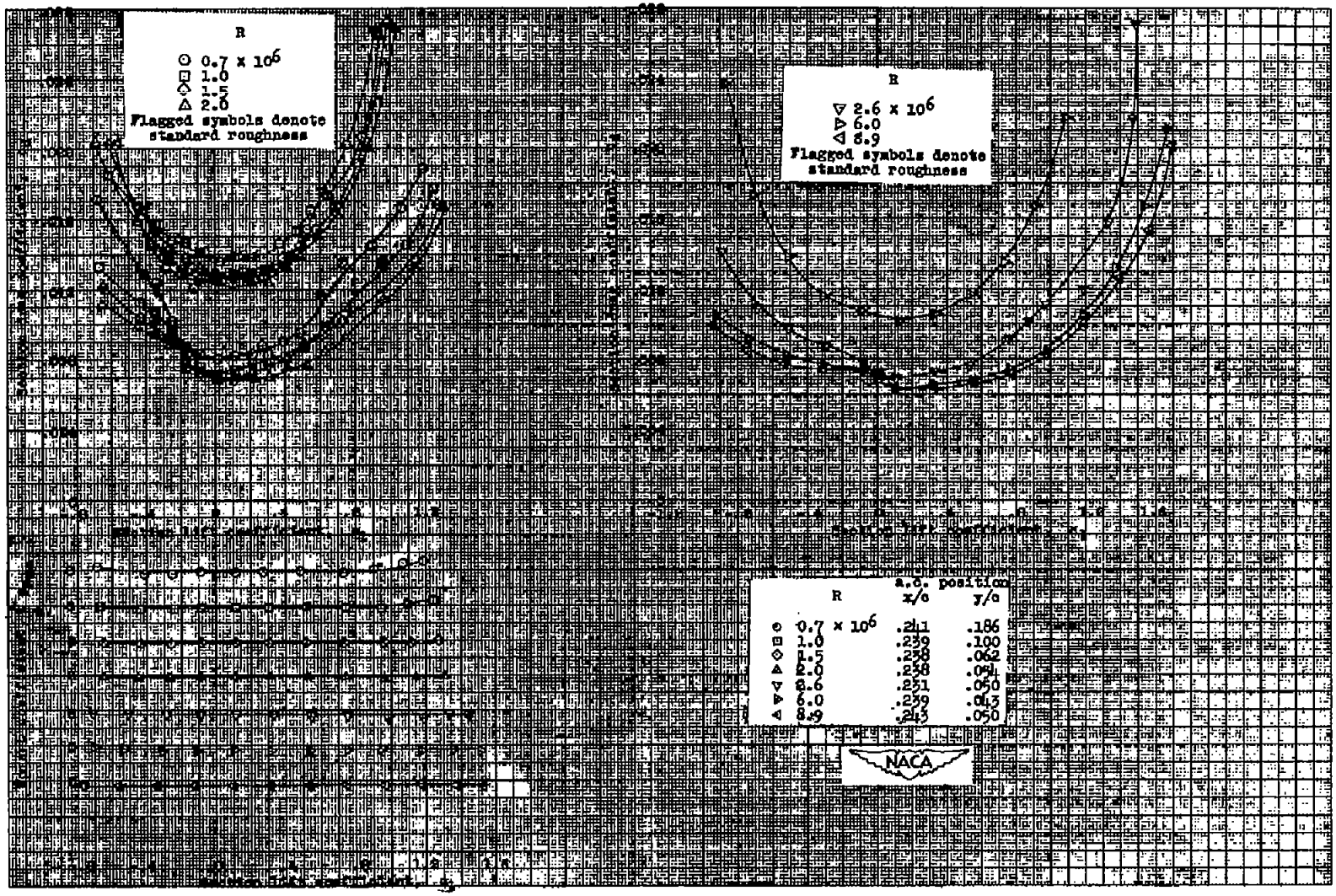

(c) Section drag characteristics and section pitching-moment characteristics about the aerodynamic center of the plain NACA 23015 airfoil section.

Figure 15.- Concluded.

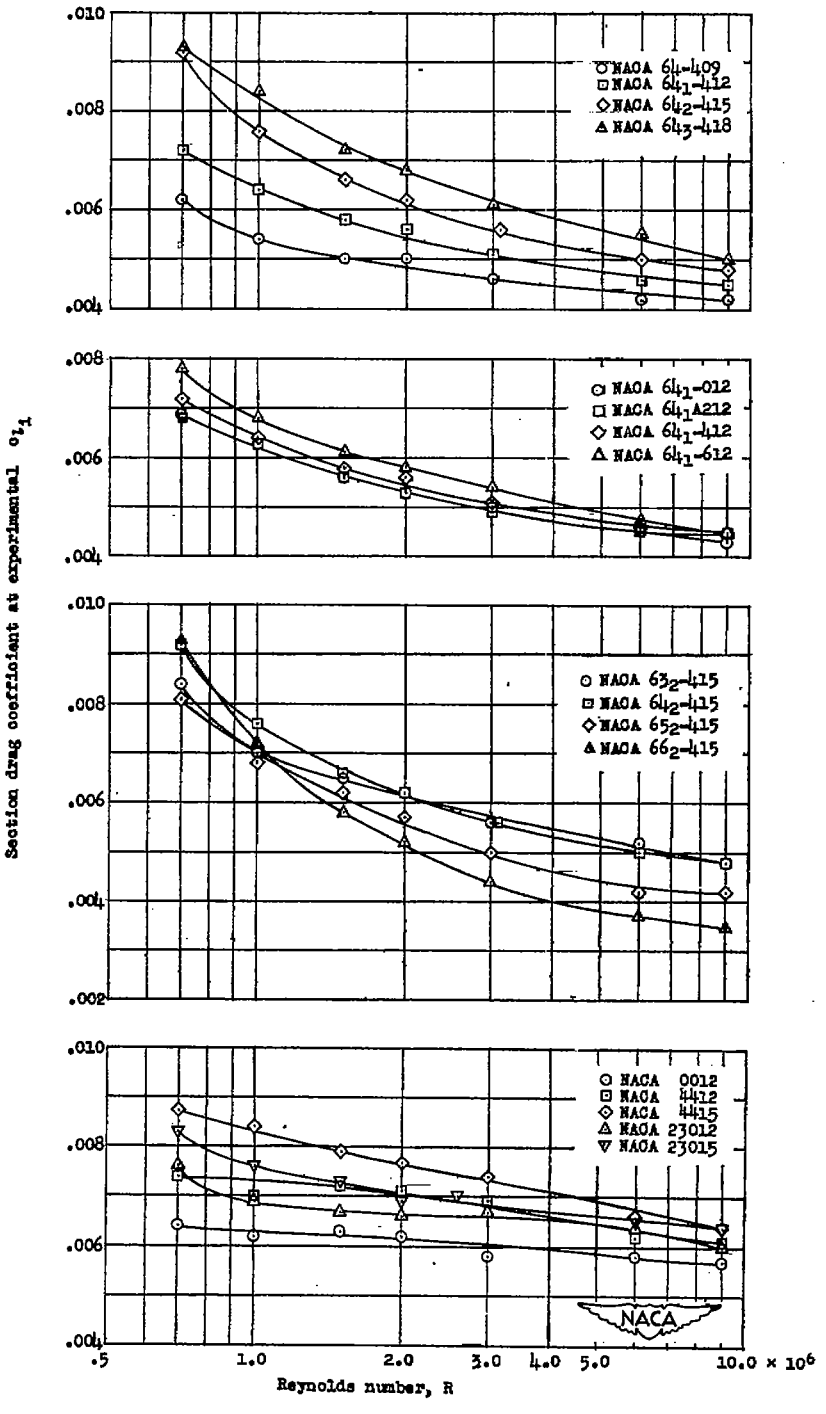

(a) Airfoils with smooth surfaces.

Figure 16.– Variation with Reynolds number of section drag coefficient at design lift coefficient for the 15 plair airfoils.

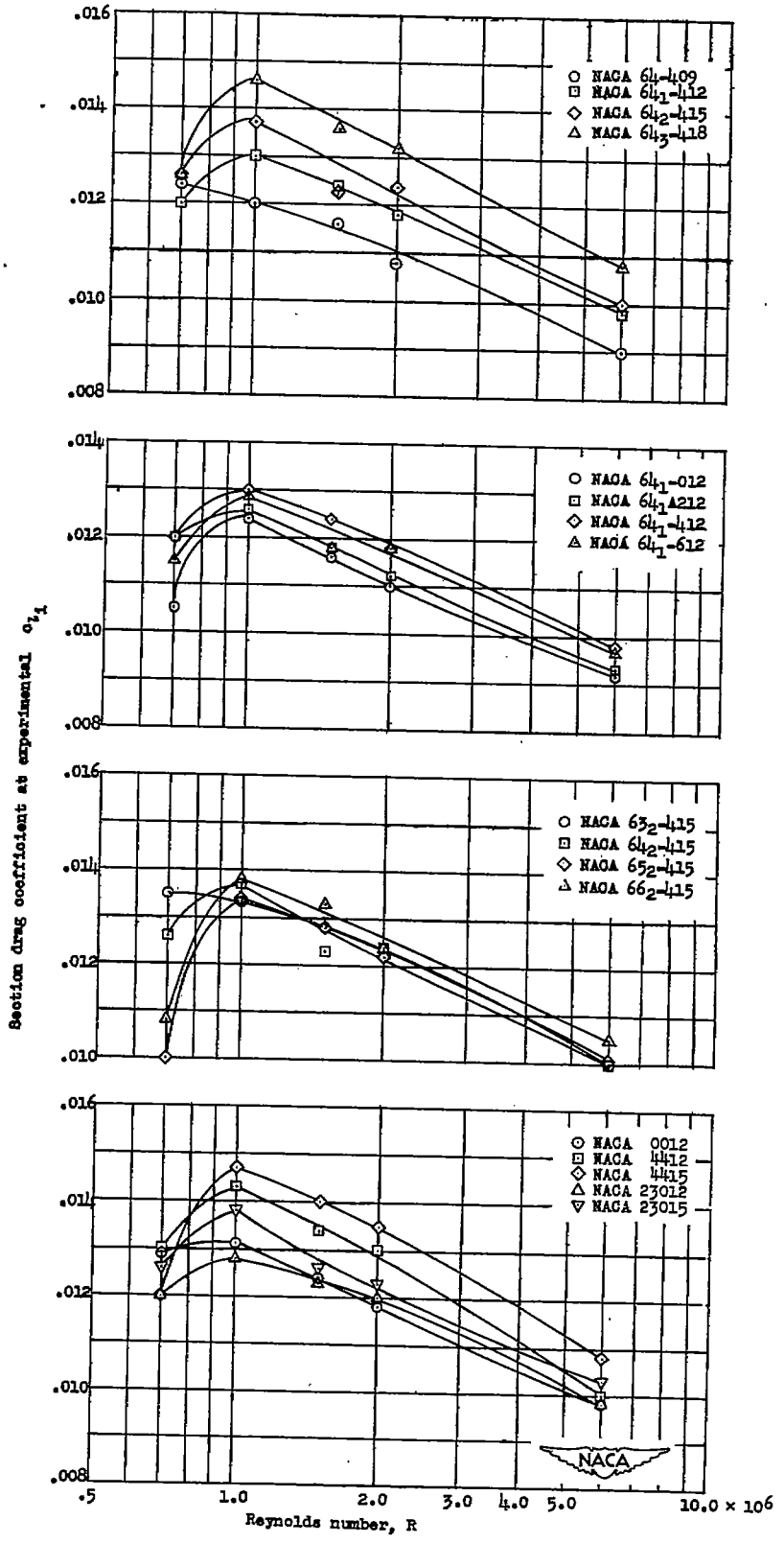

(b) Airfoils with standard leading-edge roughness.

Figure 16.- Concluded.

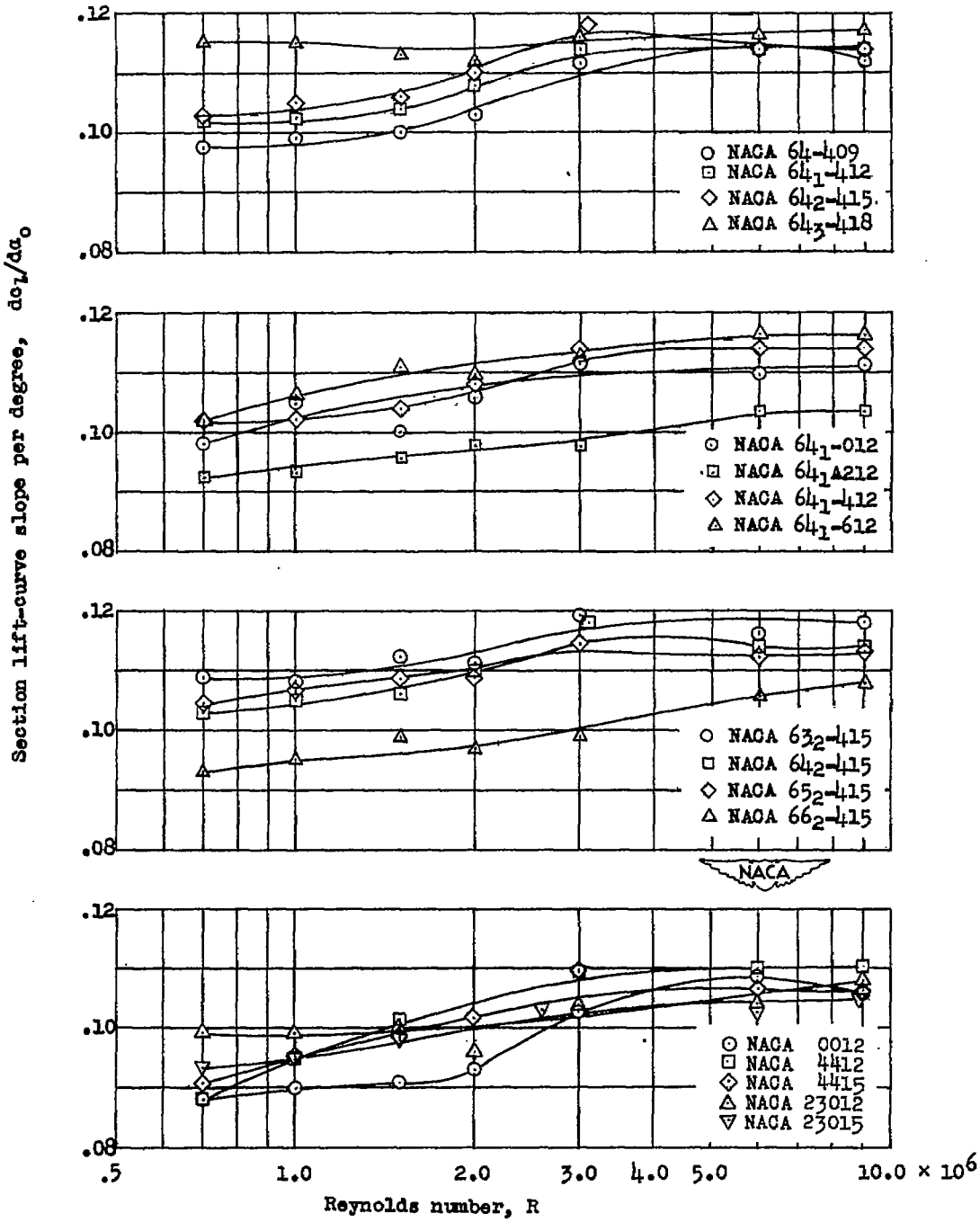

(a) Airfoils with smooth surfaces.

Figure 17.– Variation of slope of the section lift curve with Reynolds number for the 15 plain airfoils.

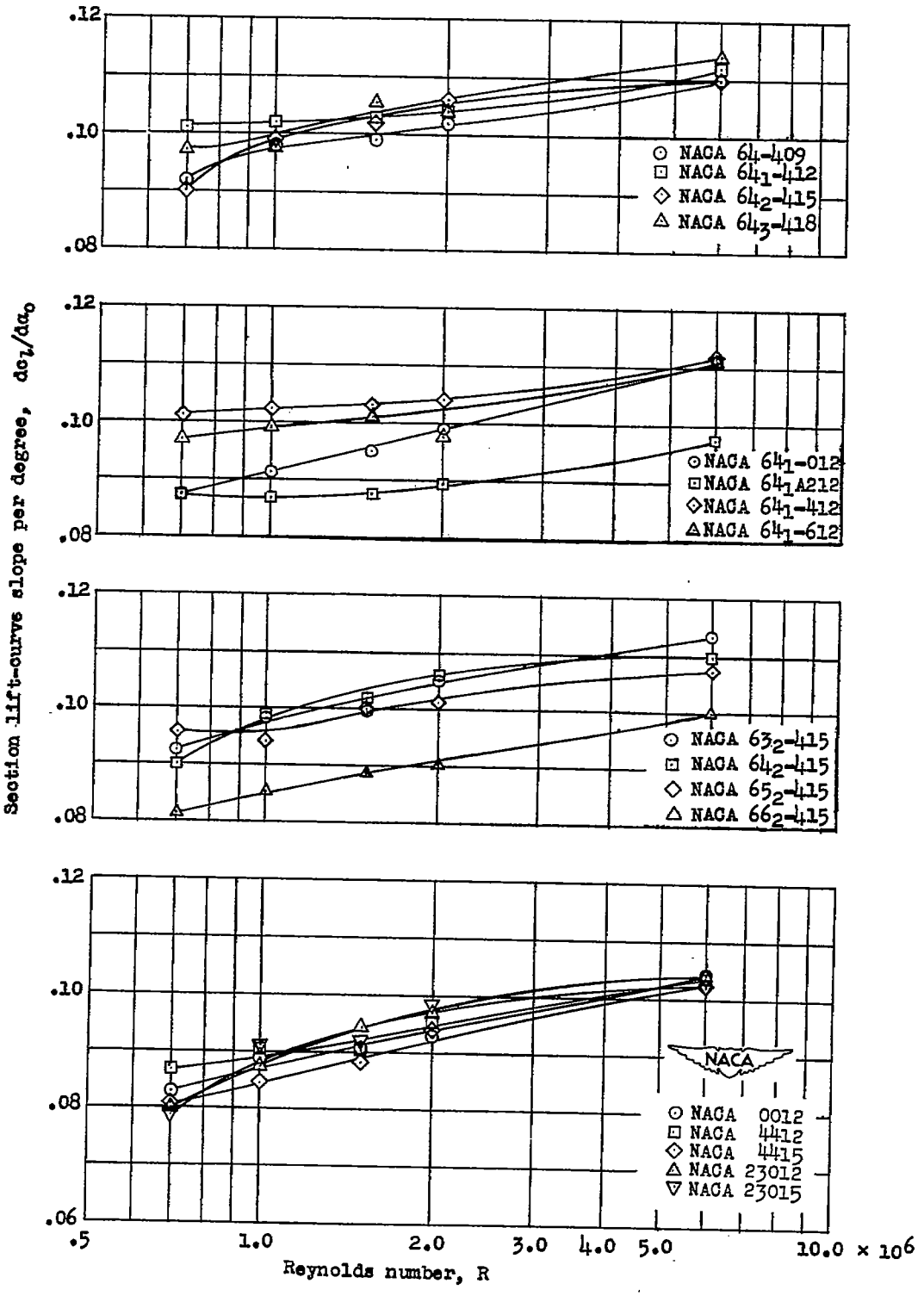

(b) Airfoils with standard leading-edge roughness.

Figure 17.- Concluded.

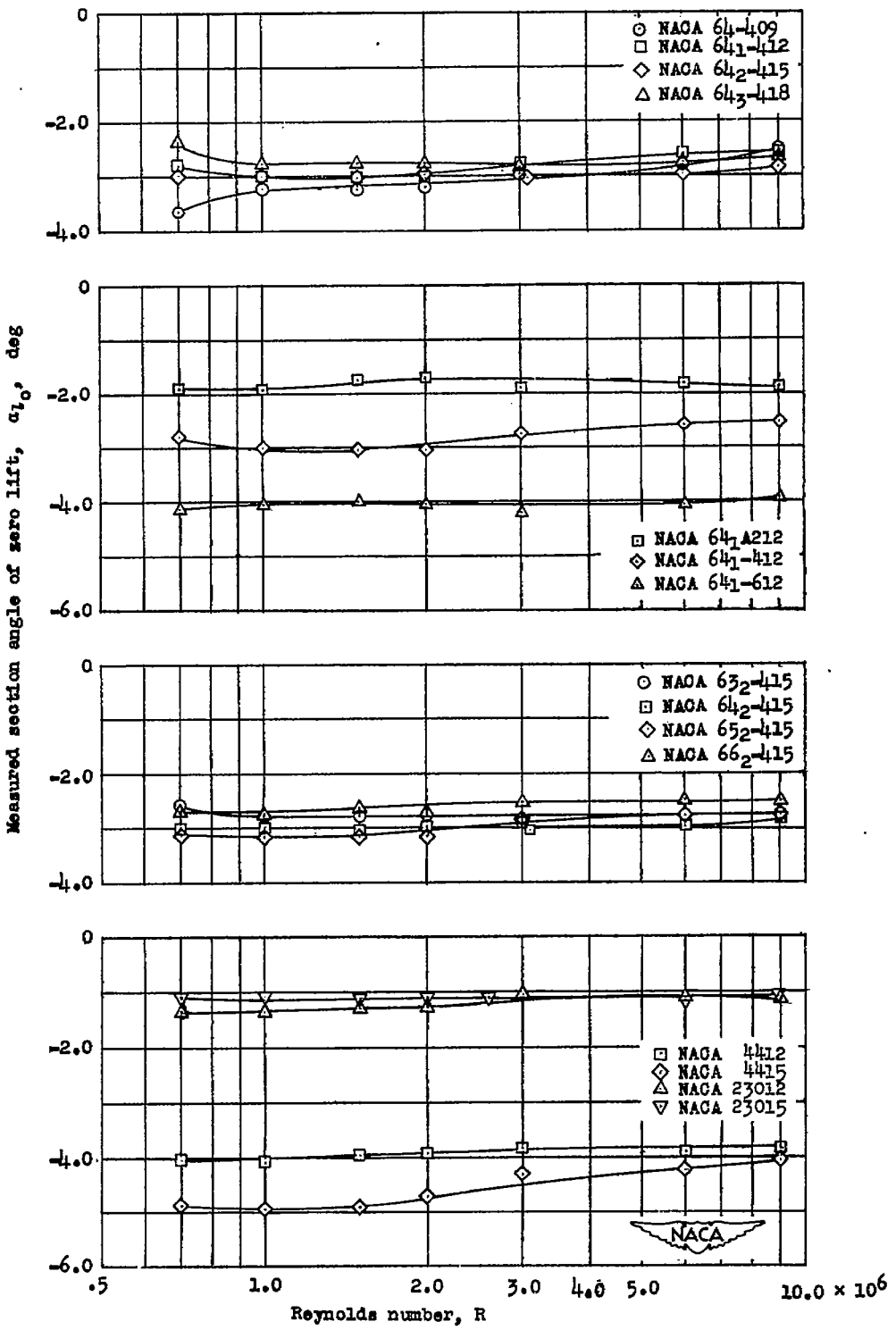

(a) Airfoils with smooth surfaces.

Figure 18.— Variation of section angle of zero lift with Reynolds number for the plain airfoils.

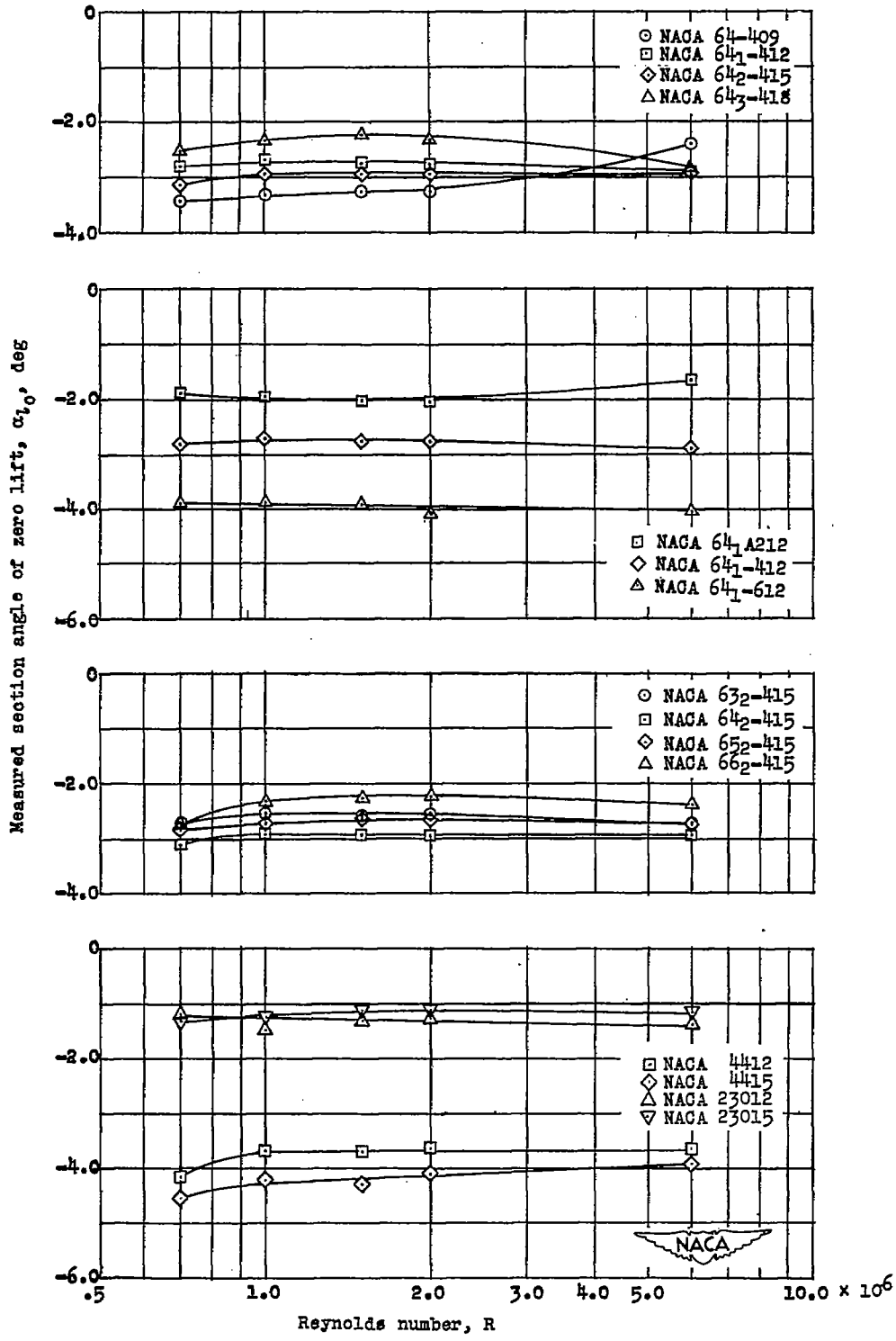

(b) Airfoils with standard leading-edge roughness.

Figure 18.– Concluded.

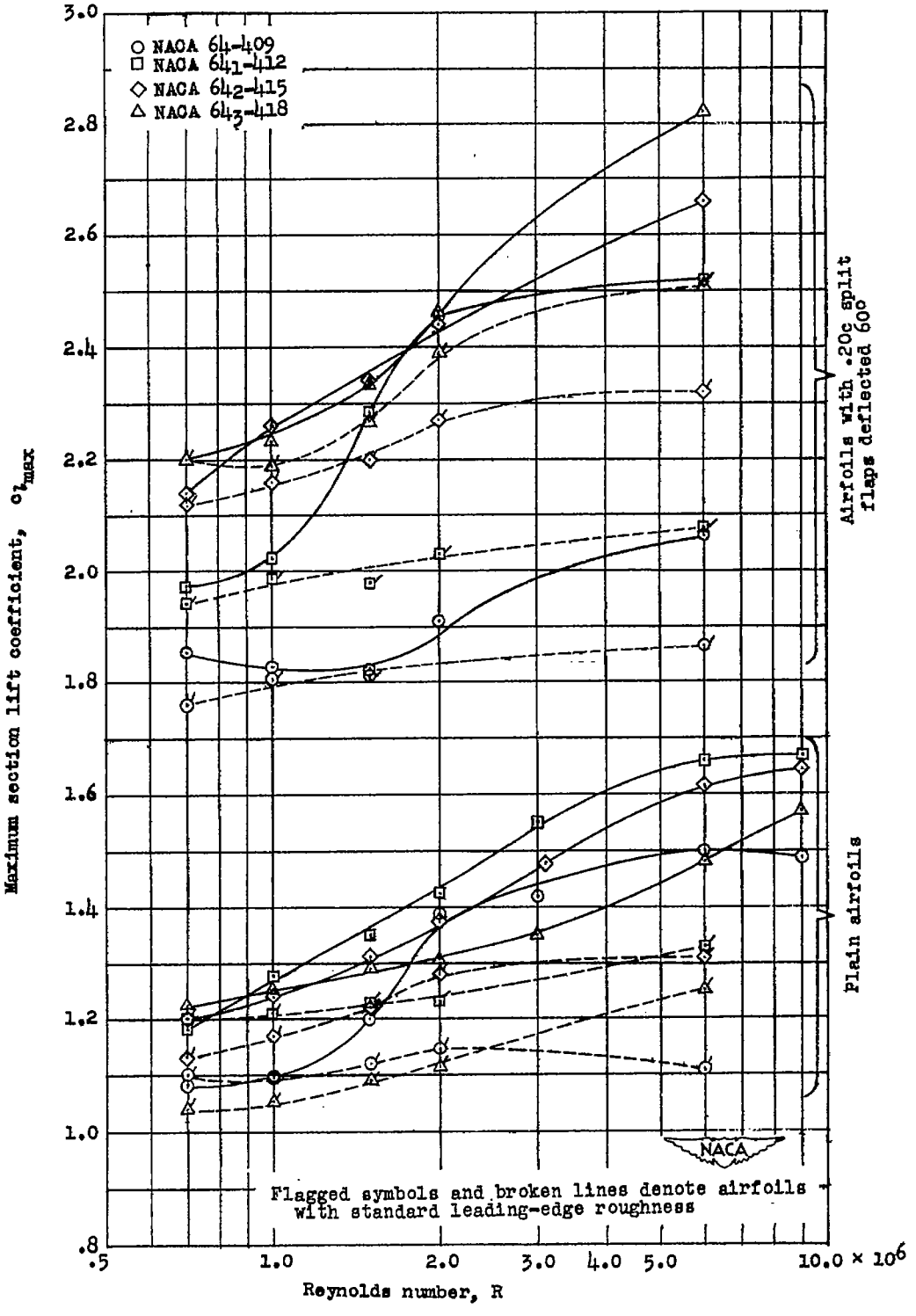

Figure 19.– Variation with Reynolds number of maximum section lift coefficient for four NACA 64–series airfoils of 0.4 design lift coefficient and various thickness.

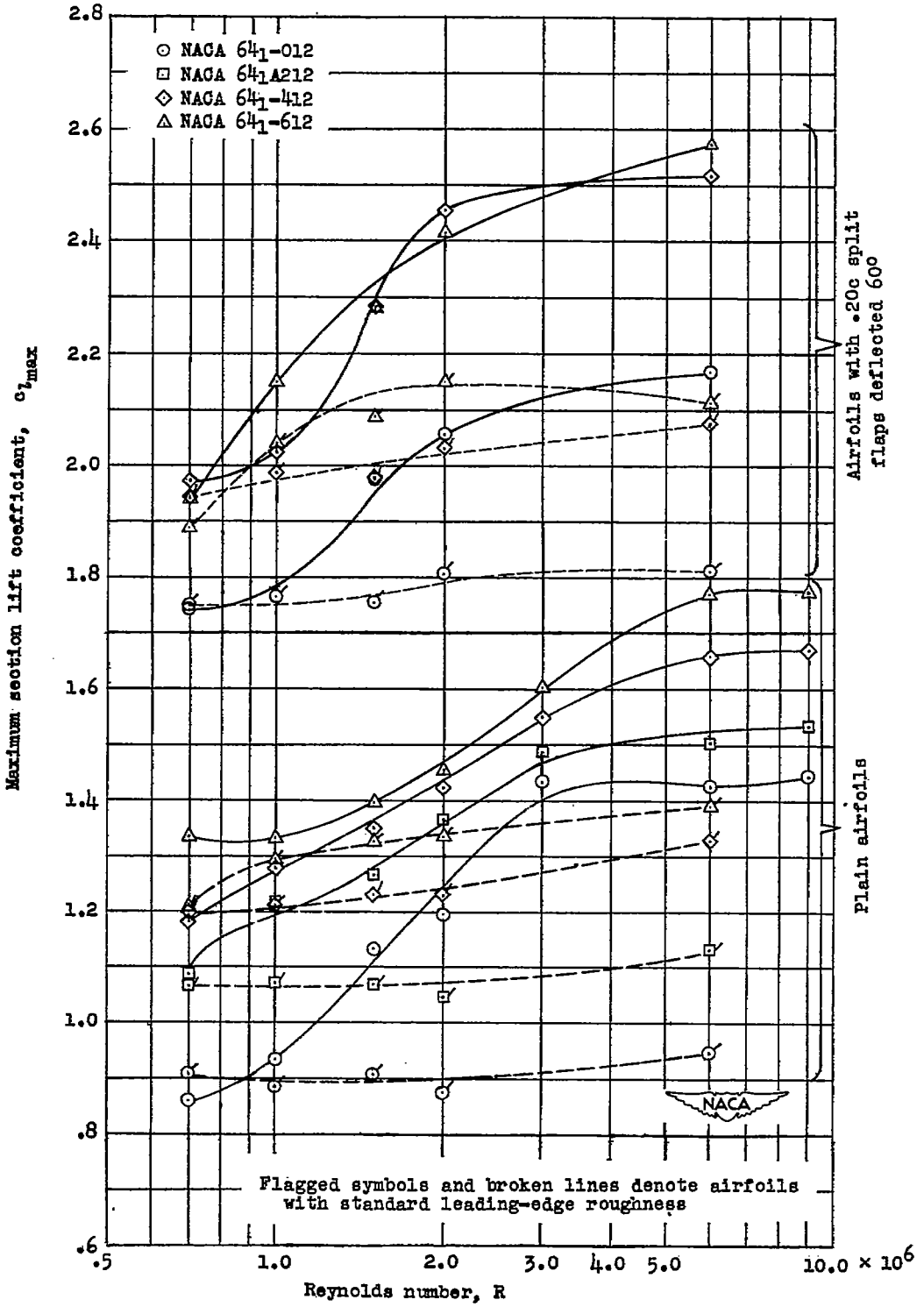

Figure 20.— Variation with Reynolds number of maximum section lift coefficient for four NACA 64-series airfoils of 0.12c thickness and various camber.

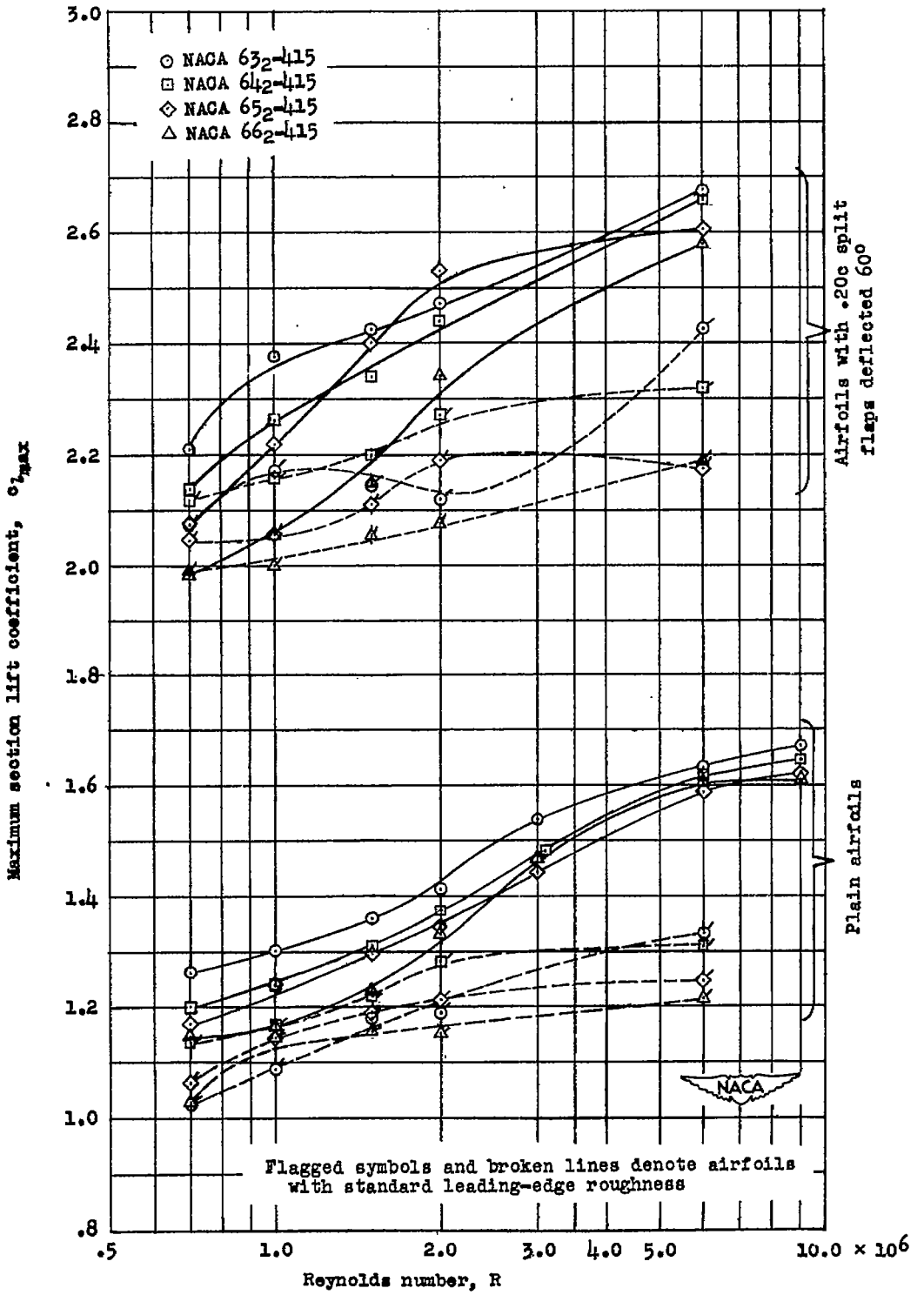

Figure 21.— Variation with Reynolds number of maximum section lift coefficient for four NACA 6-series airfoils of 0.4 design lift coefficient, 0.15c thickness, and various thickness distribution.

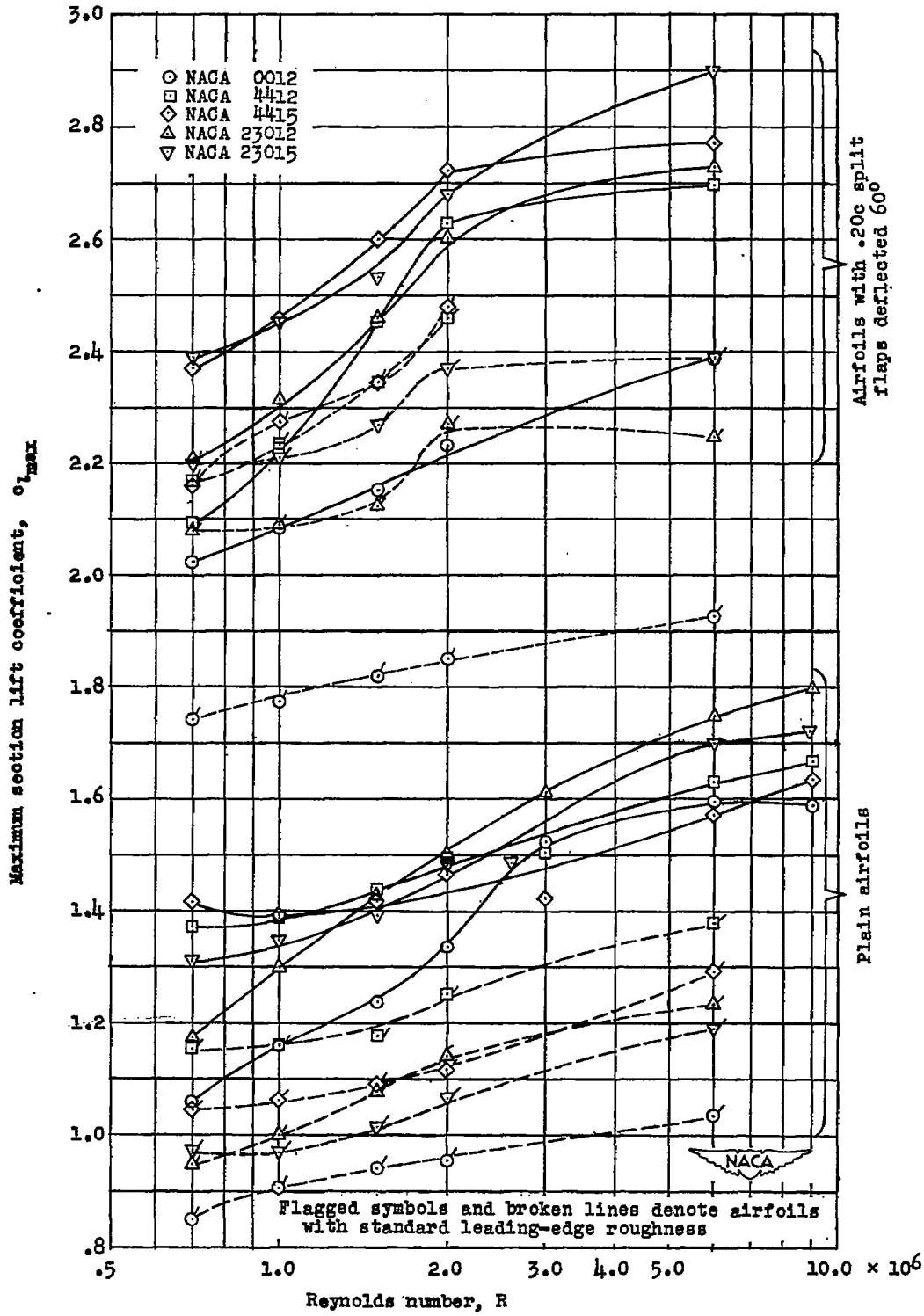

Figure 22.– Variation with Reynolds number of maximum section lift coefficient for three NACA 4-digit-series airfoils and two NACA 5-digit-series airfoils.